Potential Impacts of Stratospheric Aerosol Geoengineering on Water Yield, Crop Yield, and Rangeland Productivity in Africa

Report to the

Water Research Commission

By

Babatunde J. Abiodun[1,2] , Rhoda F. Ayedun[1] , Ashleigh Ho[1], Nokwethaba Makhanya[1], Akintunde Israel Makinde[1,2], Founi M. Awo[2], Shakirudeen Lawal[1], Gabriel Lekalakala[3], Romaric C. Odoulami[4], and Temitope S. Egbebiyi[1,4]

[1]Department of Environmental and Geographical Science, University of Cape Town

[2]Nansen-Tutu Centre for Marine Environmental Research, Department of Oceanography, University of Cape Town

[3]Department of Water and Sanitation

[4]African Climate and Development Initiative, University of Cape Town

WRC report no. 3198/1/25
ISBN 978-0-6392-0704-9

May 2025

Obtainable from:
Water Research Commission
Private Bag X03
GEZINA, 0031

This is the final report for WRC project no. C2022/2023-00782.

DISCLAIMER

This report has been reviewed by the Water Research Commission (WRC) and approved for publication. Approval does not signify that the contents necessarily reflect the views and policies of the WRC, nor does mention of trade names or commercial products constitute endorsement or recommendation for use.

Executive Summary

Rationale

Several socio-economic activities in Africa are fuelled by river basins, agricultural production and rangeland productivity. However, the productivity of these activities is increasingly threatened by climate change induced by greenhouse gases. International negotiations to reduce greenhouse gas emissions have been slow, while emissions themselves continue to rise.

Stratospheric Aerosol Geoengineering (SAG), or Stratospheric Aerosol Injection (SAI), has been proposed as a quick and cost-effective method to mitigate the temperature rise related to climate change globally. However, the implementation of SAG is still controversial due to the associated political, environmental, and socioeconomic risks, which may not be evenly distributed across the globe. Since the effects of SAG cannot be confined to its deployment location, the benefits and drawbacks of such deployment are also unlikely to be evenly distributed worldwide.

Although most research activities, discussions, and debates on SAG governance are taking place in developed countries, it is imperative for developing countries to participate, as SAG will have global implications. Also, the populace in developing countries, particularly Africa, are often the most vulnerable to environmental changes. therefore, stand to gain or lose the most from SAG implementation.

However, to participate meaningfully in the SAG discussion, Southern African stakeholders and policymakers must be well-informed about the potential socio-economic impacts of SAG in the subcontinent. The goal of this project is to investigate the potential impacts of SAG on socio-economic activities in Africa, with a focus on water yield, crop yield, and rangeland productivity in Africa.

Objectives

The specific objectives of the project are to:

- Calibrate and evaluate hydrological, crop, and rangeland models over Africa
- Examine the potential impacts of climate change and SAG intervention on water yield over the river basins in Africa
- Investigate the potential impacts of climate change and SAG intervention on crop yield over the Africa
- Study the potential impacts of climate change and SAG intervention on rangeland productivity in Africa
- Inform policy makers on potential impacts of SAG on water resources, food security and rangeland in Africa

Methodology

The project analysed a diverse range of datasets, including reanalysis products from the Global Meteorological Forcing Dataset (GMFD), as well as historical and future climate simulation datasets from the Coupled Model Intercomparison Project Phase 6 (CMIP6). It also included geoengineering climate simulation datasets from the Geoengineering Model Intercomparison Project (GeoMIP) and the Stratospheric Aerosol Geoengineering Large Ensemble (GLENS), crop yield datasets from the Food and Agriculture Organization (FAO) of the United Nations, and Geographic Information System data (such as catchment delineated shape files, land use data, topographic data, soil moisture data, vegetation types, and crop yield data).

The project was implemented in four work packages (WPs: WP1, WP2, WP3, and WP4) that ran simultaneously. WP1 focused on generating bias correction of the climate simulation datasets, while WP2, WP3, and WP4 focused on the potential impacts of climate change and SAG intervention on water yield, crop yield, and rangeland productivity, respectively. The bias correction method (called the Bias Correction and Statistical Downscaling, BCSD) was used in the study. A crop yield model, Decision Support System for Agrotechnology Transfer (DSSAT) was used to investigate the potential impacts of climate change and SAG intervention on crop yield, while a rangeland model, called the Global Rangeland model (G-Range) was used to examine the potential impacts of climate change and SAG on rangeland productivity.

Results

Influence of bias correction on simulated climate variables

The bias correction method improves the spatial distribution of simulated climate variables, such as temperature and precipitation, over Africa. Although the original CMIP6 ensemble already features a realistic spatial distribution of these variables across the continent (evidenced by high correlation values, $r \geq 0.9$), there were still substantial biases in the simulations. Specifically, the bias correction reduces the cold bias in maximum temperature and the warm bias in minimum temperature by 0.2°C and removes the dry bias in simulated precipitation over southern Africa. It also reduces the uncertainty among the simulation ensemble members. These improvements have positive implications for crops, and vegetation simulations. The improved precipitation and diurnal temperature simulation over southern Africa gives a more realistic representation of potential evapotranspiration, climate water balance, evaporation, and soil moisture in the subcontinent.

Impacts of climate change and SAG on water yield in African river basins

We examined the impact of climate change and SAG on the ten largest and most transboundary river basins in Africa: Congo, Limpopo, Niger, Nile, Ogooue, Orange, Senegal, Okavango, Volta, and Zambezi. Climate change is expected to reduce freshwater availability across most parts of Africa, except in East and Central Africa, where an increase is projected. In West and Southern Africa, climate change leads to a decrease in both precipitation and evaporation, resulting in a freshwater deficit because the reduction in precipitation is greater than that in evaporation. However, East and Central Africa experience a freshwater surplus as the increase in precipitation surpasses the increase in evaporation. Enhanced water yield is projected in the Congo (1.2%), Ogooue (5.41%), and Nile (7.1%) Basins, while a reduced water yield is expected in the remaining basins. The implementation of SAG reverses the water yield surplus and imposes a water yield deficit in the Congo (-2.8%) and Ogooue (-4.2%) Basins, and reduces the water yield surplus in the Nile Basin (6.5%). However, it reduces the magnitude of water yield deficit in Senegal, Volta, and Niger Basin, while reinforcing the deficit in Zambezi and Limpopo Basins. Given the complexity and potential trade-offs of using SAG to mitigate climate change impacts over African basins, there is a need for careful consideration and planning before implementing such techniques - this could make it necessary for transnational agreements to ensure the implementation of SAG and avoid conflicts related to water resource sharing.

Impacts of climate change and SAG on Crop Yield in Africa

We examined the impact of climate change and SAG on the yields of three crops: maize, sorghum, and soybeans. Climate change increases soybean yields in most parts of Africa, indicating that soybeans (a C3 crop) benefit more from rising CO_2 levels. In contrast, maize and sorghum (C4 crops) decrease in most parts of the continent under global warming. The application of SAG generally reduces yield deficits, although it still lowers yields in some areas where climate change projections show increases. In Southern Africa, SAG completely reverses the decline in maize yield,causes larger the decline in sorghum yield and reduces soybean yields. In West Africa, it mitigates the decline in maize yield while lowering sorghum and soybean yields. In Central Africa, SAG mitigates the declines in maize and sorghum and reduces soybean yields. In Eastern Africa, it increases maize and soybean yields, while significantly decreasing sorghum yield.

Impacts of climate change and SAG on Grassland productivity in Africa

We studied the impacts of climate change and SAG on the grassland - with shrubs, herbs, and above-ground live biomass as the focus. Climate change causes a decline in herbs and an increase in woody vegetation throughout most of Africa. The total above-ground live biomass decreases, potentially leading to less forage and fewer resources from rangelands in the future. The change in the ratio of herbs to trees and the decrease in biomass production will affect food and economic security for communities. SAG mitigates impacts of climate change on vegetation by reducing the magnitude of change and keeping vegetation closer to present-day composition and quantity. However, the effectiveness of SAI in mitigating the impact of climate change varies across regions and seasons, making it neither entirely beneficial nor detrimental.

Discussion and Conclusions

The findings from this project have several significant implications for climate science, agricultural planning, water resource management, and environmental policy.

This project produced more accurate and reliable climate model products from the CMIP6 simulation. The bias correction method significantly improves the spatial distribution of climate variables such as temperature and precipitation over Africa, reduces biases and uncertainties in climate simulations. These accurate and reliable projections are essential for understanding and predicting climate patterns, to support better informed decision-making and policy development.

The improved accuracy in temperature and precipitation simulations positively impacts crop and vegetation models. This leads to more realistic simulations of evapotranspiration, climate water balance, evaporation, and soil moisture, which are crucial for agricultural planning. Enhanced crop simulations can help farmers and policymakers develop strategies to optimize crop yields and ensure food security in the face of climate change.

The examination of climate change and SAG impacts on major African river basins highlights the challenges and trade-offs involved in managing freshwater resources. Climate change is expected to reduce freshwater availability in most parts of Africa, except for East and Central Africa. SAG implementation further complicates water yield patterns, necessitating careful consideration and planning. Transnational agreements may be required to manage shared water resources and prevent conflicts.

The findings underscore the importance of region-specific strategies to address the diverse impacts of climate change and SAG. Tailored approaches are needed to mitigate the negative impacts on water availability, crop yields, and grassland ecosystems. Ensuring sustainable development and resilience across the continent requires a comprehensive understanding of these complex interactions.

Climate change and SAG affect grasslands by reducing herbs and increasing woody vegetation. This has significant implications for rangeland resources, as reduced forage availability affects food and economic security for pastoral communities. The potential of SAG to mitigate these changes highlights the need for adaptive land management practices to maintain ecosystem health and support livelihoods.

Policymakers can use these findings to develop informed strategies to address the challenges posed by climate change and SAG. Recommendations include creating supportive policies for crop diversification, investing in climate-resilient agricultural practices, and implementing sustainable water management. Collaborative efforts and adaptive management are essential to ensure the well-being of communities and the environment.

In conclusion, these findings provide valuable insights into the interactions between climate change, SAG, and various environmental and agricultural systems. They highlight the need for targeted, region-specific strategies to address the complex challenges posed by climate change, ensuring sustainable development and resilience across Africa.

Recommendations for further research

The findings of the study can be improved in several ways. Most importantly, there is a need to extend the methodology to investigate the impact of climate change and SAG on other socioeconomic activities, such as water quality, animal production, and human health (e.g., heat stress and disease prevalence). Additionally, the impacts of climate change and SAG need to be quantified in terms of monetary gains or losses. This will help in determining the cost-effectiveness of SAG implementation and in negotiating compensation for the positive or negative impacts.

Acknowledgement

The authors would like to express their sincere gratitude to Dr B. Petja for the efficient management of the study and for showing great interest in the work.

We also extend our heartfelt thanks to the Project Reference Group for their invaluable guidance throughout the study. The Reference Group members were:

Prof T.A. Fasheun	: Tim Fasheun Group
Dr J. Botai	: South African Weather Service
Dr T. Sawunyama	: Inkomati-Usuthu Catchment Management Agency
Dr. M.J. Bopape	: South African Environmental Observation Network

Capacity building

The following postgraduate students were supported directly or indirectly from the project

1. Rhoda Adaramola (PhD student; University of Cape Town)
2. Nokwethaba Z. Makhanya (PhD student; University of Cape Town)
4. Muyiwa Oloniyo (PhD student; University of Cape Town)
3. Ashleigh Ho (Master student; University of Cape Town)

Table of content

List of Figures

List of Tables

Chapter 1: Background

This chapter provides the background for the project. It begins by exploring the impacts of climate change in Africa and outlining global efforts to mitigate the temperature-related aspects of climate change. It also highlights the aim and objectives of the project, followed by a detailed description of the datasets and methods used in the project.

1.1 Impacts of climate change in Africa

Climate change is a complex global challenge with significant impacts on various socioeconomic activities, particularly water yield, crop and grassland productivity in Africa. These impacts are especially severe because the continent relies heavily on natural resources. Moreover, existing vulnerabilities, such as inadequate infrastructure and financial constraints, further intensify the impacts of climatic variability and change across the region.

1.1.1 Impacts on Water Yield

Water yield, defined as the amount of water generated from precipitation after accounting for evapotranspiration and storage losses, is closely tied to climatic conditions. Therefore, any variability or changes in rainfall, rising temperatures, or prolonged droughts will inevitably impact hydrological systems. Across Africa, rainfall patterns are becoming increasingly erratic, with regions like East and Southern Africa experiencing extended dry seasons interspersed with sudden and intense downpours. For example, the Intergovernmental Panel on Climate Change (IPCC) noted that in Southern Africa, annual rainfall has declined over the past century, with projections suggesting further reductions in precipitation by the late 21st century (IPCC, 2019). The Sahel region exemplifies how climate change is intensifying the frequency and severity of droughts, disrupting the hydrological cycle. Conversely, regions such as East Africa are experiencing extreme weather events like catastrophic flooding, which further complicates water management efforts. Rising temperatures also exacerbate water scarcity by accelerating evaporation from reservoirs, rivers, and lakes, depleting surface water supplies. Reduced precipitation compounds these challenges, affecting groundwater recharge rates, as observed in North African aquifers. Gleeson et al. (2020) emphasized that reduced recharge, coupled with over-extraction, significantly increases the vulnerability of groundwater systems in arid zones. Additionally, wetlands and river systems, which are vital biodiversity hotspots, are under threat. For instance, Lake Chad has shrunk to a fraction of its original size, profoundly affecting the millions of people who depend on its resources. These disruptions pose serious challenges for water-dependent ecosystems and human livelihoods alike.

1.1.2 Impacts on Crop Production

Africa's agricultural sector, which employs a significant portion of the population, is particularly vulnerable to the effects of climate change. Shifting climatic conditions are disrupting traditional farming practices and creating challenges for food security. Staple crops such as maize, sorghum, and millet are highly sensitive to rising temperatures. Research shows that for every 1°C increase in temperature, yields of crops like maize could decline by up to 10% in sub-Saharan Africa (Schlenker & Lobell, 2010). Unpredictable rainfall patterns further complicate farming, particularly in areas reliant on rain-fed agriculture. Water stress during critical growing periods can result in significant yield losses. For example, in the Sahel, shorter rainy seasons and extended dry spells have severely impacted crop growth. Additionally, higher temperatures and erratic rainfall accelerate soil erosion and reduce soil fertility. Declining soil health adds to the difficulty of maintaining productivity, especially for smallholder farmers who often lack access to soil improvement resources. Rising temperatures also create favorable conditions for pests like the fall armyworm, which has devastated maize yields in many parts of Africa. Similarly, climate change increases the prevalence of plant diseases such as rusts and blights, further threatening crop yields. Changing climatic conditions are forcing farmers to adapt by altering the types of crops they grow or even abandoning traditional farming areas. For instance, coffee-growing regions in Ethiopia are becoming less suitable due to rising temperatures. On the other hand, some areas in East Africa may gain new opportunities for cultivating crops like cassava (Ramirez-Villegas & Thornton, 2015). Despite these challenges, African farmers face significant constraints in adapting to climate change. Limited access to irrigation, modern farming techniques, and financial support make adaptation particularly difficult for smallholder farmers, who form a large part of the continent's agricultural sector.

1.1.3 Impacts on Grassland Productivity

Africa's grasslands are vital ecosystems that provide grazing for livestock, support biodiversity, and act as essential carbon sinks. However, climate change is driving significant shifts in their structure and function. With rising temperatures and changing rainfall patterns, grasslands are increasingly transforming into shrublands or desert-like landscapes. This vegetation shift reduces the availability of nutritious forage for livestock, particularly in the savannas of sub-Saharan Africa (Iglesias et al., 2007). Moreover, climate change is causing persistent droughts that weaken grassland ecosystems, reducing their resilience to both climatic and human-induced stresses. Research from the Karoo region of South Africa highlights a decline in grass cover due to frequent droughts, contributing to desertification (Hoffman, 2018). Grasslands also play a crucial role in capturing and storing carbon dioxide (CO_2) from the atmosphere. However, changes in vegetation and soil health diminish this capacity, feeding into a feedback loop that exacerbates global warming. Furthermore, climate-induced changes in grasslands pose a threat to the habitats of numerous species that are dependent on these ecosystems. For example, the Serengeti is experiencing shifts in grass and tree populations, which impact herbivores that are essential for maintaining the balance of the ecosystem (Estes et al., 2012). Reduced grassland productivity also affects pastoral communities who rely on livestock for their livelihoods. Growing competition over shrinking resources often leads to conflicts, as observed in parts of East and West Africa.

Hence, a comprehensive approach is required to address the impacts of climate change on water yield, grasslands, and crop productivity. Examples of such approaches include: Water Resource Management, Grassland Restoration and Sustainable Use, Climate-Smart Agriculture, Early Warning Systems and Research, Policy and Collaboration.

1.2 Solar Radiation Modification and Global Warming

Solar radiation modification (SRM), also known as solar geoengineering, involves intentional interventions to adjust the Earth's radiation budget. This is achieved by reflecting a portion of incoming solar energy back into space or enhancing the reflectivity (albedo) of the Earth's surface or atmosphere. The primary goal of SRM is to reduce global warming and mitigate some of the adverse effects of climate change. While SRM does not directly address the root cause of climate change—greenhouse gas emissions—it has been proposed as a complementary strategy to slow warming and provide additional time for implementing mitigation and adaptation efforts. The concept of SRM is not entirely new. Natural examples, such as volcanic eruptions, illustrate how injecting particles into the atmosphere can lead to temporary cooling. For example, the eruption of Mount Pinatubo in 1991 released millions of tons of sulfur dioxide into the stratosphere, creating a reflective aerosol layer that reduced global temperatures by approximately 0.5°C over the following year. Inspired by such phenomena, researchers have been exploring various methods to replicate similar cooling effects artificially. SRM seeks to achieve these effects through different techniques for manipulating solar radiation.

The growing urgency of the climate crisis has driven interest in SRM as a potential tool to mitigate some of the most severe impacts of global warming. Despite ongoing efforts to reduce greenhouse gas emissions, the current trajectory suggests that global temperatures may exceed the 1.5°C threshold outlined in the Paris Agreement, potentially leading to catastrophic consequences. SRM could help reduce the rate of warming and limit the risk of crossing critical climate tipping points, such as the irreversible melting of polar ice caps or the collapse of major ocean currents. SRM could provide a temporary cooling effect, buying time for societies to implement long-term solutions to reduce carbon emissions. SRM could help moderate some of these impacts, potentially preventing loss of life and livelihoods. Several approaches to SRM have been proposed, each with its own mechanisms, advantages, and challenges (Fig 1). Here, we will only focus on four of them.

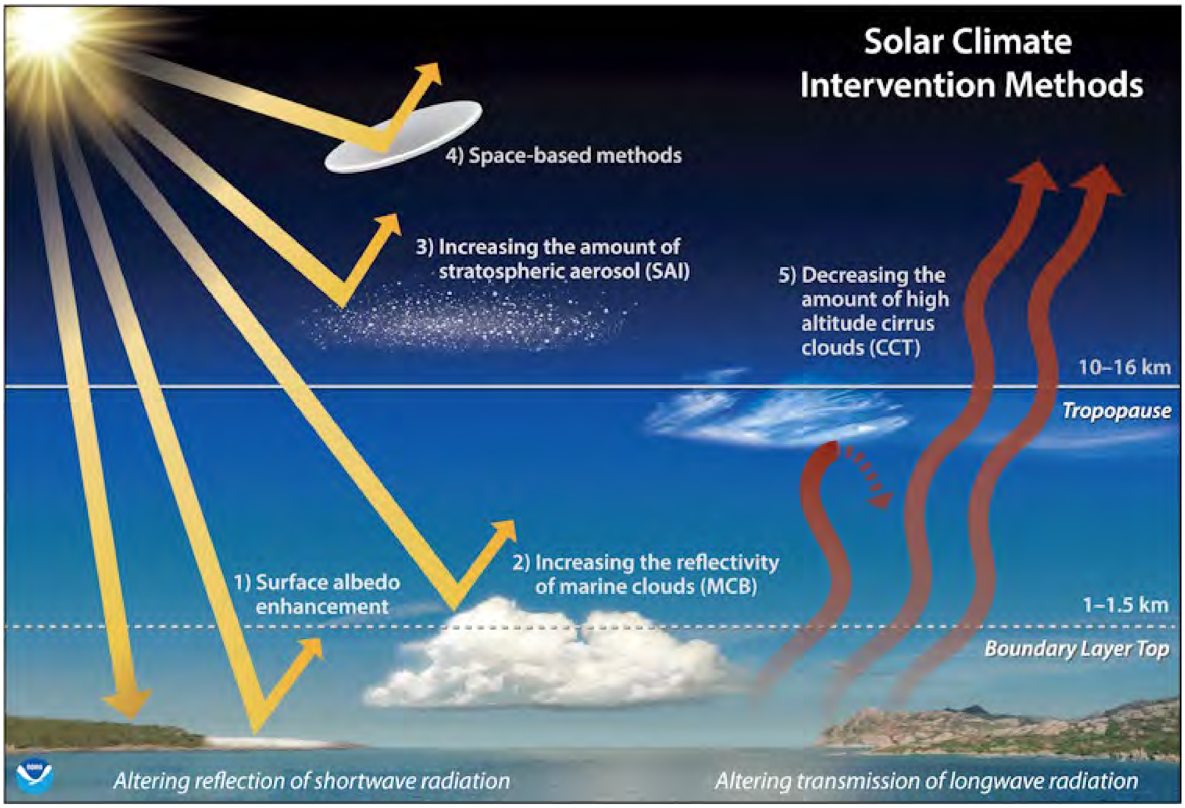

Figure 1.1 Some solar radiation modification methods (Bell et al., 2022)

1.2.1 Stratospheric Aerosol Geoengineering

Stratospheric aerosol injection or geoengineering (SAG) is one of the most studied and debated SRM methods. It involves the deliberate release of reflective particles, such as sulfur dioxide, calcium carbonate, or titanium dioxide, into the stratosphere to form a reflective aerosol layer. The aerosols scatter incoming solar radiation, reducing the amount of energy reaching the Earth's surface. This process mimics the cooling effects of large volcanic eruptions, such as Mount Pinatubo in 1991. SAI is considered one of the most cost-effective and scalable SRM methods. It has the potential to provide rapid cooling, stabilizing global temperatures within a short time frame. However, the potential side effects include changes in precipitation patterns, ozone depletion, and impacts on ecosystems. Continuous aerosol replenishment is required due to particle dispersal over time. The governance and ethical concerns about who controls and overseas deployment.

1.2.2 Marine Cloud Brightening

Marine cloud brightening (MCB) aims to enhance the reflectivity (albedo) of low-lying marine clouds by injecting fine sea salt particles into the atmosphere. These particles act as cloud condensation nuclei, increasing the number and brightness of cloud droplets. Ships or drones equipped with sprayers release seawater droplets into the air. The water evaporates, leaving behind salt particles that form brighter and more reflective clouds. MCB is regionally targeted and could be deployed over specific areas, such as coastal regions, to mitigate localized climate impacts. It uses natural components (sea salt), potentially reducing environmental risks. Limited understanding of its effectiveness and potential unintended consequences on weather patterns and ecosystems. Technical challenges in scaling up and controlling the extent of cloud modification.

1.2.3 Surface Albedo Enhancement

Surface albedo enhancement (SAE) involves increasing the reflectivity of the Earth's surface to reflect more solar radiation. This can be achieved through a variety of methods, such as using reflective materials, painting roofs white, or planting lighter-colored crops. Urban surfaces, such as rooftops and pavements, are coated with reflective materials to reduce heat absorption. Land management practices, such as planting reflective crops or managing vegetation, enhance albedo. SAE can be implemented locally with relatively low technological requirements. It provides co-benefits, such as reduced urban heat island effects. Challenges include limited global impact due to the localized nature of surface modifications. Potential trade-offs with land use and agricultural productivity.

1.2.4 Space-Based Reflectors

Space-based reflectors (SBR) involves deploying mirrors or reflective shields in space to deflect a portion of incoming solar radiation away from the Earth. With this approach, large reflective structures are positioned in orbit around the Earth or at the Lagrange Point (a stable position between the Earth and the Sun). Theoretically capable of providing precise and large-scale cooling. It has minimal impact on the Earth's atmosphere and ecosystems. The challenges include extremely high costs and technical challenges associated with launching and maintaining space-based systems. Long lead times for research, development, and deployment.

1.3 Project aim and objectives

This project aims to investigate the potential impacts of Stratospheric Aerosol Geoengineering (SAG) on socio-economic activities in Southern Africa, with a focus on water yield, crop yield, and rangeland productivity over some river basins. To achieve this aim, the project will analyze a series of climate simulations for past climate and future climate under climate change (with and without SAG) and use the simulations to force a hydrology model, crop-yield model, and rangeland model. The project intends to provide scientific information that would help the Southern African policymakers to effectively engage in the debate and negotiation on SAG implementation.

The specific objectives of the project are to:

- Calibrate and evaluate crop and rangeland models over Africa
- Examine the potential impacts of climate change and SAG intervention on water yield over Africa
- Investigate the potential impacts of climate change and SAG intervention on crop yield over Africa
- Study the potential impacts of climate change and SAG intervention on rangeland productivity over Africa

1.4 Datasets

In the project, we analysed various types of datasets, ranging from climate, hydrology, crop yield, and grassland datasets. However, only the climate datasets will be described in this chapter. Other datasets will be described chapter 3 to 5. Table 1.1 presents the three types of climate dataset used in the study while Table 1.2 shows the key meteorological variables used in datasets.

Table 1.1: The main climate variable datasets used in the project.

Dataset	**Sources**
Global Meteorological Forcing Dataset (GMFD)	https://rda.ucar.edu/datasets/d314000/
Coupled Model Intercomparison Project Phase 6 (CMIP6)	https://wcrp-cmip.org/cmip-data-access/?form=MG0AV3
The Assessing Responses and Impacts of Solar Climate Intervention on the Earth System with Stratospheric Aerosol Injection (ARISE-SAI)	https://www.earthsystemgrid.org/dataset/ucar.cgd.ccsm4.ARISE-SAI-1.5.html?form=MG0AV3
The Geoengineering Model Intercomparison Project (GeoMIP)	https://climate.envsci.rutgers.edu/geomip/
The Stratospheric Aerosol Geoengineering Large Ensemble (GLENS)	https://www.cesm.ucar.edu/community-projects/glens

Table 1.2: Climate variables used from GMFD, CMIP6, NEX-GDDP and ARISE-SAI datasets

Variable	**Description**	**Units**
hurs	Near-surface relative humidity	percentage
huss	Near-surface specific humidity	kg/kg

pre	Precipitation (in liquid and solid phases)	mm/mon
rlds	Surface downwelling longwave radiation	W/m2
rsds	Surface downwelling shortwave radiation	W/m2
sfcWind	Surface wind speed	m/s
tas	Near-surface air temperature	ºC
tasmax	Maximum near-surface air temperature	ºC
tasmin	Minimum near-surface air temperature	ºC

1.4.1 Global Meteorological Forcing Dataset (GMFD)

The GMFD is a comprehensive dataset designed to provide near-surface meteorological data for driving land surface models and other terrestrial modeling systems. This dataset is developed by the Terrestrial Hydrology Research Group at Princeton University, and it is widely used in hydrological, ecological, and climate studies to understand land-atmosphere interactions and their implications for water and energy cycles. The GMFD combines observation-based datasets with reanalysis data to create a globally consistent and long-term dataset of meteorological variables. It spans the period from 1948 to 2016, offering high temporal and spatial resolution. The dataset is available at resolutions of 1.0°, 0.5°, and 0.25°, with temporal resolutions ranging from daily to 3-hourly intervals. This flexibility makes it suitable for a wide range of applications, from global-scale studies to regional analyses. Its long-term and globally consistent nature makes it a valuable resource for understanding the interactions between the atmosphere and terrestrial systems. By providing high-resolution meteorological data, it enables researchers to address critical questions related to water resources, food security, and climate resilience. In this study, we used GMFD to bias correct the global climate simulation datasets.

1.4.2 The Coupled Model Intercomparison Project Phase 6 (CMIP6) Dataset

The CMIP6 dataset is a cornerstone of climate science, providing a comprehensive framework for understanding past, present, and future climate dynamics. CMIP6 builds on the legacy of previous phases of the project, which began in 1995 under the auspices of the World Climate Research Programme (WCRP). It represents the most advanced and collaborative effort to date, involving climate modeling groups from around the world. CMIP6 is designed to address critical scientific questions about the Earth's climate system and its response to natural and anthropogenic forcings. The dataset underpins the Sixth Assessment Report (AR6) of the

Intergovernmental Panel on Climate Change (IPCC), making it a vital resource for policymakers, researchers, and educators. The CMIP6 dataset includes simulations from over 100 climate models developed by more than 50 institutions worldwide. These models simulate the Earth's climate system, including the atmosphere, oceans, land surface, and cryosphere, for historical climate and future climate under various scenarios called Shared Socioeconomic Pathways (SSPs). In this study, we used historical and future climate simulations (SSP 2-4.5) produced by 20 models shown in Table (1.3)

1.4.3 The Assessing Responses and Impacts of Solar Climate Intervention on the Earth System with Stratospheric Aerosol Injection (ARISE-SAI) Dataset

The ARISE-SAI dataset is an extensive collection of climate model outputs designed to assess the potential impacts of solar geoengineering through stratospheric aerosol injection (SAI). As part of a broader initiative, this dataset contributes to understanding the feasibility, risks, and implications of SAI as a strategy to combat global warming. By simulating various scenarios, the ARISE-SAI dataset offers valuable insights into how SAI could affect the Earth's climate system. The dataset is generated using the Community Earth System Model, version 2 (CESM2), combined with the Whole Atmosphere Community Climate Model, version 6 (WACCM6). This sophisticated modeling framework enables detailed simulations of interactions between the atmosphere, land, ocean, and cryosphere under different SAI deployment scenarios. It includes outputs for atmospheric, land, ocean, and sea-ice components, making it a versatile and critical resource for climate research. The dataset is structured around multiple simulation scenarios, each aimed at exploring specific aspects of SAI deployment (see Fig. 2.2). For this study, we utilized the ARISE-SAI-1.5 scenario, which implements stratospheric aerosol injection in the simulated year 2035, targeting a global mean surface air temperature of 1.5°C above pre-industrial levels. This scenario is based on the SSP2-4.5 emission pathway, representing a 'middle-of-the-road' approach to future socio-economic development.

1.3 Report Outline

The report is organized into five chapters. Following this introductory chapter (Chapter 1), Chapter 2 presents the analysis and results of the bias correction of climate simulation datasets. Chapters 3 and 4 delve into the potential impacts of climate change and SAG intervention on water yield, crop yield, and rangeland productivity, respectively. Finally, Chapter 5 provides the summary and conclusion.

Table 1.3: CMIP6 models downscaled in the NEX-GDDP dataset used in the project (Source: Bridget et al., 2022)

Models	**Variant**
ACCESS-CM2	r1i1p1f1
ACCESS-ESM1	r1i1p1f1

CanESM5	r1i1p1f1
CMCC-ESM2	r1i1p1f1
GFDL-CM4	r1i1p1f1
GFDL-ESM4	r1i1p1f1
HadGEM3-GC31-LL	r1i1p1f3
INM-CM4	r1i1p1f1
INM-CM5	r1i1p1f1
KIOST-ESM	r1i1p1f1
MIROC6	r1i1p1f1
MIROC-ES2L	r1i1p1f2
MPI-ESM1	r1i1p1f1
MPI-ESM1	r1i1p1f1
MRI-ESM2	r1i1p1f1
NESM3	r1i1p1f1
NorESM2-LM	r1i1p1f1
NorESM2-MM	r1i1p1f1
TaiESM1	r1i1p1f1
UKESM1	r1i1p1f2

Chapter 2. Bias correction of global climate model simulations

This chapter presents the application of the bias correction on the CMIP6 dataset and discusses the extent to which it improves the quality of the dataset.

2.1 Background

Global climate models (GCMs) are powerful tools for simulating climate systems. All past and future climate simulations in CMIP6 are built on GCMs. However, numerous studies have shown that the outputs of these models can differ significantly from observational data, primarily due to their coarse spatial resolution (Maraun, 2016; Randall & Fichefet, 2007). For example, the horizontal resolution of most CMIP6 simulations is 2°, which is too coarse for direct use in regional-scale studies. As a result, GCM outputs are typically statistically bias-corrected and downscaled before being applied to climate impact simulations (Ehret et al., 2012; Maraun, 2016).

While bias-correction methods statistically match GCM simulations to observation data to remove systematic biases in the simulations, the statistical downscaling methods transform the coarse-scale GCM simulations to a much finer scale through trained transfer functions (Li et al., 2010). Several bias-correction and statistical downscaling methods have been well documented and used in literature (Bürger et al., 2010; Werner & Cannon, 2016). However, some sophisticated bias-correction methods can also downscale GCM simulations. An example of suchmethod is the Bias Correction and Spatial Disaggregation (BCSD) method introduced by Wootten et al.(2021). The BCSD first unifies GCM and observation datasets into the same grid by interpolation. Then it removes the average, variation, and tendency biases in GCM outputs by adjusting their average and probability distribution. Finally, it transforms the coarse spatial resolution of the GCM to the required resolution through interpolation. The downscaling error of BCSD is usually within the range allowed in most hydrological models such as variable infiltration capacity (Bürger et al., 2010; Werner & Cannon, 2016). This makes BCSD popular and widely used, especially in coupling GCMs with hydrological models. Therefore, we used BCSD for statistical bias correction and downscaling of climate simulations in this project.

The CMIP6 simulations were downscaled and biased corrected by the National Aeronautics and Space Administration (NASA), who made the high-resolution and bias-corrected dataset publicly available as the Global Daily Downscaled Projections (NEX-GDDP-CMIP6, hereafter NEX-GDDP) dataset (https://registry.opendata.aws/nex-gddp-cmip6/). Detailed descriptions of how the NEX-GDDP was generated are given in Thrasher et al (2022). The statistical downscaling algorithm used to create the NEX-GDDP dataset is a daily variant of the monthly (BCSD) method described in Wood et al.(2002). A single variant from each of the 20 models (Table 1.3) listed was used for the dataset. The historical experiment was downscaled over the years 1950–2014, while the SSP experiments were downscaled over the years 2015–2100.

2.2 Performance of CMIP6 and Bias corrected datasets (NEX-GDD) in Africa

The NEX-GDDP dataset was developed to support the scientific community in studying the impacts of climate change at local to regional scales and to enhance public understanding of future climate patterns at the level of individual towns, cities, and watersheds (Thrasher et al., 2022). While the dataset has undergone a quality control process, Bridget et al. (2022) highlighted the importance of regional and local evaluations before using it for climate impact studies. Therefore, we found it essential to evaluate the performance of the NEX-GDDP dataset over Africa and several river basins across the continent. This evaluation involved comparing the performance of the NEX-GDDP dataset against the original CMIP6 dataset to determine how effectively the BCSD method improves the quality of CMIP6 simulations.

Twelve major river basins within the African region were selected for evaluation (Fig. 2.1). These are the largest and most transboundary basins in Africa, making them excellent representatives of other river systems across the continent. Their sizes vary greatly, from the Ogooué Basin, spanning 223,400 square kilometers, to the vast Congo Basin, covering 3,699,100 square kilometers. The number of countries sharing these basins also differs significantly, ranging from three nations for the Juba-Shibeli Basin to 11 for the Nile Basin. Similarly, the population living within these basins varies, with the Okavango Basin hosting 800,000 people, while the Nile Basin is home to a staggering 280 million inhabitants. These 12 basins are vital for driving socio-economic activities such as agriculture, mining, power generation, and industrial development in their respective regions. They play an essential role in supporting sustainable development across Africa. For instance, the Zambezi and Limpopo Basins attract visitors worldwide, offering breathtaking sites like Victoria Falls and opportunities to see iconic wildlife like the "Big Five" in Kruger National Park. Meanwhile, the Lake Chad Basin supports local communities by providing water for farming, fishing, and grazing. The Nile Basin is a cornerstone for agricultural productivity, irrigating more than 5.5 million hectares of land, with the potential to expand this coverage to 10.4 million hectares. The Niger Basin contributes significantly to energy generation, producing 7,000 GWh of hydropower, with an untapped potential of up to 30,000 GWh. However, these basins face critical challenges. Drought continues to drive desertification, degrade land, exacerbate poverty, and spark conflicts over dwindling resources. Given the broad scope of this study, this report focuses on the results for three key Southern African river basins: the Limpopo, Orange, and Okavango.

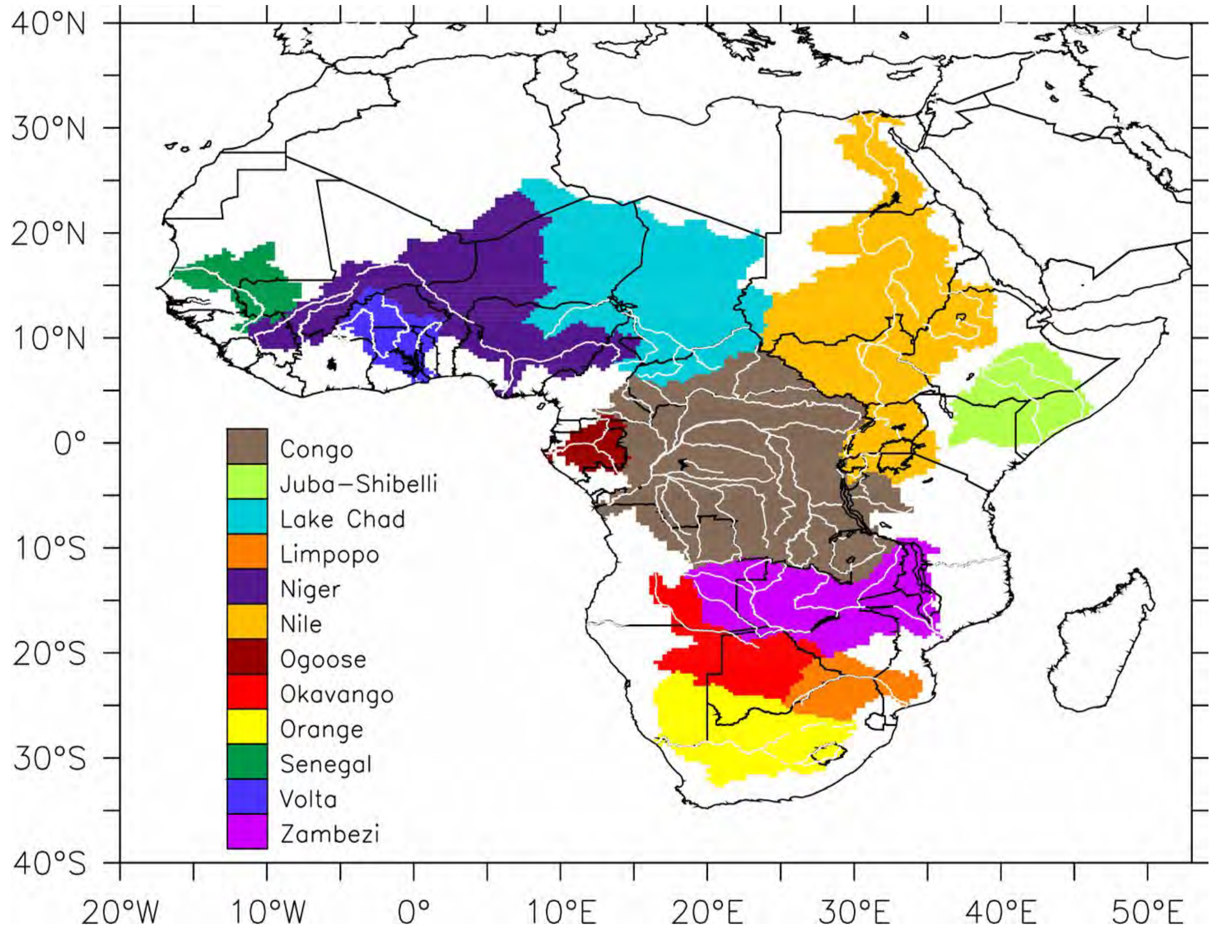

Figure 2.1: Map of Africa showing the 12 major river basins used in the project. The white lines on the basins show the rivers.

2.2.1 Spatial distribution of climate variables over Africa

The bias correction (i.e., BCSD) method improves the spatial distribution of the simulated climate variables (temperature and precipitation) over Africa (Figs. 2.2-2.4). Although the original CMIP6 ensemble features realistic spatial distribution of the variables over the continent (as evidenced by the high correlation values; r ≥ 0.9), there are substantial biases in the simulations (Figs. 2.2-2.4). For instance, the root mean squares (RMSEs) error is ≥ 2^{o}C for the maximum and minimum temperature (Tmax and Tmin) and ≥ 20 mm/month for the precipitation. Due to the implementation of the BCSD, the RMSEs are much lower in the NEX-GDDP dataset. More specifically, the BCSD lowers the cold bias in Tmax and warm bias in Tmin 0.2^{o}C (Fig. 2.2 and 2.3), meaning that it increases the diurnal range of the simulated temperature and brings it closer to the GMFD observation. It also removes the dry bias in simulated precipitation over southern Africa (Fig 2.3). Furthermore, it reduces the inter-model differences as shown in the Taylor diagrams (Fig. 2.5).

All these corrections will have good implications in hydrology, crop and vegetation simulations. For example, the increase in precipitation and the diurnal temperature over southern Africa would foster a more realistic simulation of potential evapotranspiration, climate water balance, evaporation, and soil moisture over the sub-continent. The extent to which the correction improves the quality of other climate and climate-impacts variables will be quantified in subsequent studies in the project.

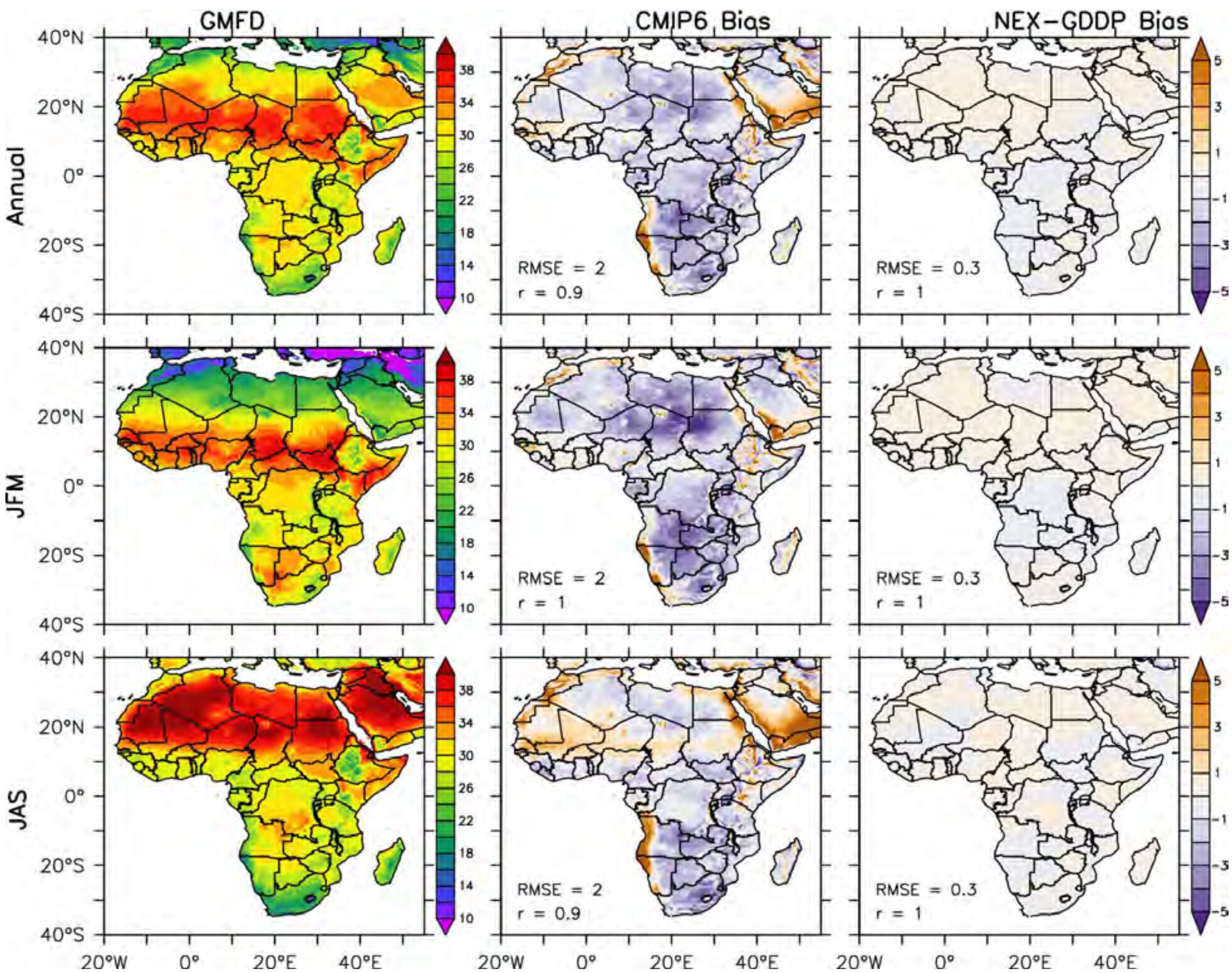

Figure 2.2: The influence of NEX-GDDP bias correction on CMIP6 simulated maximum temperature (Tmax, °C) over Africa (1970 - 2000). The first, second, and third rows show the annual, January-March (JFM), and July-September (JAS) mean, respectively. The first column (GFMD) shows the reference data while the second and third columns (CMIP6 and NEX-GDDP) show the bias in CMIP6 simulations before and after the bias correction, respectively. The root-mean-square error (RMSE) and the spatial correlation (r) of the simulations with reference to GMFD results are indicated.

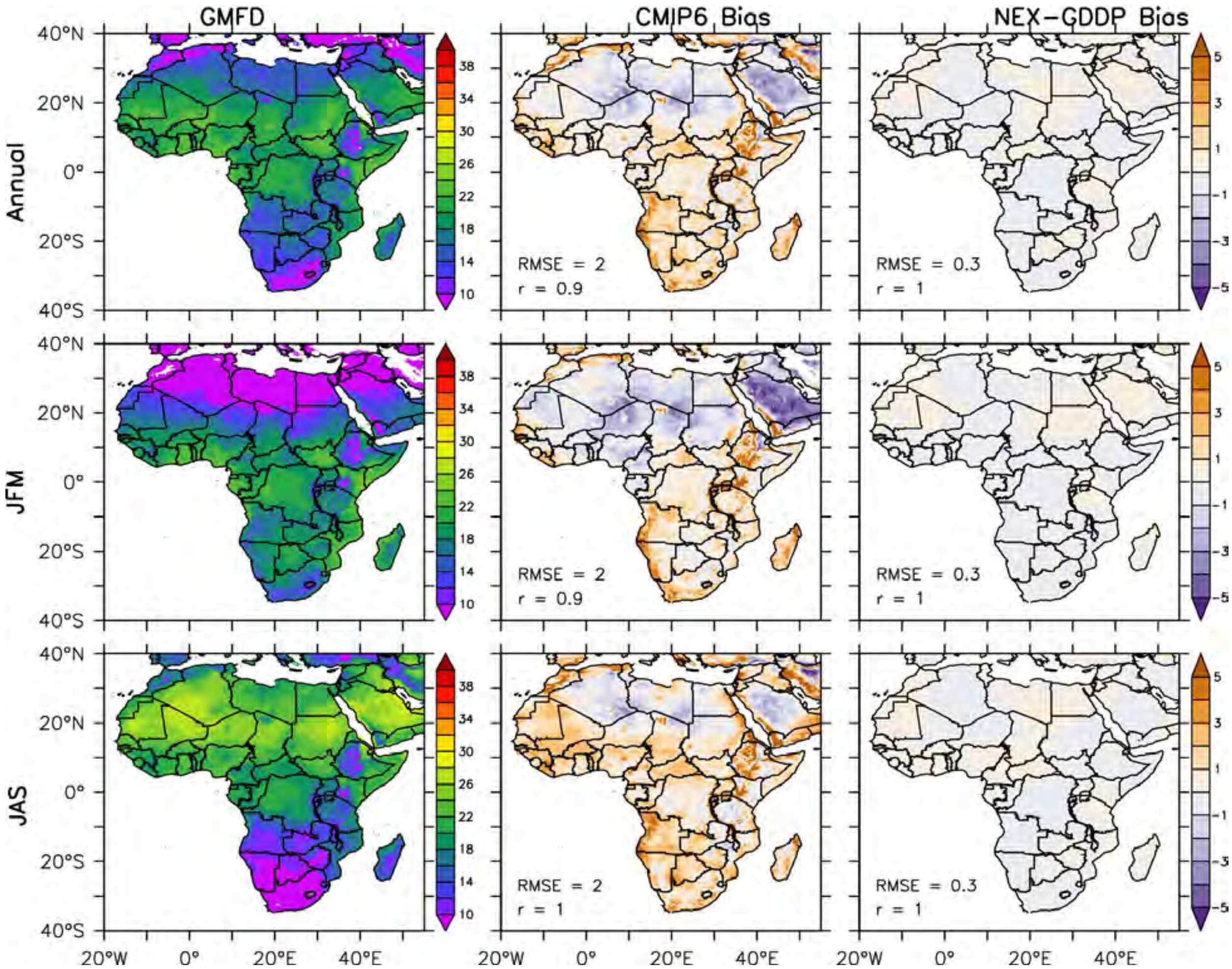

Figure 2.3: Same as Figure 2, but for minimum temperature (Tmin, °C).

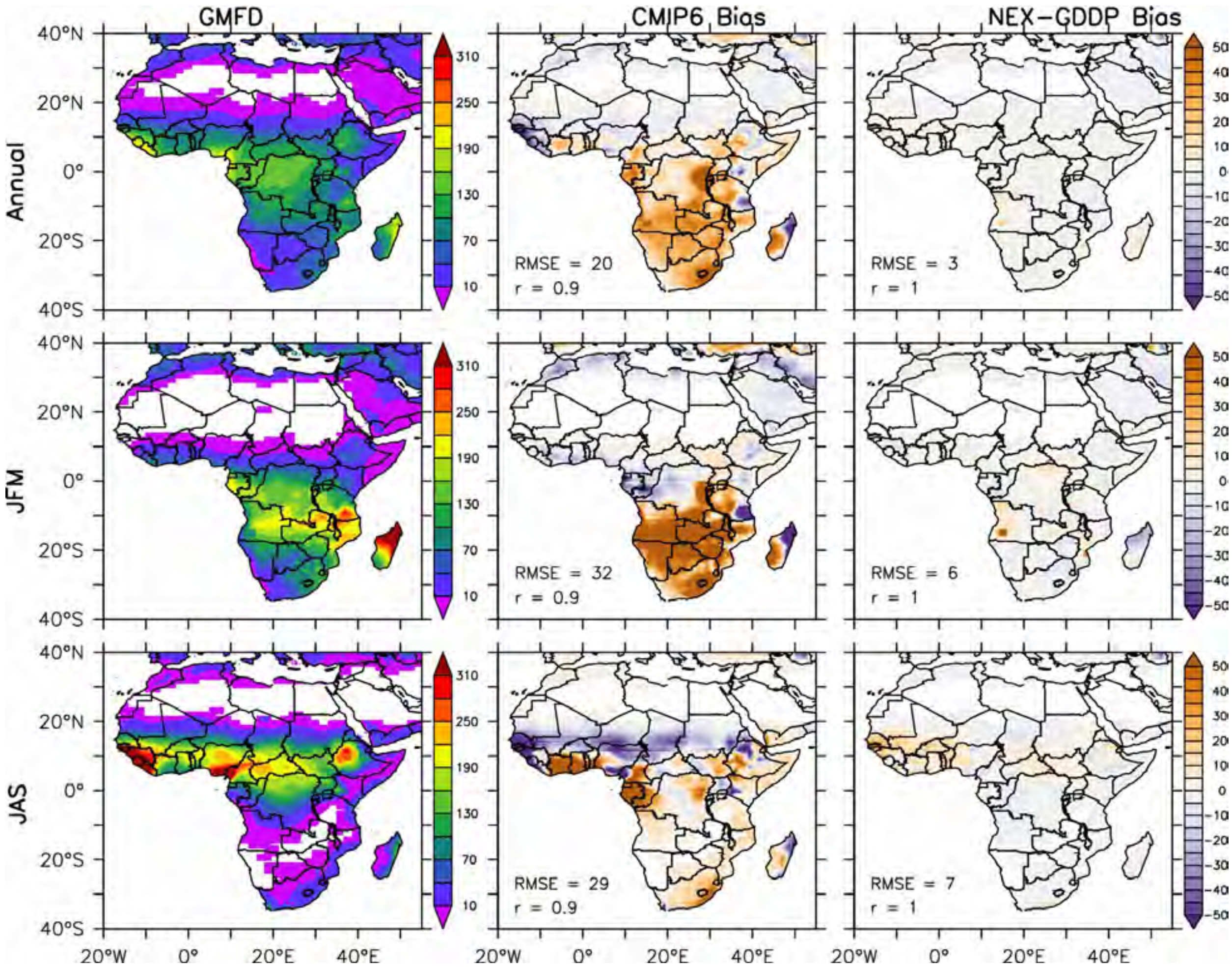

Figure 2.4: Same as Figure 2, but for precipitation (mm/month)

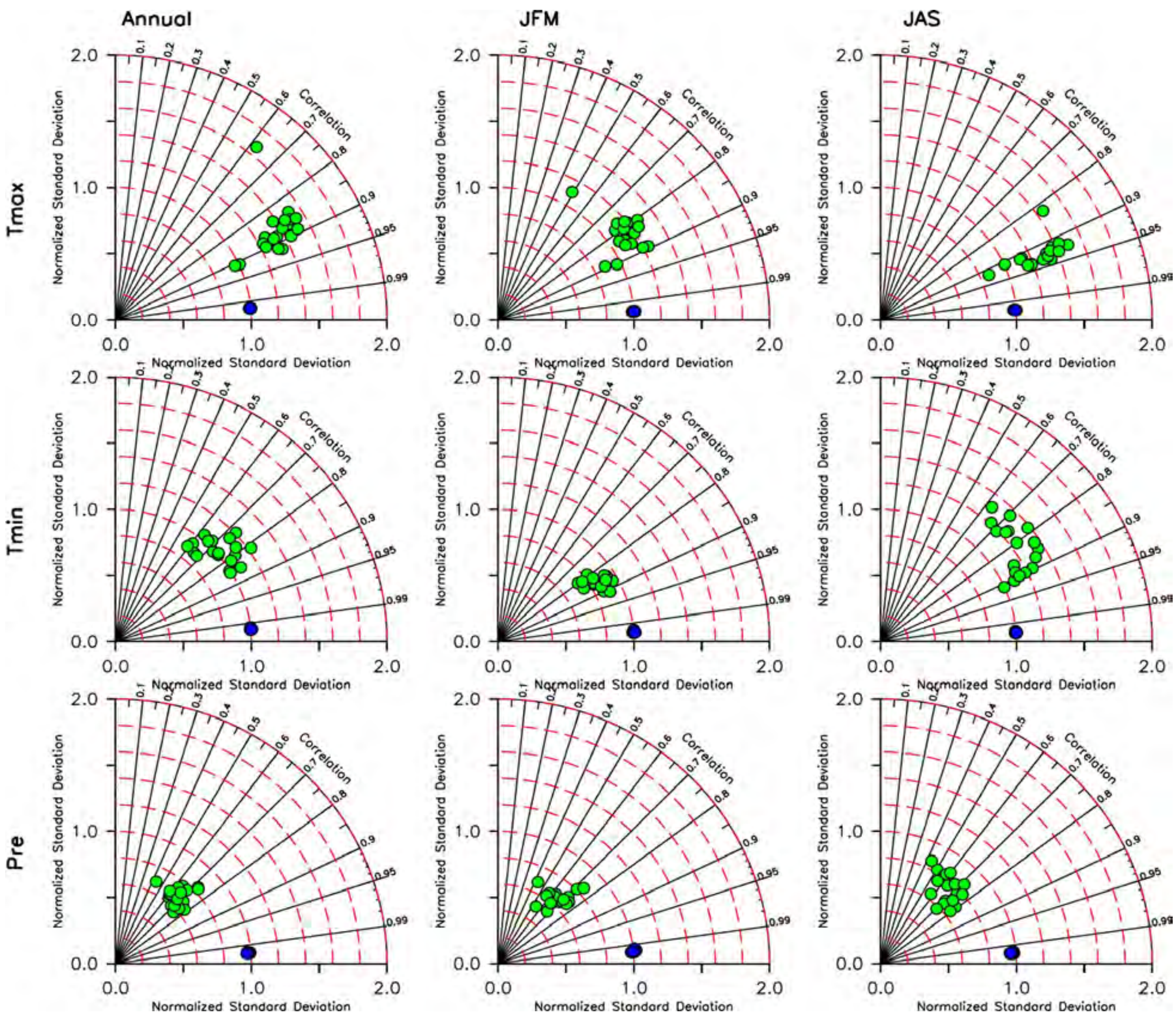

Figure 2.5: Taylor diagram showing the performance of CMIP6 maximum temperature (Tmax), minimum temperature (Tmin), and precipitation (Pre) simulations over Africa before (green dots) and after (blue dots) the NEX-GDDP bias correction, in terms of normalized standard deviation and spatial correlation of the simulations with reference to GMFD.

2.2.2 Annual cycle of climate variables over the basins

The bias correction also improves the annual cycles of the climate variables over the basins (Figs. 2.6-2.8). As expected, the original CMIP6 dataset gives credible simulations of the annual cycles but with huge biases (up to 10^{o}C for temperature and > 80 mm month^{-1} for precipitation). The direction of the biases differs across the variables, fluctuates with months, and varies among the models. However, the bias correction drastically reduces the magnitude of the bias for all the variables (to less than 10^{o}C for temperature and < 20 mm month^{-1} for precipitation). In addition, it reduces the spread of the simulation ensemble members and makes the ensemble mean to follow the GMFD results more closely. This is expected to enhance the simulations of hydrological and plant-physiological processes as well as reduce the level of uncertainty in the simulations. The extent to which this happens will be quantified later in the project.

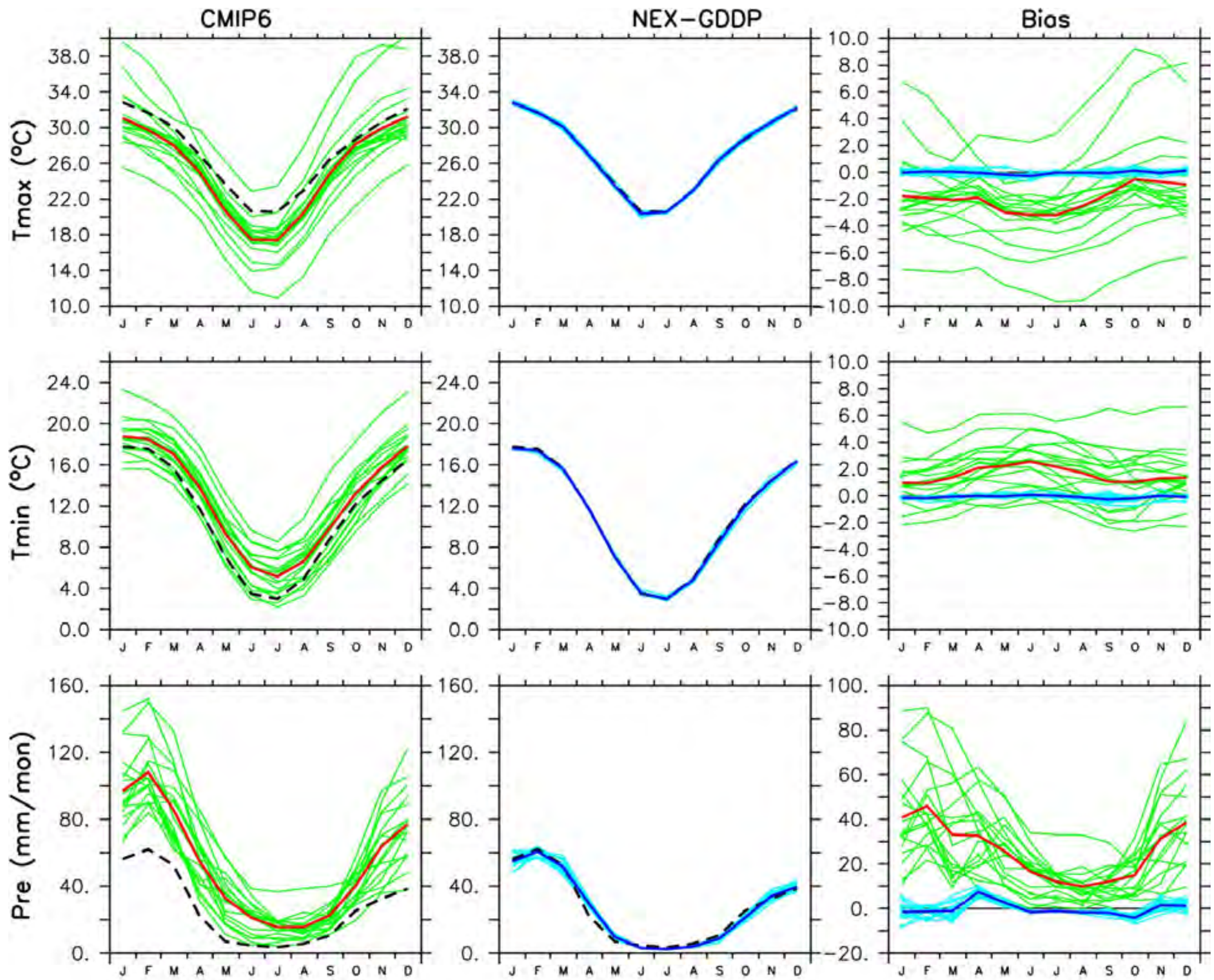

Figure 2.6: Comparison of CMIP6 simulated maximum temperature (Tmax), minimum temperature (Tmin), and precipitation (mm month^{-1}) climatology before and after the NEX-GDDP bias correction (CMIP6 and NEX, respectively) over the Limpopo River basin. The last column shows the associated biases. The thick black dashed lines show the GMFD results. The thick red and blue lines show the ensemble mean of CMIP6 simulations before and after the bias correction (respectively) while the thin green and red lines show the corresponding individual simulations.

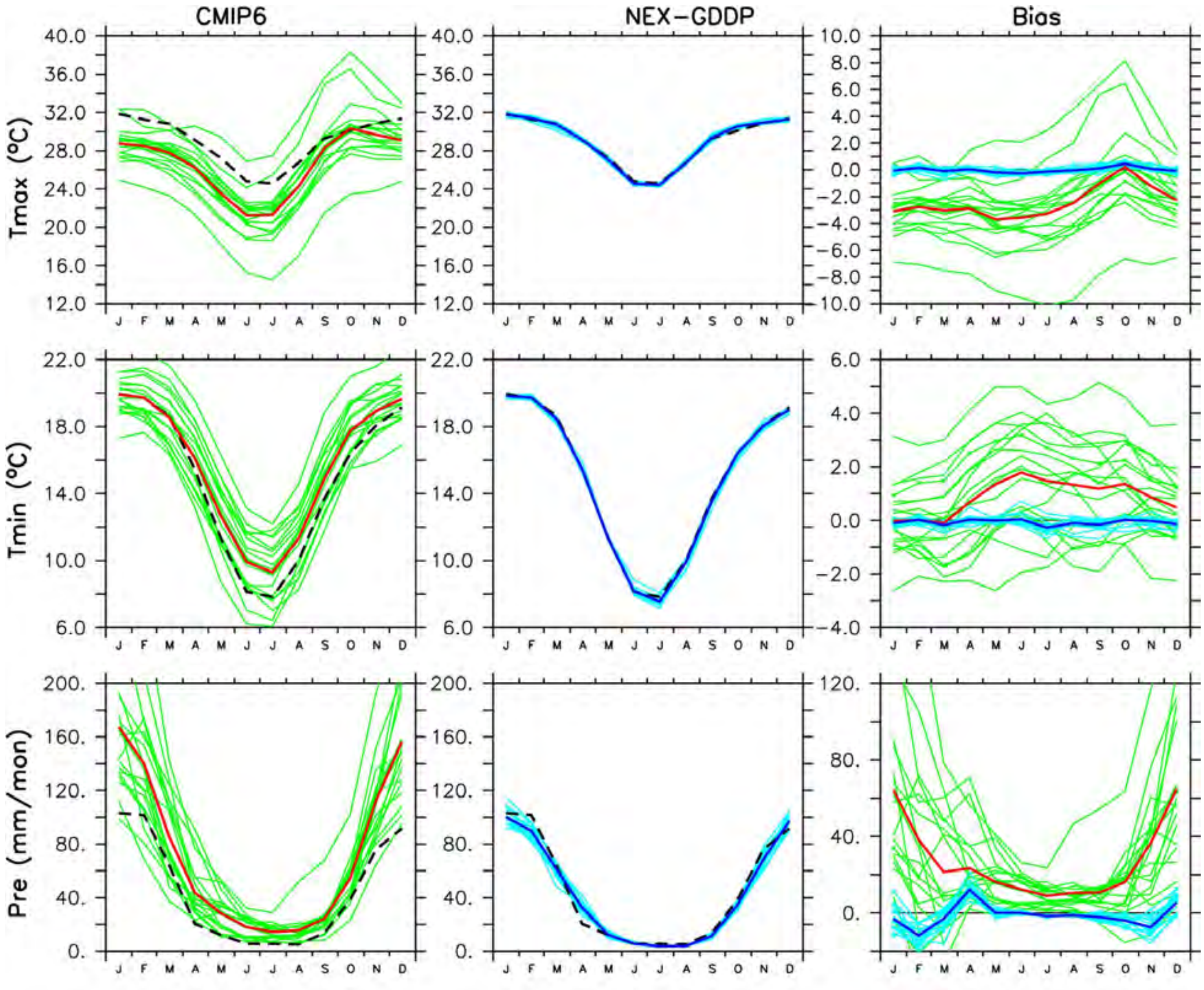

Figure 2.7: Same as Figure 6 but for the Orange River basin.

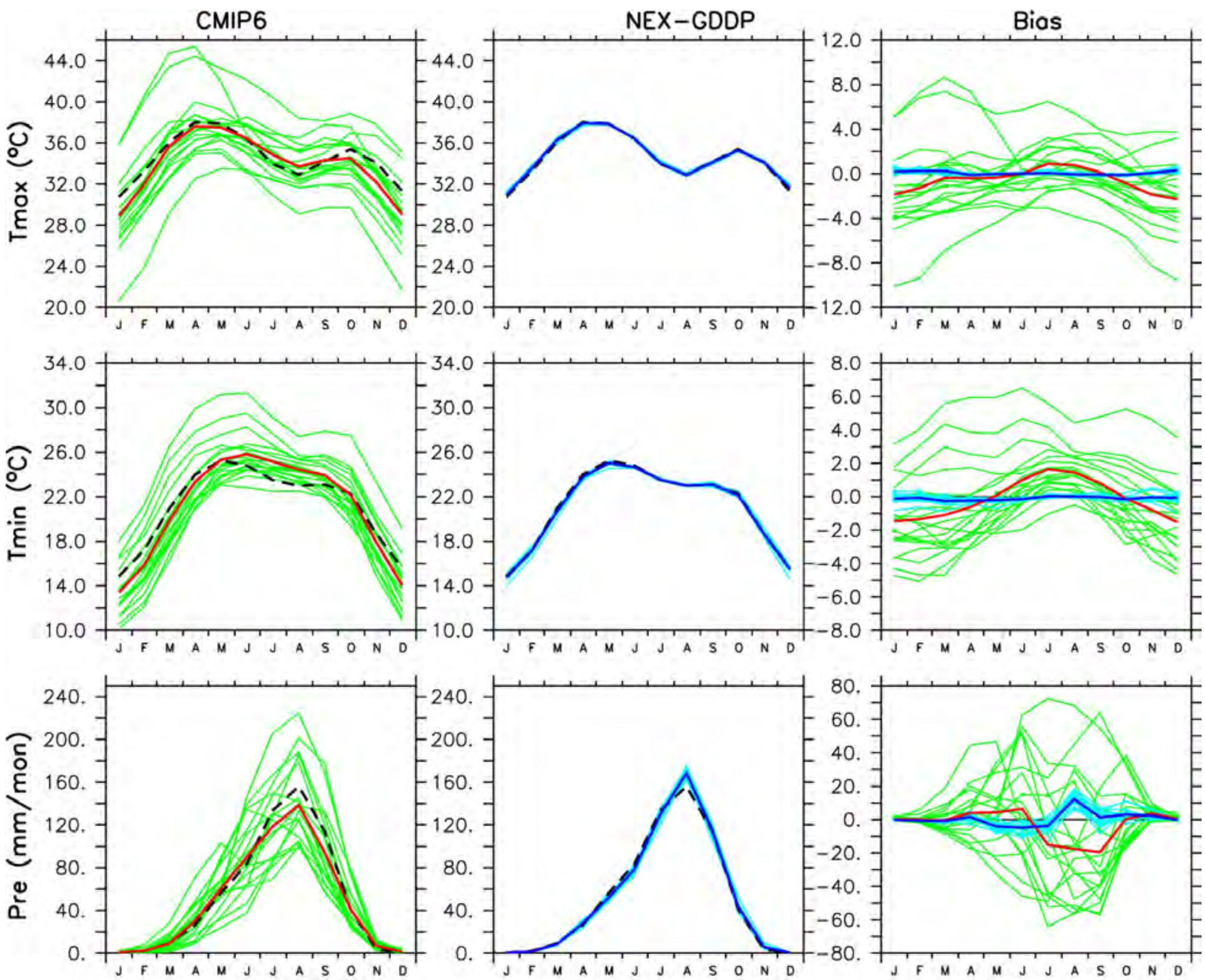

Figure 2.8: Same as Figure 6 but for the Okavango River basin.

2.2.3 Relationship among the climate variables over the basins

BCSD is an example of a univariate bias-correction method, which adjusts climate variables independently of one another. However, this approach does not account for spatial and inter-variable correlations between variables (Wilcke et al., 2013). These correlations, such as the relationship between air temperature and precipitation, are crucial when modeling multivariate drought indices like the Standardized Precipitation Evapotranspiration Index (SPEI) (Cannon, 2016).

Research has demonstrated that while univariate quantile mapping preserves the inter-variable dependencies present in the raw climate model output data, it may not fully capture the localized interdependencies observed in real-world data (Wilcke et al., 2013). Therefore, it becomes important to evaluate how BCSD manages these inter-variable dependencies within the river basins studied. Figures 2.9 through 2.11 illustrate that BCSD modifies the simulated inter-variable relationships and, in most cases, brings them closer to the observed relationships.

Overall, the scatter-plot patterns generated using NEX-GDDP show a stronger alignment with observed data compared to the original NEX-GDDP outputs. Additionally, the plots appear more clustered in the NEX-GDDP data after BCSD correction compared to those from CMIP6 simulations.

Encouraged by these promising results, we applied BCSD to bias-correct the global climate datasets used in this study (Table 1.1). The corrected climate data was then utilized to drive simulations for crops and rangelands.

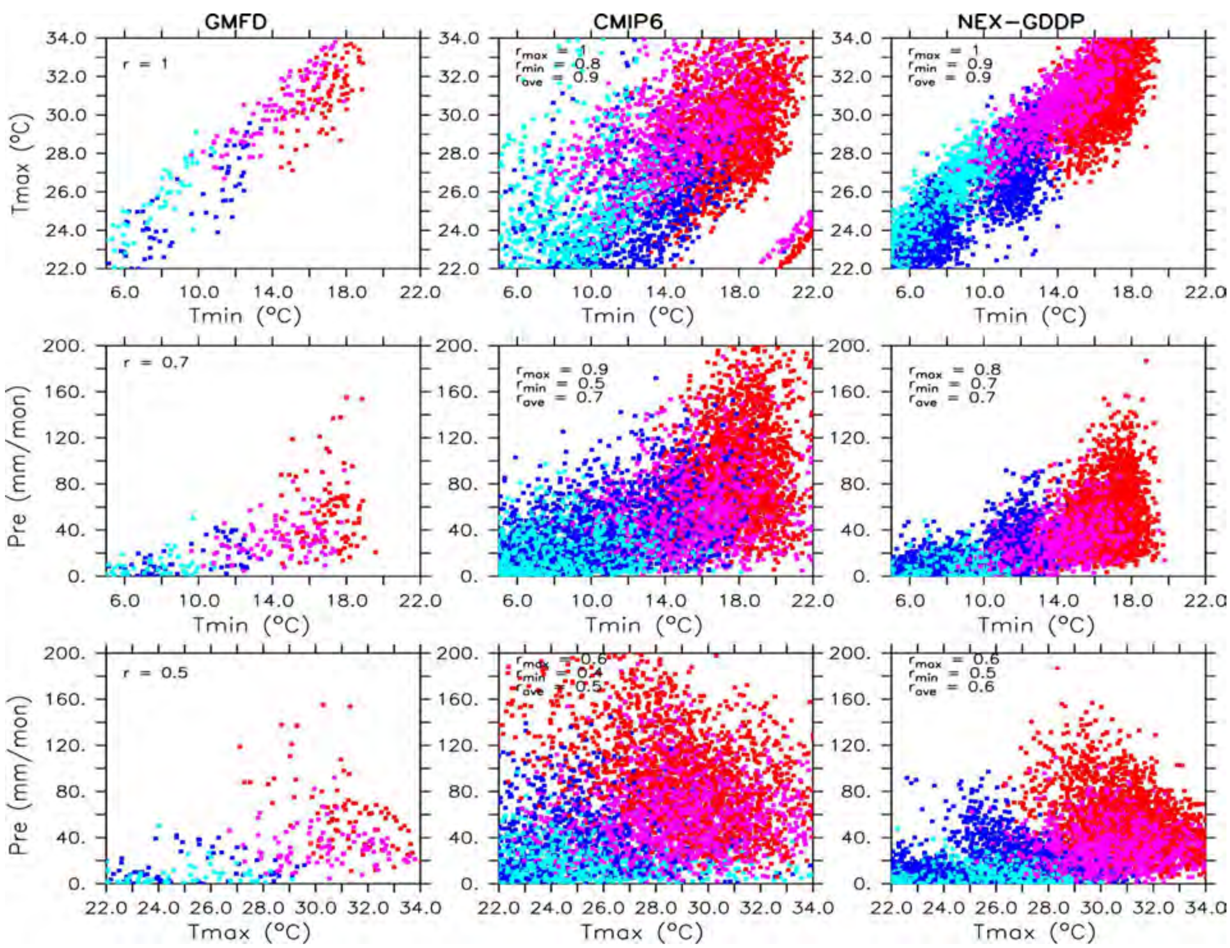

Figure 2.9: Scatter plots showing the correlations among the monthly mean of the climate variables (Tmax, Tmin and Pre) over the Limpopo River basin. Different colours show the results for different seasons: December-January-February (DJF, red); April-May-June (AMJ, blue), July-August-September (JAS, light blue), October-November-December(OND, purple).

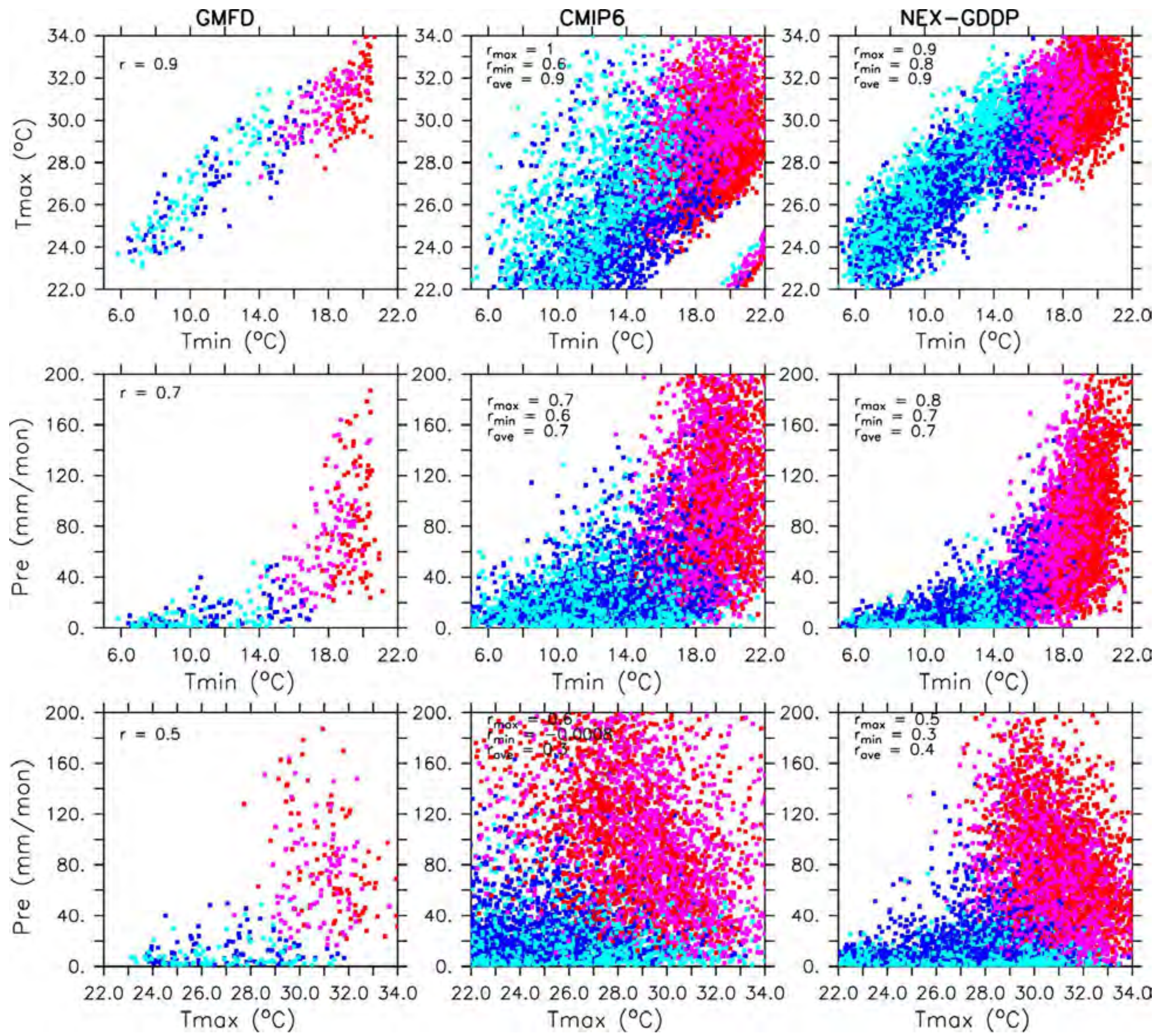

Figure 2.10: Same as Figure 9 but for the Orange River Basin.

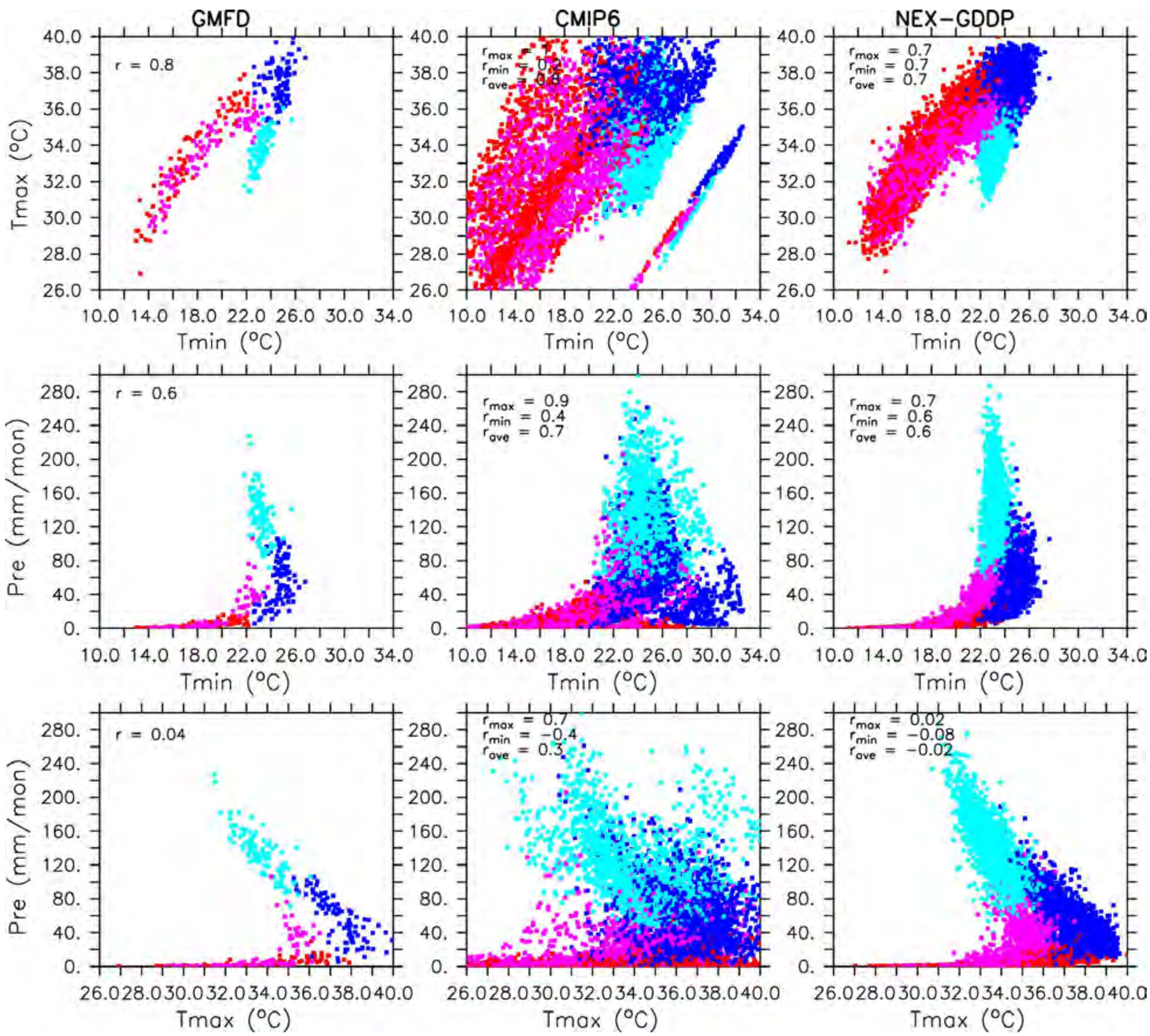

Figure 2.11: Same as Figure 9 but for the Okavango River basin.

Chapter 3: Potential impacts of climate change and SAG on water yield in Africa

This chapter reports our study on impacts of climate change and stratospheric aerosol injection (SAI) or stratospheric aerosol geoengineering (SAG) on water yield in Africa.

3.1 Methodology

We analyzed the ARISE-SAI simulation datasets and examined the impacts of climate change and Solar climate intervention on water yield across 10 major river basins in Africa (Fig 3.1). The ARISE-SAI simulation datasets are already described in Chapter 2. Water yield is defined as the amount of freshwater generated from base flow, interflow, and overland flow originating from groundwater and precipitation within a watershed. It is one of the model output variables in the ARISE-SAI dataset.

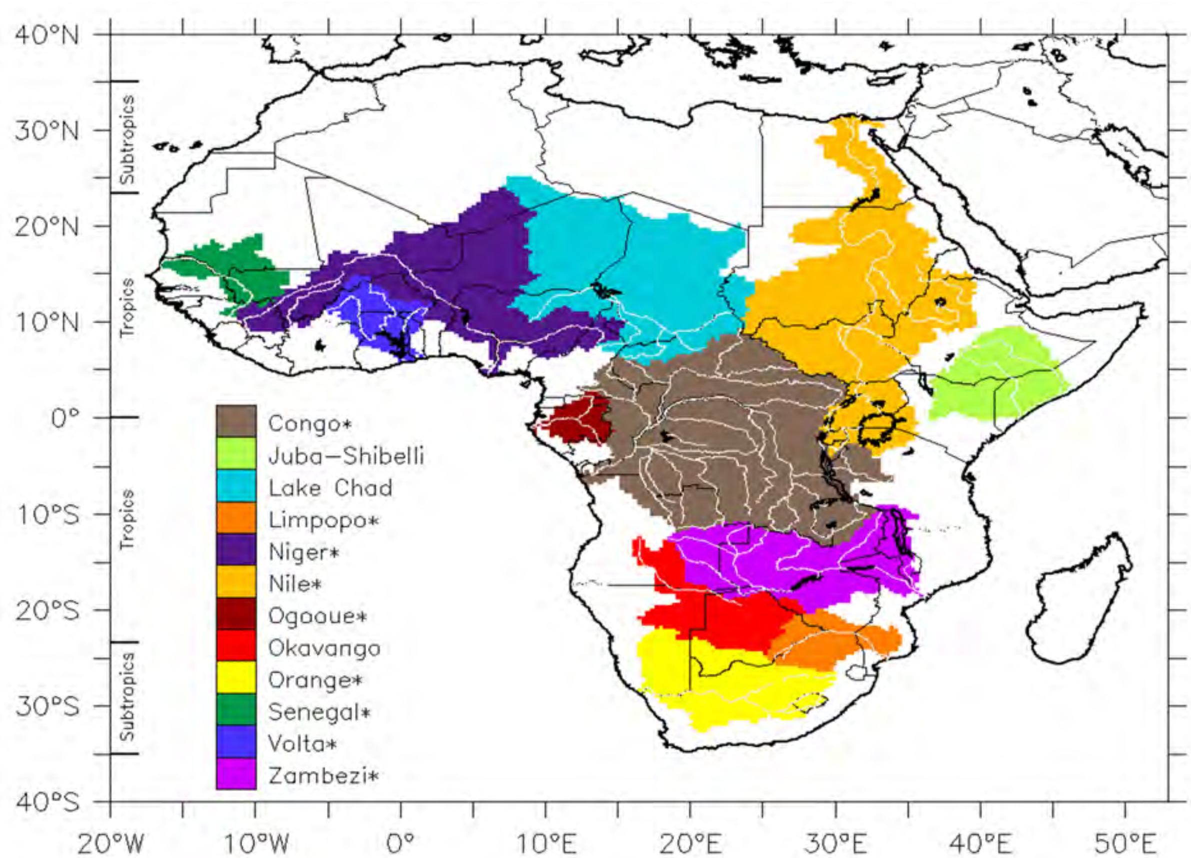

Figure 3.1: Map of Africa showing the major river basins in Africa. The selected 10 river basins used in the study is indicated with asterisk (*). Modified after Abiodun et al., (2021).

Three ARISE-SAI simulation dataset were analyzed in this study. The first dataset (PRS) provides present-day climate simulation (2017 - 2032). The second dataset (CC) simulates future climate (2049 - 2069) under the SSP2-4.5 scenario. The third dataset (SAI) simulates future climate (2049

- 2069) with the implementation of SAI. The difference between CC and PRS (CC minus PRS) depicts the impacts of climate change relative to the present day. The difference between SAI and PRS (SAI minus PRS) indicates the impacts of SAI implementation relative to the present day. The difference between SAI and CC (SAI minus CC) depicts the impact of SAI implementation relative to the SSP2-4.5 warmed world.

Figures (3.2) and (3.3) present the results of the analysis for evaporation, precipitation, resulting net water flux (evaporation minus precipitation), and river basins. The net water flux is a good indicator of freshwater availability in a region because it shows whether the region is experiencing a net loss or gain of water from the atmosphere. A positive value means more water is evaporating than precipitating, leading to a net loss of freshwater, while a negative value indicates the opposite.

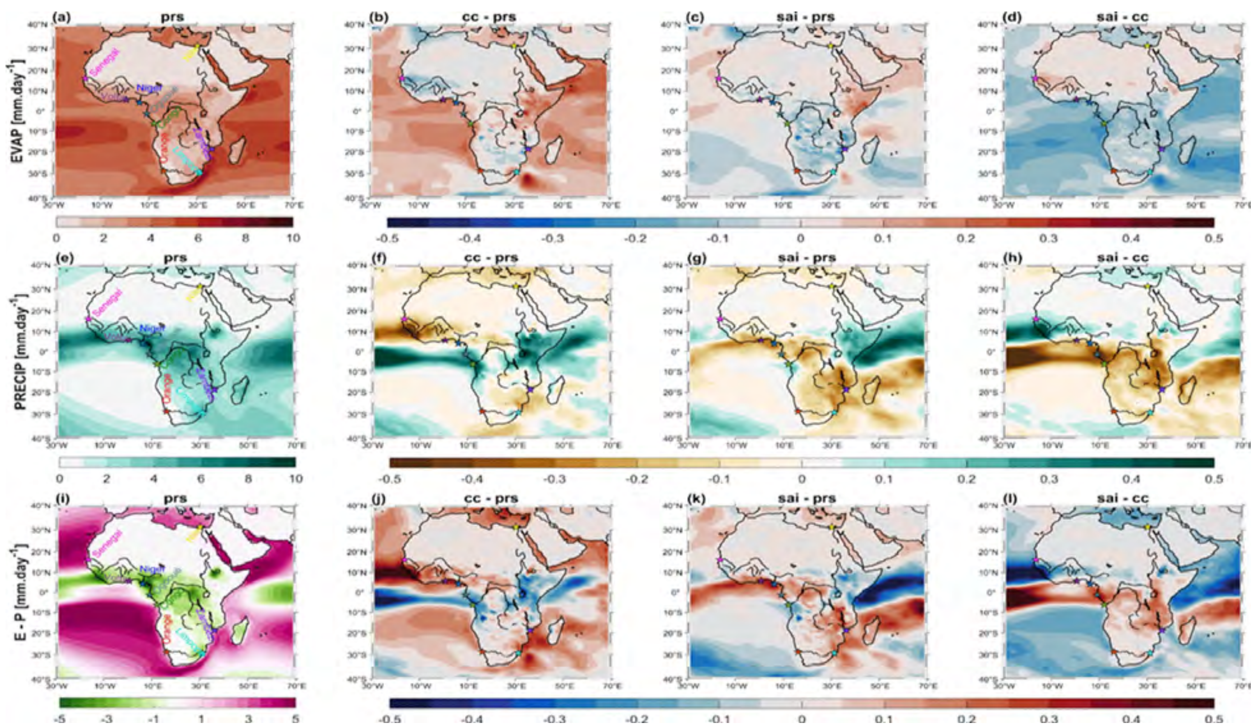

Figure 3.2: The spatial distribution of evaporation (upper row), precipitation (middle row) and evaporation minus precipitation (lower row) over Africa during the present-day (prs) and the potential changes due climate change (cc) and stratospheric aerosol injection (sai).

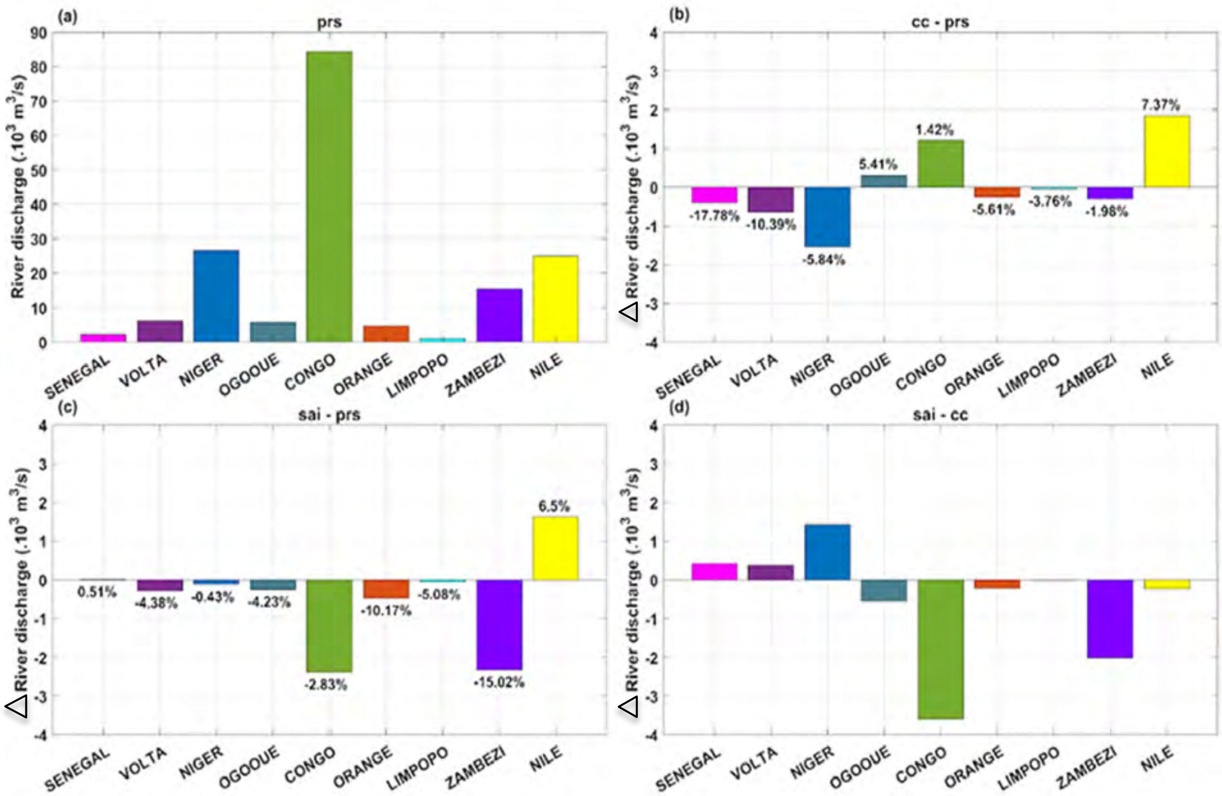

Figure 3.3: Water yield in the selected 10 river basins in Africa and the projected changes (Δ) due climate change (cc) and stratospheric aerosol injection (SAI).The percentages of these river discharge changes related to the present-day climate are shown in Figures 3.3.b and 3.3.c

3.2 Impacts of Climate Change on Freshwater

Climate change is projected to reduce freshwater availability across most parts of Africa, except in East and Central Africa, where an increase is expected. These changes come primarily through changes in precipitation, which indirectly influence evaporation rates. In West and Southern Africa, climate change causes a decrease in both precipitation and evaporation. However, since the reduction is greater for precipitation than for evaporation, the net result is a freshwater deficit. Conversely, in East and Central Africa, a freshwater surplus occurs because the increase in precipitation exceeds that of evaporation. This increase in precipitation is potentially associated with the intertropical convergence zone, which regulates rainfall across the entire equatorial region.

The projected changes in freshwater availability influence water yield in the selected 10 river basins, which represent the major rivers across Africa that flow into oceans. The figure indicates that climate change enhances water yield in the Congo, Ogooue, and Nile Basins (by 1.42%, 5.41%, and 7.1%, respectively) but reduces it in the other seven basins (by 2.0 - 17.78%). This is not unexpected because the Congo and Ogooue Basins reside in Central Africa, where a freshwater surplus is projected, and the Nile Basin has its tributaries in East Africa, where a freshwater surplus is projected. In contrast, other basins reside in West or Southern Africa, where freshwater deficits are expected.

3.3 Impacts of Stratospheric Aerosol Injection

Figure (3.2) shows that while SAI mitigates the impacts of climate change in some instances, it can overcompensate for or enhance the impact in others. For example, while it offsets the freshwater deficit in West Africa, it reverses the freshwater surplus in parts of Central and East Africa and exacerbates the freshwater deficit in Southern Africa. Consequently, SAI negates the positive influence of climate change on the water yield in the Congo and Ogooue Basins, resulting in a net reduction in water yield with respect to the present-day climate. It also lowers the projected increase in the water yield over the Nile Basin by about 1%. Nevertheless, with respect to climate change, it enhances the water yield in the Senegal, Volta, and Niger Basins while reinforcing the decreasing water yield in the Zambezi Basin. It is essential to view these results in light of our previous studies, in which we analysed other SAI datasets under different scenarios to provide information on how SAI could alter impacts of climate change over river basins in Africa (e.g., Abiodun et al. (2021; 2024) and Fotso-Nguemo et al. (2024)).

In Abiodun et al. (2021), we investigated how the SAI (Stratospheric Aerosol Injection) intervention could mitigate the effects of RCP8.5 warming on drought characteristics across the 12 largest and most transboundary river basins in Africa (as shown in Fig. 3.1). The analysis utilized two climate simulation datasets from the GLENS Project—control and feedback scenarios. To identify and characterize droughts in these basins, we employed two drought indices: the Standardized Precipitation Index (SPI) and the Standardized Precipitation Evapotranspiration Index (SPEI). While SPI is solely based on precipitation to characterize drought conditions, SPEI considers both precipitation and Potential Evapotranspiration (PET), making it a more comprehensive measure. The gap between the projections for SPEI and SPI was used as an indicator of the impact of enhanced atmospheric evaporative demand driven by RCP8.5 warming on drought projections. This gap not only highlights the range of uncertainty in future drought conditions but also points to opportunities for mitigating drought risks within these basins. The findings of the study suggest that SAI intervention may counteract the effects of climate change on temperature and atmospheric evaporative demand (Fig 3.4). However, a significant observation is that while sufficient SAI levels to compensate for temperature changes would overcompensate for precipitation impacts, this could result in a climate water balance deficit in tropical regions. Furthermore, the study shows that SAI intervention narrows the gap between SPEI and SPI projections. This is achieved by reducing SPEI drought frequency through lower temperatures and reduced atmospheric evaporative demand, while simultaneously increasing SPI drought frequency due to decreased rainfall. This narrowing of the gap reduces the level of uncertainty concerning future changes in drought frequency. Importantly, these findings have significant implications for future drought management within the basins. While SAI may lower the upper limit of future drought stress, it simultaneously raises the lower limit. This dual effect underscores the need for careful and adaptive strategies to manage drought risk in these critical areas.

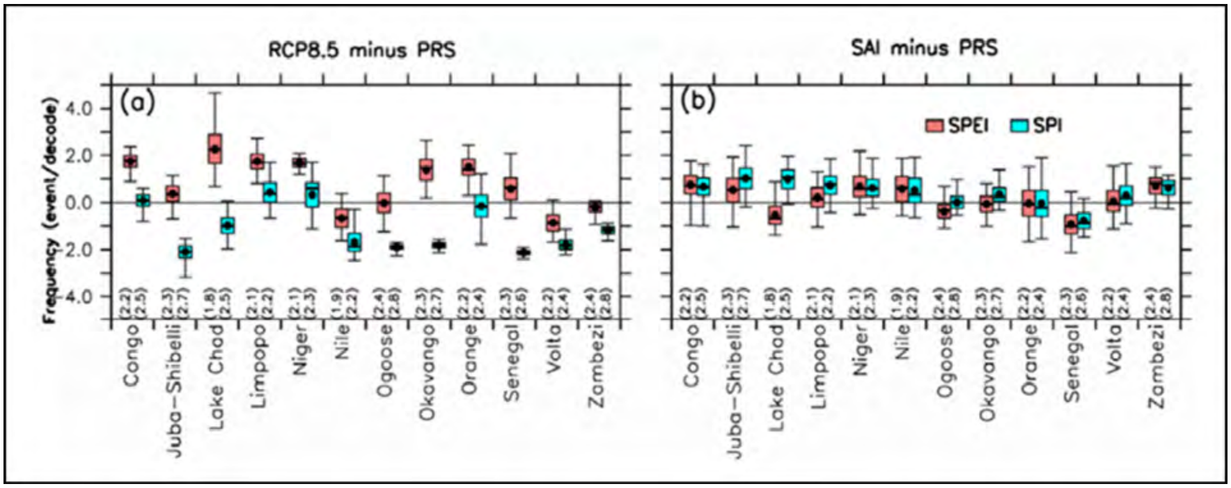

Figure 3.4: Projected changes in frequency of SPI and SPEI moderate droughts over the major river basins in Africa. Modified after Abiodun et al. (2021)

Fotso-Nguemo et al. (2024) examined how SAI (Stratospheric Aerosol Injection) could influence water availability across four major river basins in Central Africa: the Niger Basin, Lake Chad Basin, Cameroon Atlantic Basin (CAB), and Congo Basin (CB). To conduct this analysis, the study defined a potential water availability index as the ratio of precipitation to potential evapotranspiration. This index was calculated using climate data from the ensemble-mean simulations in Phase 6 of the Geoengineering Model Intercomparison Project. The study focused on two Solar Radiation Management (SRM) simulation experiments: stratospheric sulfate aerosol injection (G6sulfur) and global solar dimming (G6solar). The findings revealed a significant reduction in water availability—up to 60%—particularly in the CAB under high radiative forcing scenarios by the end of the 21st century (Fig. 3.5). However, SAI methods demonstrated the potential to significantly alleviate this deficit, increasing water availability by as much as 50% in the affected river basins. Notably, the CAB showed the greatest improvement when global solar dimming was applied. Our findings in Fotso-Nguemo et al. (2024) align with existing studies, suggesting that while SAI can mitigate some water availability deficits, it may exacerbate these issues in specific regions, such as the Congo Basin.

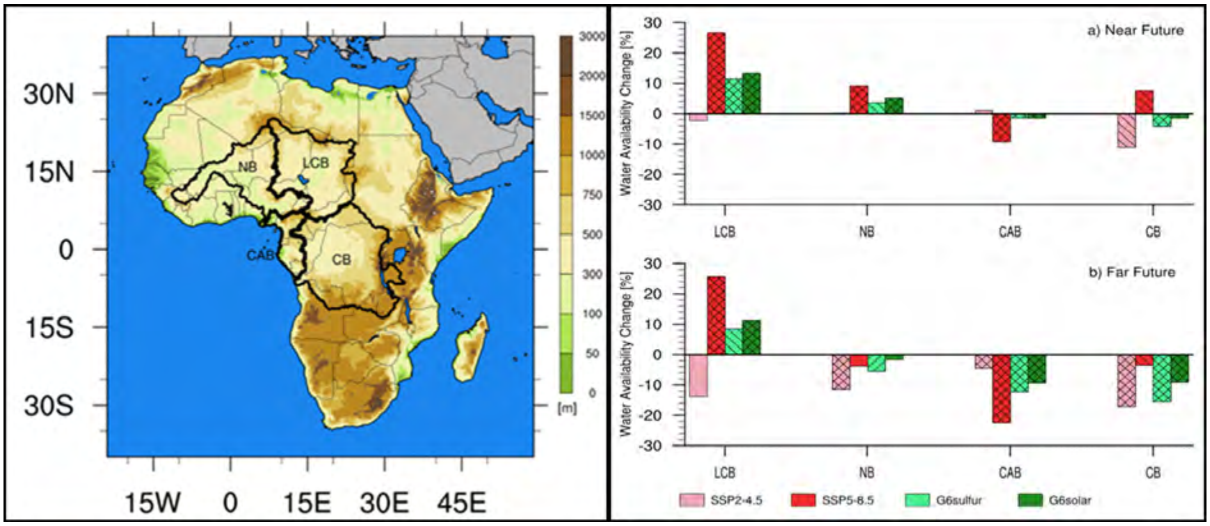

Figure 3.5. Left Panel: Mean topography (in meter; shaded) of the African domain, Outlines in bold delineate the contour of the main Central African river basins, including: Niger Basin (NB), Lake Chad Basin (LCB), Cameroon Atlantic Basin (CAB) and Congo Basin (CB). Right Panel B: Changes in the annual potential water availability index (in %, with respect to the 1985–2014 baseline period). Modified after Fotso-Nguemo et al. (2024).

3.4 Implication for stakeholders and policy makers

Our findings have several implications for river basin stakeholders and policymakers. The findings highlight the complexity and potential trade-offs of using SRM techniques and argue for careful consideration and planning when implementing SRM techniques to manage climate change impacts on water resources in Africa. Given that SRM can alter water yield differently across Africa, river basin policy makers in African countries will need to cooperate to manage the shared water resources responsibly, ensuring that any SRM activity does not unfairly impact one country's water supply or lead to political tensions. There is a need for transnational agreements that ensure that the implementation of SRM technologies is coordinated and includes mechanisms for resolving conflicts related to water resource sharing.

Policymakers will need to prioritize investments in climate change adaptation, especially in river basins that could face increasing vulnerability due to potential SRM impacts. This could involve updating water management strategies, improving infrastructure to handle potential disruptions (e.g., better irrigation systems or water conservation measures), and strengthening disaster preparedness plans. National policies may need to integrate both mitigation and adaptation strategies into broader climate action plans, which include addressing the impacts of SRM on river basins. Additionally, there is a need for scientific dialogue among policymakers, researchers, and international organizations to make informed decisions about whether to pursue SRM, especially in the context of Africa's vulnerability to climate change.

Chapter 4: Potential impacts of climate change and SAG on crop yield in Africa

In this chapter we present the results of our study to investigate the potential impacts of climate change and SAI on crop yield in Africa using a crop model called DSSAT model. We start by giving a comprehensive description of the DSSAT model before discussing the results.

4.1 DSSAT model

DSSAT is a suite of 42 crop simulation models designed to simulate crop growth, development, and yield by capturing the interactions within the soil-plant-atmosphere system (E. P. K. Boote et al., 2019). It takes into account factors such as soil conditions, crop characteristics, weather patterns, and management practices. One of its standout features is the ability to evaluate crop model outputs against experimental data. This allows users to compare simulated results with real-world observations, ensuring greater accuracy and reliability (E. P. K. Boote et al., 2019). Before applying a crop model to real-world decision-making or recommendations, it is crucial to validate the simulated outcomes by thoroughly comparing them with experimental data. DSSAT has proven to be incredibly versatile, finding applications across various domains. These include precision farming and on-farm management, regional analyses of climate variability and climate change impacts, gene-based modelling for breeding programs, water resource planning, greenhouse gas emission assessments, and ensuring long-term sustainability through the monitoring of soil organic carbon and nitrogen balances.

Although the DSSAT crop model is a widely used and calibrated process-based crop model in Africa, it is generally used at a plot scale because it uses climate and soil data of a particular point to generate yield for a point. Most of the studies that use the DSSAT crop model usually use a few plots to represent an entire area. For instance, Zingyere et al. ((2014) and (2015)) that used DSSAT to study the impact of climate change on crop yield in Southern Africa used one study site each in three Southern Africa countries but this may not be enough to make decisions at a regional level. To address this challenge, a python code was written to run DSSAT spatially, and this code allows us to supply the DSSAT model with soil, climate data, different cultivars and planting windows in format that DSSAT understands, and it then generates crop yield for each grid that is stored in a NETCDF file.

Although management in terms of cultivar type or irrigation and fertilizer use may vary from place to place, varying planting dates. However, some cultivars are generally used across a region and also it is difficult to model all the cultivars used in a grid because within a local community several cultivars can be used by different farmers. For instance, Abate et al., (2017) study found that nearly 500 maize cultivars were grown across 13 African countries during the 2013/2014 main crop season. Sixty-nine percent of these cultivars each occupied less than 1% of the total maize area, while only two cultivars covered more than 40%, and four occupied over 30% of the area. Therefore we used cultivars that are more expansive for a specific region to simulate yield and we planted them under rainfed conditions. Another major challenge is planting dates that vary from place to place. To address the issue of varying planting dates, we used the automatic planting function in DSSAT where we give the model a planting window. The planting window is the time frame during which sowing could occur, and the automatic planting function uses soil moisture level in the first 30 cm at 50% to determine the right time to sow. In cases where the planting did not occur across the window period the planting is forced on the last day of the planting window.

4.2 Calibration and evaluation of the DSSAT model

Calibrating and evaluating process-based models such as DSSAT over Africa can be quite challenging due to the scarcity of quality observation datasets in the region. We utilized some data from the Agricultural Model Intercomparison and Improvement Project (AgMIP) developed the Global Gridded Crop Models (GGCMs) for calibrating process-based models, although the dataset is poorly developed for Africa (Elliott et al., 2015). At experimental stations, crop experiment data is often incomplete, with some records providing only the planting date, latitude, and longitude but lacking information on harvested yield. Despite these challenges, we utilized the information available to calibrate the model. Studies ((Xiong et al., 2008, 2016) suggest that when calibrating and validating crop models at a regional scale, particularly for climate change impact assessments, the focus should be on capturing agricultural production trends rather than estimating precise farm-level yields, given the constraints of limited geographical data and model. Hence, the Food and Agriculture Organization (FAO: https://www.fao.org/faostat/en/#data/QCL) data was used in evaluating the DSSAT model in this study after calibrating the model with the information we were able to get.

4.2.1 Datasets

The Global Meteorological Forcing Dataset (GMFD) daily data (solar radiation, maximum temperature and minimum temperature and precipitation) was used during evaluation of the model. The GMFD data is reanalysis data. The dataset is created by integrating a range of global observation-based datasets with the NCEP/NCAR reanalysis. The soil data used is the HC27 soil profile database created by Koo Jawoo and Dimes John (2013). These 27 soil profiles were developed according to three criteria that crop models are most sensitive to: soil texture, rooting depth (as an indicator of water availability), and organic carbon content (as an indicator of fertility). Each category was divided into three levels using boundary conditions derived from a meta-analysis of WISE 1.1 soil profiles measured in cropland areas across Sub-Saharan Africa.

4.2.2 Crop management

This section presents the different crop management used in calibrating and setting up the model simulation. Crop management varies from place to place, and it includes planting dates, cultivar types and fertilizers among several.

4.2.2.1 Planting window

We obtained planting window information for each crop from the Global Yield Gap Atlas (GYGA) website, Agmip and for countries not covered by both, we sourced data from the FAO website (https://www.fao.org/giews/countrybrief/). For example, in many West African countries, maize is typically planted in April in the southern regions, while the northern regions begin planting in June or July. In such cases, we assigned different planting windows accordingly. Similarly, in Southern Africa, some areas are planted in October, while others start in December. We ensured that all these variations in planting windows were incorporated into the Python code.

4.2.2.2 Cultivar types

The information about the maize cultivars was obtained from Global Yield Gap Atlas (GYCA), AgMip and Abate et al.(2017) that summarizes different cultivars used in different countries in Africa. For instance, we used the Obatanpa cultivar already present in DSSAT over western Africa and some parts of central Africa because it is one of the most widely used cultivars in the region (Abate et al., 2017). It retains its original name, Obatanpa, in Ghana and Zambia, while in Mali, it is known as Dembanyuman, In Nigeria, it is called Sammaz14, and in Uganda, it goes by Longe5 (or Nalongo) (Abate et al., 2017)). For other regions, we selected cultivars commonly used in Africa that are already included in the DSSAT cultivar file and are closely similar to those present in the area. No new cultivars were introduced beyond those available in DSSAT, as calibrating a specific cultivar requires extensive experimentation. Additionally, most experimental trials in the region are not designed to measure the specific parameters needed for DSSAT calibration. For Sorghum, cultivars that are already calibrated over Africa were used in the simulation. For instance, a cultivar called W. Africa cultivar already present in DSSAT was used over western Africa and some parts of central Africa. Also, MN1500 cultivar in DSSAT as obtained in Mengistu et al.(Mengistu et al., 2016) was used over some parts of southern Africa because it is already in use in the region. For soybeans, not much information is known about its cultivars for crop modelling. The challenge is not about knowing the names of the cultivars but to get the parameters of the cultivars in a form that can be used by the DSSAT crop model. To overcome this, we used some of the cultivar that has a similar maturity date to what is planted.

4.2.2.3 Fertilizer and irrigation

We simulated and planted under rainfed conditions that no irrigation was applied. Low input of fertilizers was added to areas that had poor soils for maize and over South Africa, Northern Africa for sorghum. The low input of fertilizer added was 15 kg/ha as applied by Srivastava et al. (2025) during spatial crop modelling over Africa.

4.2.3 Evaluation Metrics

To evaluate the spatial performance of the DSSAT model, we compared simulated crop yields with FAO time-series data for maize, sorghum, and soybean in countries with available data from 1980 to 2009. To do this, we averaged the simulated crop yields over each country and compared them with FAO country-level data. However, for a few countries in the Sahel region, as well as Namibia, South Africa, and Somalia—where both suitable and unsuitable areas for crop production exist—we only averaged yields over areas where the crops are grown. This averaging methodology was also applied in a recent spatial study by Sultan et al. (2023) focusing on West Africa. The model was evaluated using three statistical measures: coefficient of determination (R^2), percentage bias (Pbias), and relative root mean square error (RRMSE). These measures were selected because no single metric can fully assess model performance, as each has its own strengths and limitations (Kobayashi & Salam, 2000; Legates & McCabe, 1999).

4.2.4 Results

This section presents model evaluation using FAO data for maize, sorghum and soybean. It also presents the sensitivity of maize and sorghum to low levels of fertilizers.

4.2.4.1 Maize

The crop model performs moderately well, capturing over 60% of the variability in observed data ($R^2 = 0.624$) with an low level error (RRMSE = 0.29) and slight underestimation (PBIAS = -4.39%) for maize yield (Fig. 4.1). It performed well in most countries but underestimated yield in South Africa and overestimated yield in Central Africa (Figure 4.1). We excluded Northern Africa from the DSSAT model evaluation because the observed yields are extremely high due to irrigation. The underestimation in South Africa may be due to averaging over multiple grid points. However, Figure 4.4b shows areas where simulated yields exceeded 2000 kg/ha, which closely aligns with observations. The overestimation in Central Africa could be attributed to the region's fertile soil and substantial rainfall, which exceeds levels in Southern and Northern Africa. Additionally, the yield data observed in Central Africa are scarce; we found no experimental data on the AgMIP website for this region. FAO yield data, often a mix of estimated and observed values, may also introduce discrepancies between FAO and DSSAT yields. Despite these challenges, the DSSAT model's predictions were reasonably close to FAO data. Overall, its current performance is encouraging and sufficient for the sensitivity study we conducted.

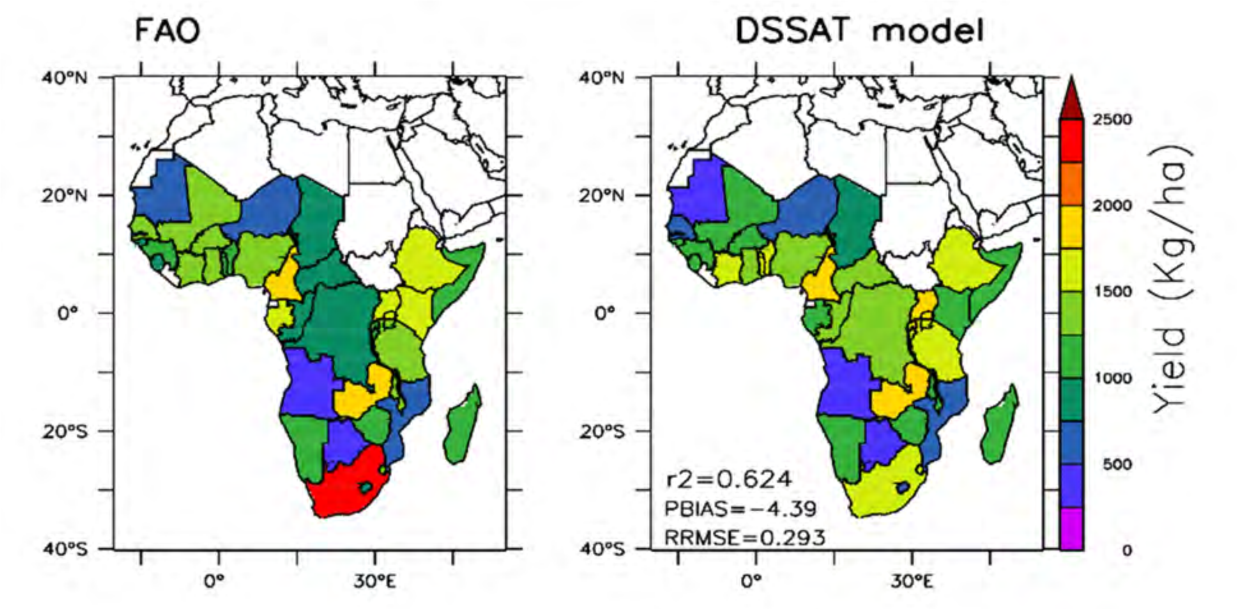

Figure 4.1: A Comparison between FAO data and simulated DSSAT model for maize yield over Africa

4.2.4.2 Sorghum

The model performs well in simulating sorghum yield, with strong predictive power (R^2 = 0.8) and an acceptable level of error. While it slightly underestimates yield (PBIAS = -12%) performance of DSSAT model was good for sorghum (Fig. 4.2). It however underestimates yield in South Africa, Niger and Mauritania. The underestimation may likely be due to averaging over multiple grid points because Figure 4.4d shows areas where simulated yields closely align with observations. Overall, the results are still reliable for most applications, making the model suitable for analysis and decision-making for sorghum.

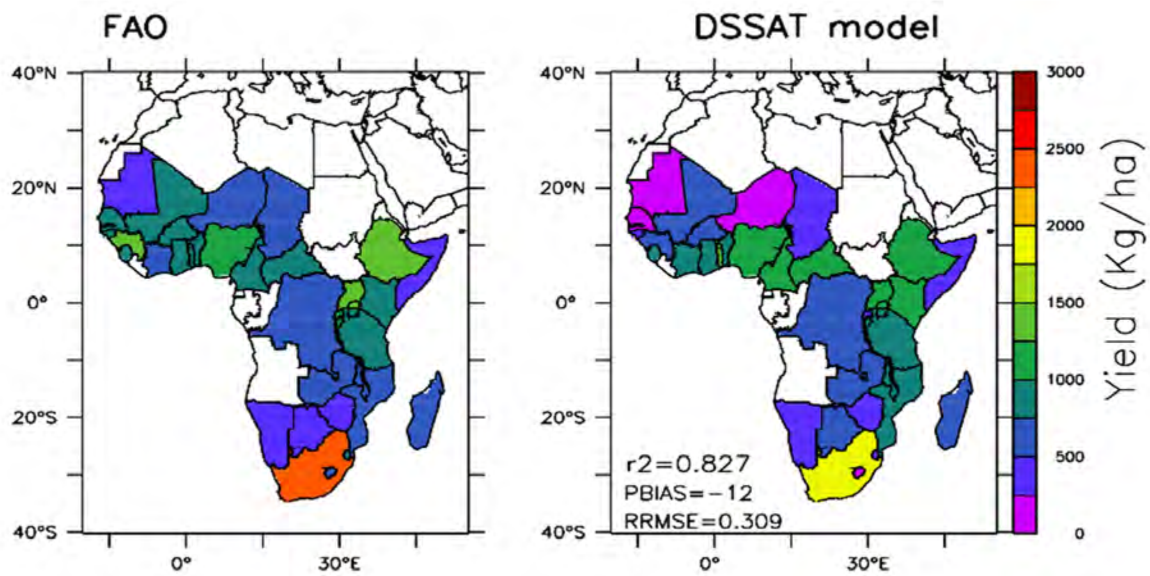

Figure 4.2: A Comparison between FAO data and simulated DSSAT model for sorghum yield over Africa

4.2.4.3 Soybean

The model performs well for soybeans, with a strong correlation ($R^2 = 0.75$), minimal bias (PBIAS = 4%), and relatively low error (RRMSE = 0.237) (Fig. 4.3). Although it slightly over estimated yield in some areas and slightly under estimates in Mali and Zimbabwe, however, the overall performance for soybean was good. These values suggest the model provides reliable and accurate predictions, making it suitable for further analysis and application.

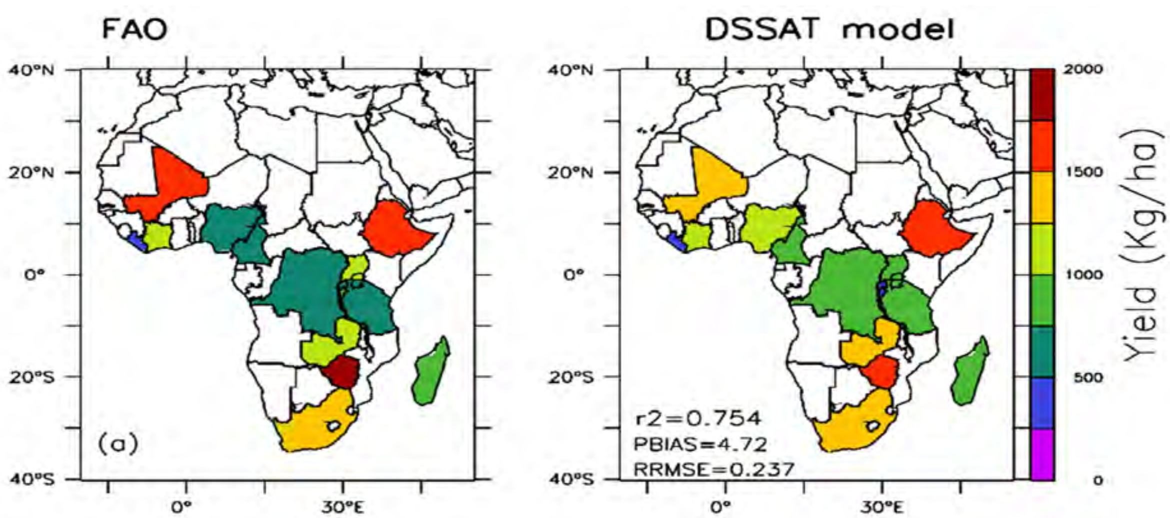

Figure 4.3: A Comparison between FAO data and simulated DSSAT model for soybean yield over Africa

4.2.4.4 Sensitivity of Maize and Sorghum to low level fertilizer input

The model shows and responds positively to the addition of fertilizers for both Maize and Sorghum (Fig.4.4). Yield estimates generated by the model align with expected agronomic responses. The model accurately simulates the beneficial effects of fertilizer application, with higher nutrient levels leading to enhanced maize and sorghum productivity. Although fertilizers seem beneficial, smallholder farmers still plant sorghum without the use of fertilizers however, for maize most smallholder farmers presently use fertilizers ranging from low to high input.

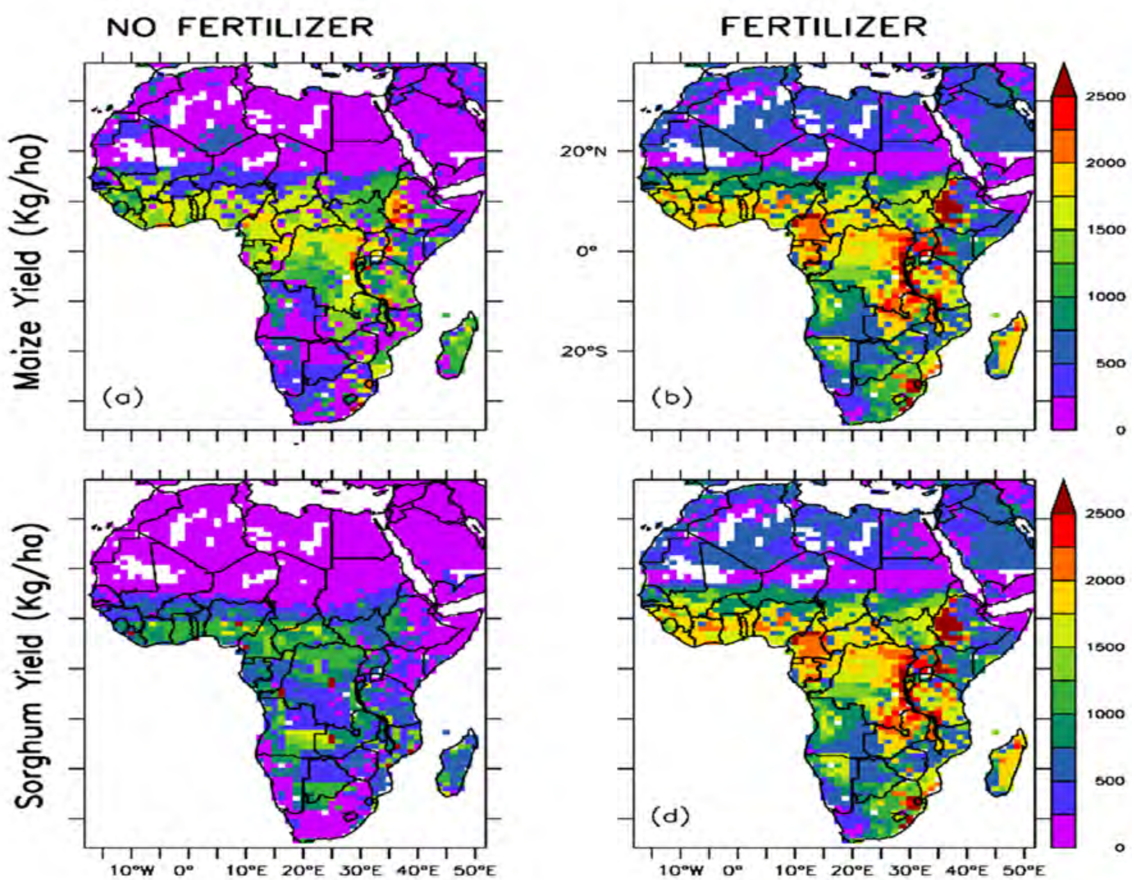

Figure 4.4: A Comparison between simulated fertilized at 15 kg/ha and no added fertilizers for maize and sorghum yield over Africa

In conclusion, the overall performance of the DSSAT model was good, with strong predictive ability for sorghum and soybean and moderate performance for maize. It effectively captured yield variability, with acceptable levels of error and bias. While maize simulations showed moderate accuracy, the model performed well for sorghum and soybean, making it reliable for crop yield simulation and suitable for sensitivity analysis. The performance of DSSAT was satisfactory for use as a spatial model across Africa. Although DSSAT is a process-based model, it performed well with minimal parameterization, likely due to previous calibrations over Africa. Additionally, the automatic planting function in DSSAT enhances its suitability for spatial applications, contributing to its robust performance in this study.

4.3 Simulating the Potential Impact of Climate Change and Stratospheric Aerosol Geoengineering on Crop Yield in Africa

We employed the use of a spatial DSSAT crop simulation model approach to assess the potential impact of SAG on crop yield. This approach integrated climate model projects with crop simulation models to evaluate yield under different climate experiments. The climate simulation datasets used for the study were obtained from the Coupled Model Intercomparison Project version 6 (CMIP6) and the Assessing Responses and Impacts of Solar climate intervention on the Earth system with Stratospheric Aerosol Injection (ARISE-SAI). All the simulations were produced by the CESM-WACCM. The dataset contains 10 ensemble members which were passed individually into crop models. Also, the ARISE-SAI data introduced SAG intervention in the year 2035 to keep the warming at 1.5^{o}C. The simulation datasets can be grouped into three:

1. The present-day climate simulation, from CMIP6, extends from 2015 to 2035 (20 years); hereafter, Reference.
2. The future climate projection under the SSP2.45 scenario (without SAI intervention), from CMIP6, extends from 2049 to 2069 (20 years); hereafter, SSP245.
3. The future climate projection under the SSP2.45 scenario with SAI intervention, from ARISE-SAI, extends from 2049 to 2069 (20 years). The SAI intervention targets keeping the global warming at 1.5^{o}C; hereafter, GEO

Before the climate data listed above was used in simulating crop yield, it was bias-corrected with GMFD data.

We maintained the cultivars and planting windows used during calibration and a low level of 15 kg/ha was added to only maize as used by Srivastava et al.(2025) for spatial crop modelling in Africa. The soil data used is the HC27 soil profile database created by Koo Jawoo and Dimes John (2013). These 27 soil profiles were developed according to three criteria that crop models are most sensitive to: soil texture, rooting depth (as an indicator of water availability), and organic carbon content (as an indicator of fertility). Each category was divided into three levels using boundary conditions derived from a meta-analysis of WISE 1.1 soil profiles measured in cropland areas across Sub-Saharan Africa. To simulate the potential impacts of climate change and SAG on crop yields, DSSAT simulations were forced with present day data (Reference), climate change data at SSP4-25 (SSP45), and climate projection in which SAG intervention has been implemented to limit the warming to 1.5°C (GEO). Furthermore, we included the CO2 scenario for SSP245 for all the scenarios.

4.3.1 Impacts of climate change and SAG on climate variables.

This section presents the impact of climate change and SAG some climate variables that are important to crop production. The climate variables discussed are solar radiation, maximum and minimum temperature and precipitation.

4.3.1.1 Solar Radiation

Climate change is projected to increase Solar radiation across most regions in Africa but the pattern and magnitude of increase is not homogenous across the   month and region. The maximum observed increase is up to 0.8 mJ/m²/day (Figure 4.5). The spatial plot for July, August, and September (JAS) revealed that most regions in Africa project an increase in solar radiation under the SSP245 scenario (Figure 4.5i). Southern Africa seems to have an increase in solar radiation across all months for climate change with the highest increase occurring in JFM in South Africa. Figure 4.5 shows a projected increase in solar radiation as a result of projected change under the ssp245 scenario during the most region growing season. For instance, from approximately 1°S northward, most regions above the equator experience a planting season from April to September for many crops and for the most part had an increase in solar radiation during this period. Also, regions south of latitude 1°S, where the planting season typically occurs from September to March, also had increased solar radiation during the July–September (JUL/AUG/SEP) and October–December (OCT/NOV/DEC) periods. This therefore suggests that increased solar radiation could potentially benefit crop yields in Africa. Solar radiation is a key driver of crop photosynthesis, influencing the formation and development of plant organs and ultimately determining crop yields. For instance, in the northern transition zone (NTZ) of Karnataka, India, Munnoli et al. (2023) found that increasing solar radiation by 10% and 20% increased the yield by 42% and 46%, respectively.

SAG intervention, when compared to the reference period, reduced solar radiation over most places in Africa. There is also the possibility of solar radiation reducing crop yield over Africa as a result of SAG intervention.. For instance, Yang et al (2019) found that a decrease in solar radiation after silking can cause a drop in maize grain yield and biomass in china. Similarly, Munnoli et al. (2023) found that reducing solar radiation by 10% and 20% decreased the yield of Kharif sorghum by 61% in India. While the impact of changes in solar radiation on crops in Africa remains uncertain, increased solar radiation has the potential to improve crop yields, a maximal increase of approximately 0.8 mJ/m²/day under the SSP245 scenario, representing less than a 5% increase. Such a small change may have negligible effects on crop productivity. Additionally, since Africa lies around the equator and already receives ample sunlight, solar radiation may not be a primary limiting factor for crop growth. Other climatic factors, such as temperature and rainfall, could offset any potential benefits of increased solar radiation.

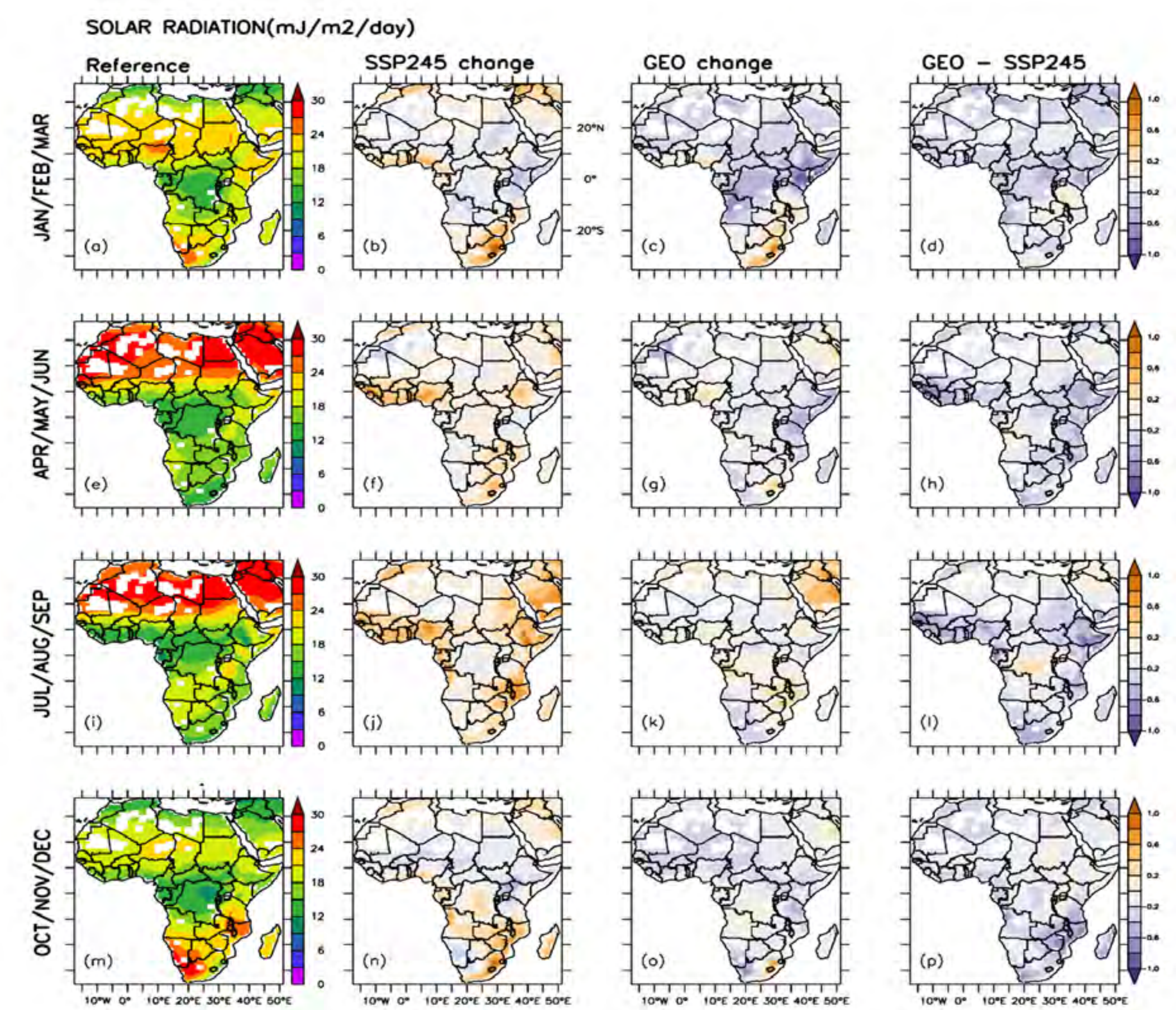

Figure 4.5: Projected Average 3-Monthly Change in Solar Radiation Impact for SSP245 and SAG (2050–2069) in mJ/m2/day. The simulation is an average of 10 ensemble members and the reference period from 2015 to 2034.

4.3.1.2 Temperature

The ARISE data both Tmax and Tmin are projected to increase by 1 to 2 degree celsius across Africa under the ssp245 scenario however, the intensity and spatial spread varies across months and places (Figure 4.6 and 4.7). For Tmax, the region that seems to have the highest increase across all months is Southern Africa however, these high temperatures over the region are highest at around OCT/NOV/DEC and it enters into JAN/FEB/MAR (Fig. 4.6). This period corresponds to the most crop growing season in the region and an increase in Tmax may affect crop yield negatively. Also, most part of west africa and some part of central africa projects the highest increase in Tmax during APR/MAY/JUN and this period is the start of the crop growing season in the region. Maximum temperature is very crucial to photosynthesis because it reflects the temperature during the day and higher temperatures accelerate photosynthesis and respiration rates but may also increase water stress under elevated transpiration (Kirschbaum, 2004). Unfortunately, most regions of Africa project an increase in Tmax during most crop growing seasons under the ssp245 scenario during the 2050 to 2069 period.

Although there is generally an increase in Tmin across all the months and places, Southern Africa seems to have one highest increase from across all the months with the Jul/Aug/Sep having the highest spread of increase in the region (Figure 4.7). Increased Tmin may promote plant growth in drier, colder areas (Li et al., 2023). Increases in Tmin may be beneficial for farmers that plant during winter, especially winter wheat (Rosenzweig & Tubiello, 1996). The result shows that SAG intervention at keeping the warming at 1.5 lowers the increased Tmax and Tmin as a result of climate change but not completely (Figs. 4.6 and 4.7). The reduction of elevated Tmax can potentially reduce heat stress on crops associated with rising temperatures. While SAG may alleviate heat stress, the reduction in minimum temperatures in certain regions could lead to freezing conditions, posing risks for crops in areas exposed to extreme cold. This impact may be particularly unfavorable for winter planting in the southernmost parts of Africa, where colder minimum temperatures could harm crop establishment and growth.

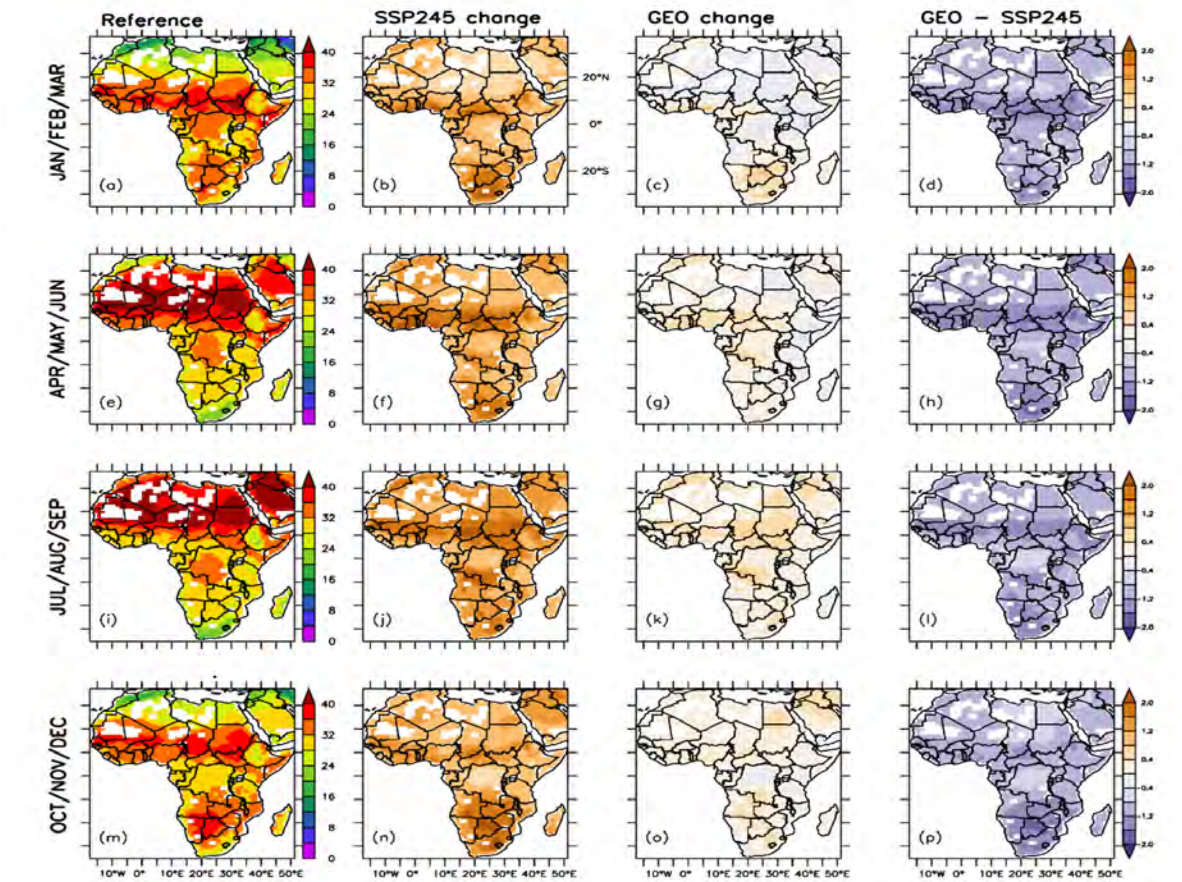

Figure 4.6: Projected Average 3-Monthly Change in Maximum Temperature Impact for SSP245 and SAG (2050–2069) in degree celsius/day. The simulation is an average of 10 ensemble members and the reference period from 2015 to 2034.

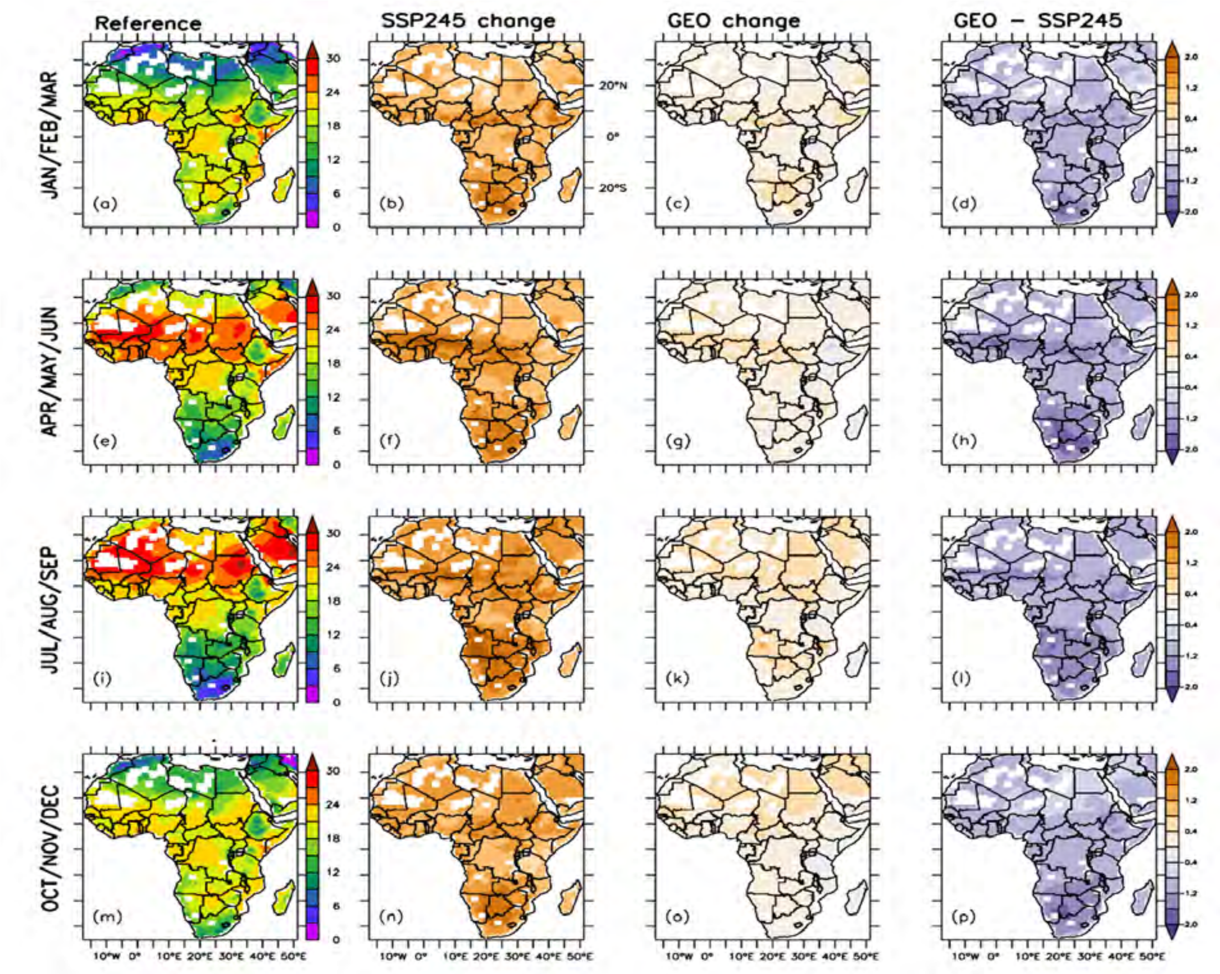

Figure 4.7: Projected Average 3-Monthly Change in Minimum Temperature Impact for SSP245 and SAG (2050–2069) in degree Celsius/day. The simulation is an average of 10 ensemble members and the reference period from 2015 to 2034.

4.3.1.3 Precipitation

In Fig. 4.8, climate change under the ssp245 scenario projects decrease in most areas with some areas experiencing more than 20% decrease in precipitation, however, the time of the decrease differs from place to place. When considering the growth seasons and the time each area receives most of their rainfall, West Africa seems to experience the highest decrease ranging from 8 to 18% in rainfall during the APR/MAY/JUN period which is essential for the start of the crop growing season in the region however, the decreased in April to June may not be felt because the region region is one of the areas that receives the highest rainfall in Africa. Also, there seems to be no notable changes in the July to August months especially over the southern part of West Africa. Furthermore, Although Southern Africa seems to have the highest decrease of more than 20% in precipitation however, this great decrease is experienced during the JUL/AUG/SEP in which present climate shows little rainfall during those months. The main season where most of the rainfall is collected is from October to March, and the result projects a 4 to 8% decrease in the OCT/NOV/DEC and slight decrease in the southernmost part Jan/Feb/March. The only area that seems to experience a slight increase during its main rainy season is East Africa. Since precipitation plays a crucial role in crop production across Africa, where up to 70% of food is produced on small farms practising rainfed agriculture (Berkowitz, 2021), projected decrease in precipitation will most likely decrease yield in Africa.

The effect of SAG intervention on precipitation varies across different months and regions in Africa. Fig 4.8 projects that SAG intervention will most likely reduce precipitation and exacerbate the decline in precipitation because of climate change over Southern Africa and the south part of East and Central Africa. While, over Western Africa, SAG intervention did offset the decline in precipitation but not completely. This implies that SAG could potentially minimize the decline in precipitation in West Africa and cause further decline in other parts of Africa.

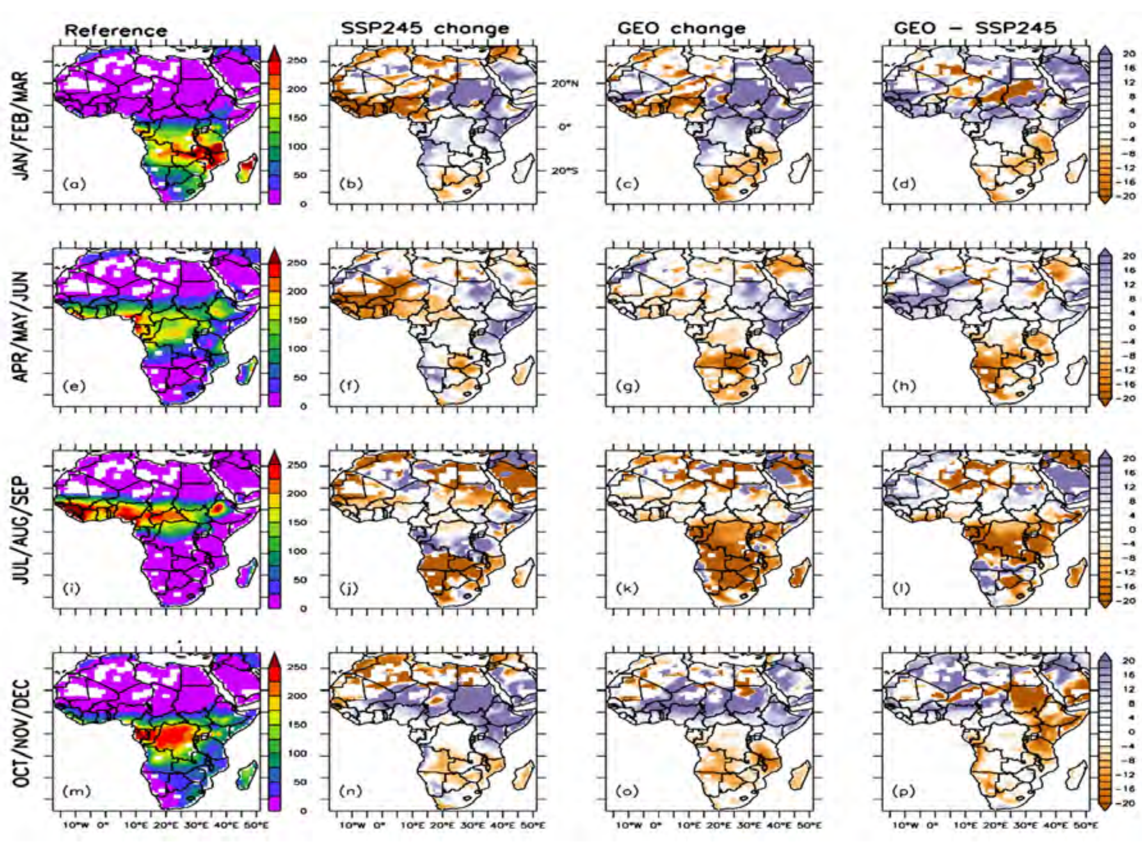

Figure 4.8: Projected Average 3-Monthly Percentage Change in Precipitation Impact for SSP245 and SAG (2050–2069). The simulation is an average of 10 ensemble members and the reference period from 2015 to 2034.

4.3.2 Potential Impact of climate change and SAG on crop yield

The projected impact of climate change and geoengineering varies among crops and locations. This section shows the projected impact of climate change and geoengineering on maize, soybean and sorghum yield. It also highlights how each crop extracts moisture from the soil and their varying evapotranspiration (ET) rates. ET and water uptake varies from plant to plant because of their different physiology. Maize and Sorghum are both C4 plants but they still vary in physiology.

4.3.2.1 Maize

Maize yield is projected to decline across most parts of Africa, except for a few areas experiencing slight increases under the SSP245 scenario (Figure 4.9b). The highest decrease, of 20% or more, is observed in some places in Southern Africa like Zambia, Botswana, Malawi and Mozambique, likely due to increased maximum temperature during the growing season (Fig. 4.6). The impact of climate change can also be seen in the amount of extractable soil moisture when the plants reach maturity which is about 10 to 15 days before harvesting. The amount of soil moisture available in the soil at crop maturity generally declined under projected change. Several factors such as temperature, rainfall, leaf size, evapotranspiration and the crop water use may be responsible for the decline. Although the decline in extractible SM may not truly reflect increase/decrease grain yield because it is the total moisture remaining after grain production, it points out the demand of water by the atmosphere. Except for the Northern part of Africa where ET seems to increase, other regions had a decline in ET during the crop growing season most likely as a result of decrease in crop yield.

Applying SAG did not completely offset the negative impact of climate change but it lowered it. It offsets the negative decline of maize yield in almost all places in Africa except for northern Africa and the east part of south Africa where there is not much change (Figure 4.9). This indicates that increased temperature is one of the major contributing factors to the decline of maize in Africa under the SSP245 scenario. According to Prasad et al. (2018), maize is more sensitive to high temperatures, with optimal growth occurring at cooler temperatures than sorghum and pearl millet. Although the result shows that ET slightly increased when SAG was applied despite lowering temperature, this is because when a plant produces a higher grain yield, evapotranspiration (ET) rate often increases (Bai et al., 2024; Djaman et al., 2013). Therefore, in places where SAG increased yield there is a slight increase in ET and vice versa.

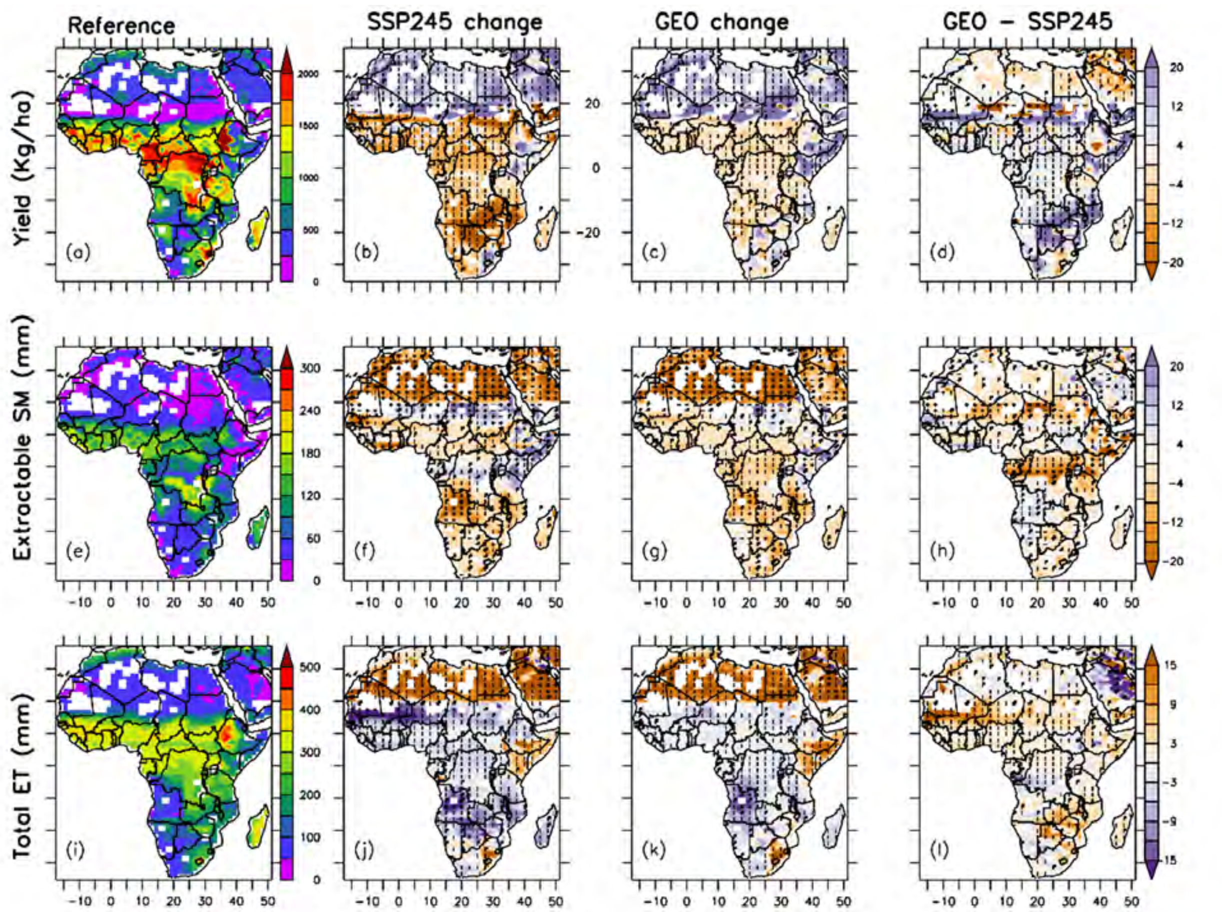

Figure 4.9:Projected percentage change maize yield, Extractable soil moisture at crop maturity, Total actual evapotranspiration during the growing season (planting to harvesting) for SSP245 and SAG for 2050 to 2069. The simulation is an average of 10 ensemble members and the reference period is from 2015 to 2034. The vertical lines indicate that 60% of the ensembles result in a change that exceeds natural variability. The horizontal lines indicate that 70% of the ensembles agree with the sign of the change.

4.3.2.2 Sorghum

Sorghum yield is projected to decline across most of Africa, except for a few areas experiencing slight increases under the SSP245 scenario (Fig., 4.10) and the extent of decline varies among locations. The highest decline of 20% or more, is observed in the Sahel region of West Africa, likely due to the region's arid climate and poor soil conditions. In contrast, Southern Africa shows the second highest decline, with sorghum yield decreasing by up to 16% in some places, this decline may be as a result of increased Tmax during planting season or decreased rainfall during the growth season (Figure 4.10 and 4.6). Similar to maize, the amount of SM that can be extracted at maturity also decreased except for the upper part of western Africa, the sahel region where extractable SM increases despite the reduction of yield in the region. This may be due to several crop failures as a result of poor soils and lesser growth at time of crop maturity may likely lead to decrease in soil moisture demand in the area.

Applying SAG generally increases sorghum yield where temperature-induced declines are significant, but in other areas, it exacerbates yield loss due to reduced precipitation. It offset and lowered sorghum yield decline in the Sahel part of western Africa and Northern Africa and some few places in Southern Africa, and all these areas experienced yield loss above 10% (Figure 4.10). While it increases the decline of sorghum yield in other parts of Africa ranging from areas that had slight increase in yield to areas that had declined less than 10% (Fig. 4.10). Increase in yield after SAG intervention in areas where the decline in yield is above 10%, indicates that increase in temperature was what exacerbates the decline in sorghum yield, therefore, the decreased Tmax was beneficial to those areas. Furthermore, other regions that did not benefit from the decrease in temperature indicate that decline in precipitation is affecting sorghum yield..

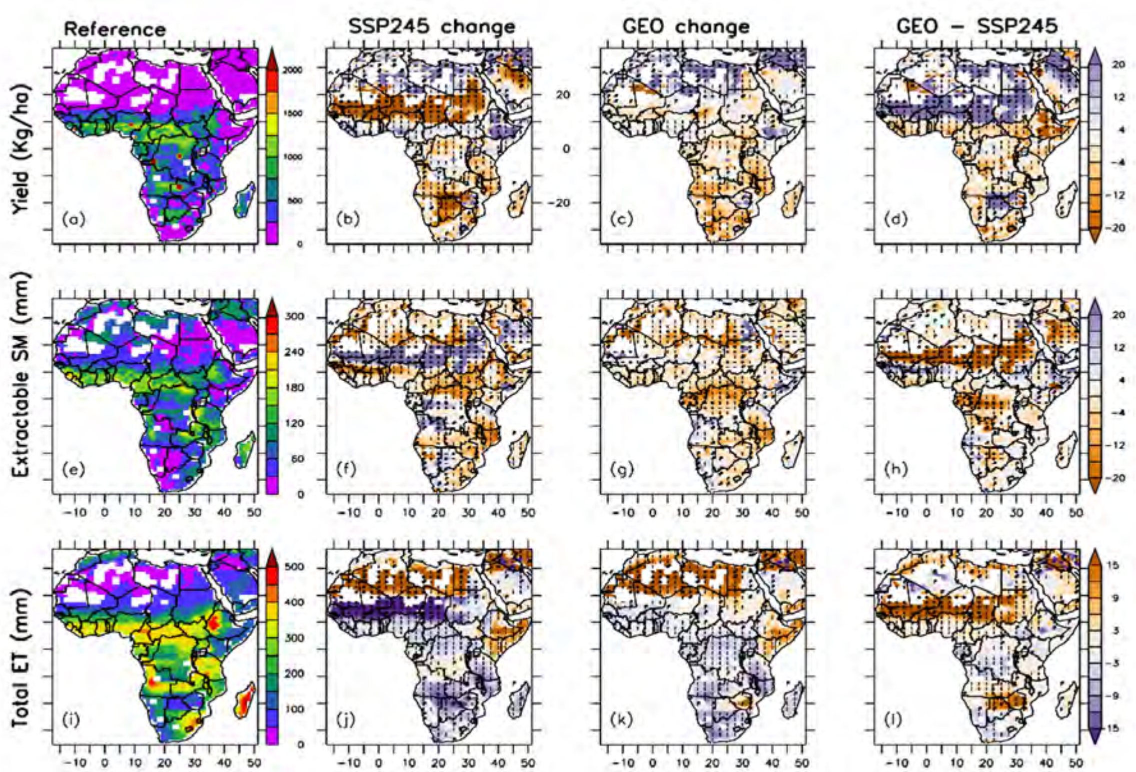

Figure 4.10: Projected percentage change sorghum yield, Extractable soil moisture at crop maturity, Total evapotranspiration during the growing season (planting to harvesting) for SSP245 and SAG for 2050 to 2069. The simulation is an average of 10 ensemble members and the reference period is from 2015 to 2034.The vertical lines indicate that 60% of the ensembles result in a change that exceeds natural variability. The horizontal lines indicate that 70% of the ensembles agree with the sign of the change.

4.3.2.3 Soybean

Soybean is projected to increase under the SSP245 scenario in several places in Africa except for the Sahel part of West Africa , Northern Africa and some places in Southern Africa (Fig. 4.11). Substantial increases ranging to as high as 25% under SSP245 scenario may be a result of soybean which is a C3 crop benefitting from increasing levels of CO_2. For instance, MacCarthy et al. (2022) found that when ambient present CO_2 level was used to project impact of climate change under RCP 4.5 and 8.5, soybean yield decreased by 3.2% and 9.2% respectively however when the CO_2 projection for each scenario was added soybean, yield increased by 18% and 31% respectively. Similarly Durodola & Mourad (2020) showed that soybean yields are projected to increase by up to 40% under RCP 8.5 due to CO_2 fertilization effects in Nigeria and this can be seen in our results in Fig. 6 over the Southern part of West Africa. Furthermore, due to increased crop yield under the SSP245 scenario, ET experienced an increase when compared to maize and sorghum.

Other varied factors such high temperature, low rainfall and poor soil could be responsible for decline in North Africa and the Sahel part of west Africa, and Southern Africa. For instance, Northern Africa and the Sahel part of West Africa are mostly desert and arid climate, where crop yield is normally poor because of soils, high temperature and low amount of rainfall. Furthermore, in some places in Southern Africa, soybean yield declines from 10 to 20 % under the SSP245. This may be as a result of increased Tmax during the growing seasons. Although there is a reduction in precipitation over Southern Africa during the crop growing season, however the decline during the crop growing season is not high when compared to other regions, a high increase in Tmax in the crop growing season could have led to a decrease in soybean yield. Despite the fact that soybean, which is a C3 plant, has the capacity to benefit more from increased CO_2 levels, some places in Southern and Northern Africa still experienced a decrease in yield due to high temperature or low rainfall.

The application of SAG can help to offset soybean yield declines in some regions while slightly reducing gains in others (Figure 4.11). It offsets the negative decline of soybean yield in Southern Africa, Sahel part of West Africa and North Africa, though not entirely (Fig. 4.11). This may be as a result of reduction in Tmax when SAG is applied (Fig. 2a). According to Burroughs et al., (2023) who conducted a field experiment to understand the effect of increased temperature on soybean yield, found that increased temperatures reduce soybean yield by decreasing leaf area index, pod production, seed size, and harvest index. Therefore, any intervention to decrease temperature in areas of soybean decline will be beneficial to soybean. However, for areas such as southern part of West Africa, central Africa, Eastern Africa that experienced an increase in soybean yield under the SSP245 scenario as a result of increased CO_2 levels, application of SAG slightly reduced yield but the reduction is still a positive increase in yield if compared to the reference period. The slight decrease may be as a result of decrease in precipitation in most places as a result of SAG intervention. The reduction in yield in some of these places is evident in the decrease of ET in Soybean when you compare GEO to SSP245.

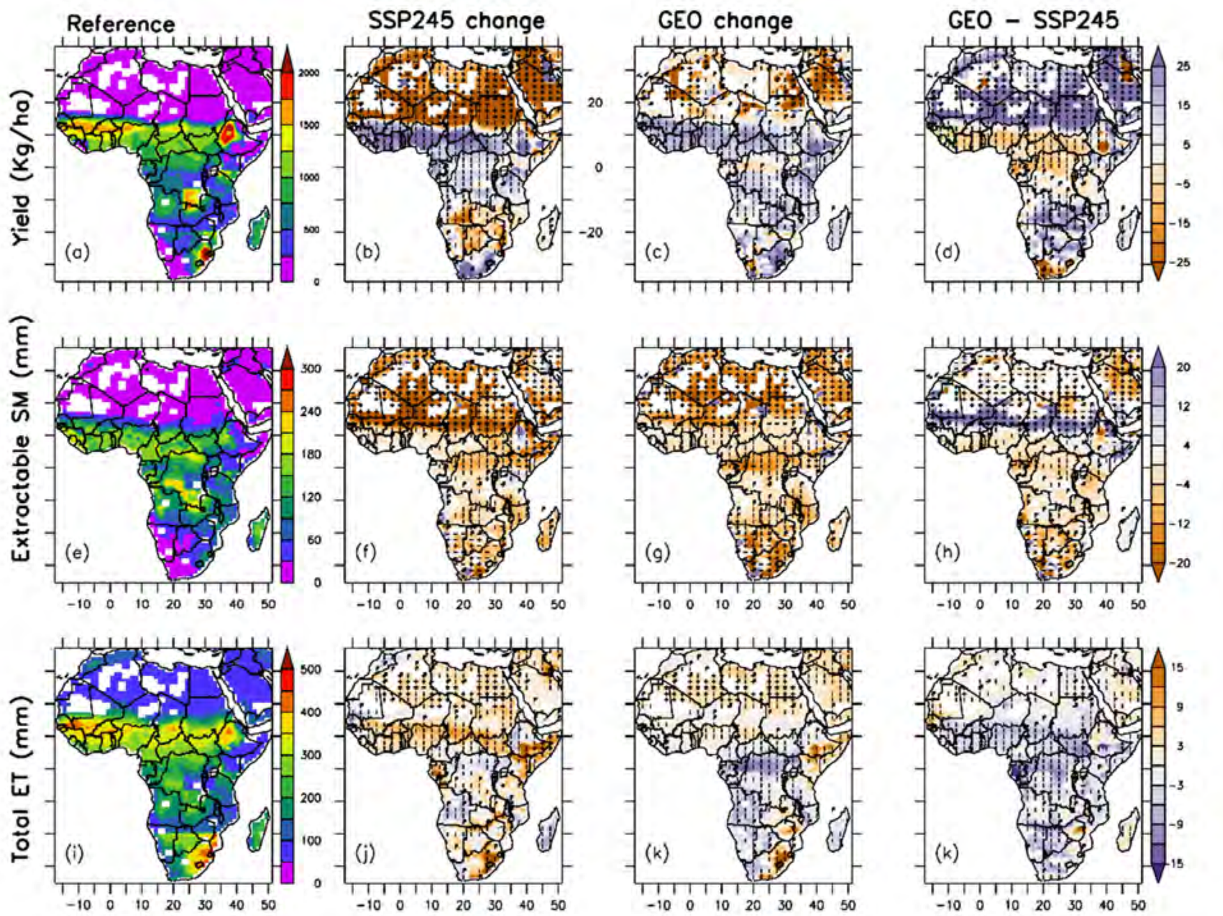

Figure 4.11:Projected percentage change of soybean yield, Extractable soil moisture at crop maturity, Total evapotranspiration during the growing season (planting to harvesting) for SSP245 and SAG for 2050 to 2069. The simulation is an average of 10 ensemble members and the reference period is from 2015 to 2034. The vertical lines indicate that 60% of the ensembles result in a change that exceeds natural variability. The horizontal lines indicate that 70% of the ensembles agree with the sign of the change.

4.3.4 Regional summary of potential climate change and SAG on crop yield in Africa

The projected impact of climate change varies across regions and crops (Figure 4.12). Over the Sahel part of Western Africa, maize is projected to increase by 8%, while sorghum and soybean is projected to decrease 27% and 20%. In contrast, Northern Africa, which is the region that extends the Sahel part of Western Africa, projects an increase of about 18% for maize and about 9% for sorghum while soybean projects a decrease of about 30%. Despite the increase in maize and sorghum over Northern Africa and maize over the Sahel of Western Africa, it may not significantly increase yield because yield in the area is generally low under rainfed conditions because of poor soils, high temperature and low rainfall.

In the Southern part of West Africa, maize is projected to decrease by 8% while sorghum and soybean is projected to increase by 10% and 15% respectively. Also, over Central Africa, maize and sorghum are projected to decrease by 7% and 6% while soybean is projected to increase by 10%. Similarly, over Southern Africa, maize and sorghum are projected to decrease by 10% and 5% while soybean is projected to increase by 16%. Furthermore, East Africa seems to be the least affected by climate change, where maize yield projection only declined slightly 2% while sorghum increased by 37% and soybean by 3%.

The application of SAG generally decreases the negative decline of yield because of climate change; however, it reduces yield in areas of positive increase in yield as a result of climate change (Fig. 4.12). Over Northern Africa and Sahel part of West Africa, it slightly reduces maize yield while it increases sorghum and soybean yield. Furthermore, Over the southern part of West Africa, it mostly decreased the decline for maize while it reduced sorghum and soybean yield over the region. Over Central Africa, SAG reduced the decline in maize and sorghum and slightly reduced soybean yield over the region. Finally, In Eastern Africa, it increased maize and soybean yield, while it significantly decreased sorghum yield from 37% to about 10%. It completely offset the decline of maize in Southern Africa while it slightly increased the decline of sorghum yield and reduced soybean yield over the region.

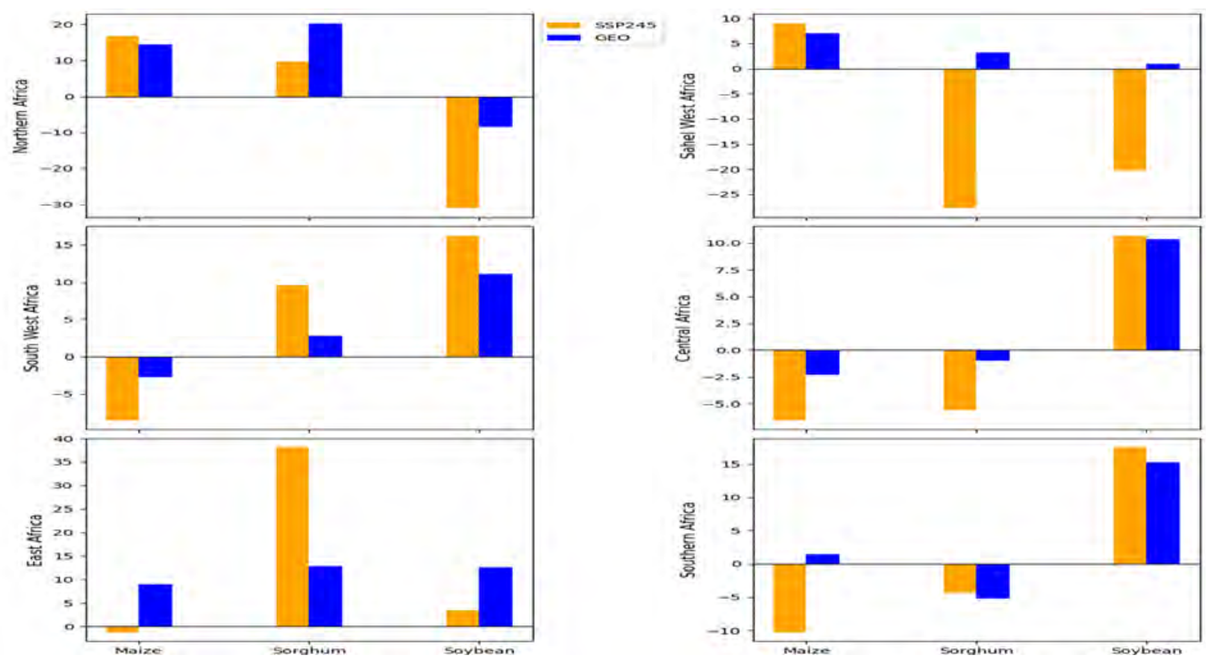

Figure 4.12: A Comparison of Maize, Sorghum and Soybean Yield Percentage Change for Climate Change (SSP245) and Geoengineering (GEO) across different Regions from 2050 to 2069 in Africa.

4. Conclusion

Among the three crops, soybeans, which is a C3 crop, seem to benefit more from increasing levels of CO_2 than the other crops under the SSP245 scenario. Maize and Sorghum may not really benefit from increasing levels of CO_2 because they are C4 crops. Overall, under the SSP245 scenario, there is a projected decline for maize in most places, decrease in some places for sorghum while soybean projects an increase in most places in Africa .

Application of SAG did offset yield decline caused mainly by increased temperature. It generally reduced the decline of maize yield because of its sensitivity to temperature. It also does the same for sorghum in regions where the decrease in sorghum is above 10%. However in regions which have below 10% decrease and positive increase in yield under the SSP245 scenario, it slightly decreased yield of sorghum. Similarly, for soybean SAG also slightly reduced the decline of soybean in regions where projected impact is negative. However, it decreases yield slightly in places where there is a positive yield of soybean.

Overall, SAG can help offset the decline in maize and the extreme decline in sorghum and soybean. However, it may reduce yields in areas where sorghum and soybean show a positive or no increase in yield, as well as in regions where the decline in sorghum is less than 16%. We acknowledge that more models are still needed to examine the impact of SAG on crops in Africa. Also, there is a need to examine more classes of crops because we only examined cereals and soybean which is legume.

Chapter 5: Impact of Climate Change and Stratospheric Aerosol Injection on Rangeland Productivity in Africa

In this chapter we present the results of our study to investigate the impact of climate change and SAI on crop yield in Africa using a rangeland model called the G-Range model. We give a comprehensive description of the G-Range model before discussing the application of the model for the study.

5.1 G-Range Model

G-Range is a global rangeland model for simulating how rangelands change over time (Boone et al., 2018; Boone R., Conant R., Hilinski T., 2011). It uses spatial data and parameters to describe plant growth in different landscape units. By combining this information with a computer code that represents ecological processes, the model simulates soil nutrients and water dynamics, vegetation growth, fire, and the impact of both wild and domestic animals. The model divides the world into square cells, and it simulates ecosystem dynamics in rangeland cells (Fig. 5.1).

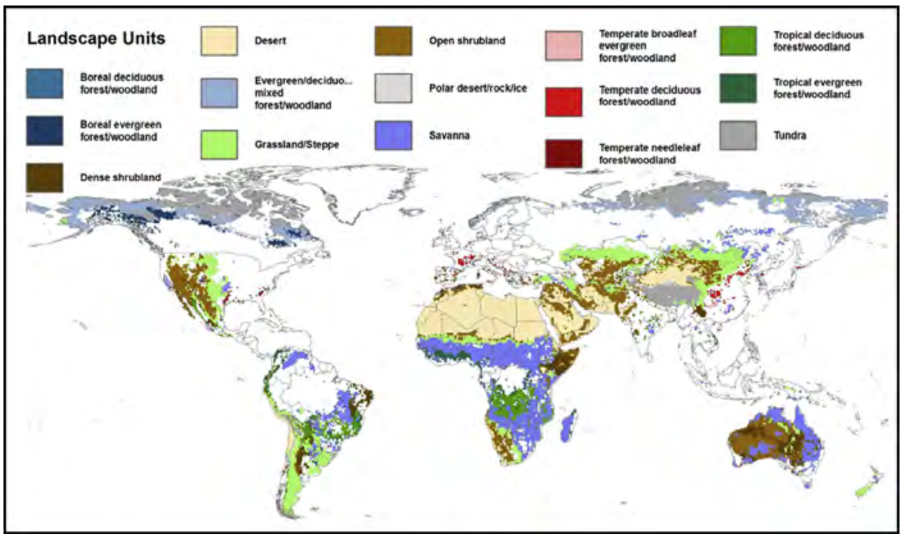

Figure 5.1: The simulation domain of the G-Range model, showing active G-Range simulation surface. Parameter sets are divided among rangeland "landscape units" (i.e., biomes). Rangeland versus non-rangeland grid cells were defined on the basis of land cover types (USGS, 2008) (source:(Sircely et al., 2019)).

5.2 Model Calibration and Evaluation

The G-Range model was globally calibrated by Sircely et al. (2019). The calibration process began with a sensitivity analysis of the model parameters and involved adjusting them until a global-scale calibration was achieved. This approach ensured that the model accurately represented various global data layers, focusing on the year 2006 or, where applicable, average values across all available years. In particular, emphasis was placed on the new G-Range parameters that govern vegetation dynamics in the plant population submodels. For the calibration process, global layers were utilized, including CENTURY model outputs (Henderson et al., 2015) for plant-available soil water, decomposition coefficients (DEFAC), soil organic carbon, annual net primary production (NPP), potential evapotranspiration (PET), and soil surface temperature. These layers were further complemented by additional global layers for annual evapotranspiration (Zhang et al., 2010), snow-water equivalent (Armstrong et al., R., Brodzik MJ, Knowles K., Sovoie M., 2009), soil C:N ratio (Batjes, 2002), Tier 1 live carbon density (Ruesch A., 2008), and leaf area index (LAI) derived from ISLSCP II NDVI (Sietse, 2010).

Sircely et al. (2019) evaluated the performance of G-Range at global and station scales (Fig. 2). They assessed the ability of the model to simulate ecosystem dynamics at large scales based on its ability to generate outputs across diverse data points from various locations and years. The primary central function of the model is to simulate and forecast biomass production, with particular focus focusing on net primary production (NPP) and vegetation composition (herbaceous and woody cover). To ensure that the model was suitable for global-scale application, the study established criteria for evaluating its performance across different scales and set benchmarks based on the absolute and percent differences between the model outputs and evaluation data. The results showed that, at both global and site scales, the difference in G-Range total net primary production (TNPP; aboveground + belowground) from MODIS TNPP was generally within the established benchmarks for acceptable margin of model error, both in absolute and percent difference (see Fig. 5.2). However, in savannas, G-Range exceeded the percentage difference benchmark for TNPP at both global and site scales. For tropical evergreen forests (“tropical evergreen forest and woodland”), the model surpassed the absolute difference benchmark at site scales, but not at global scales.

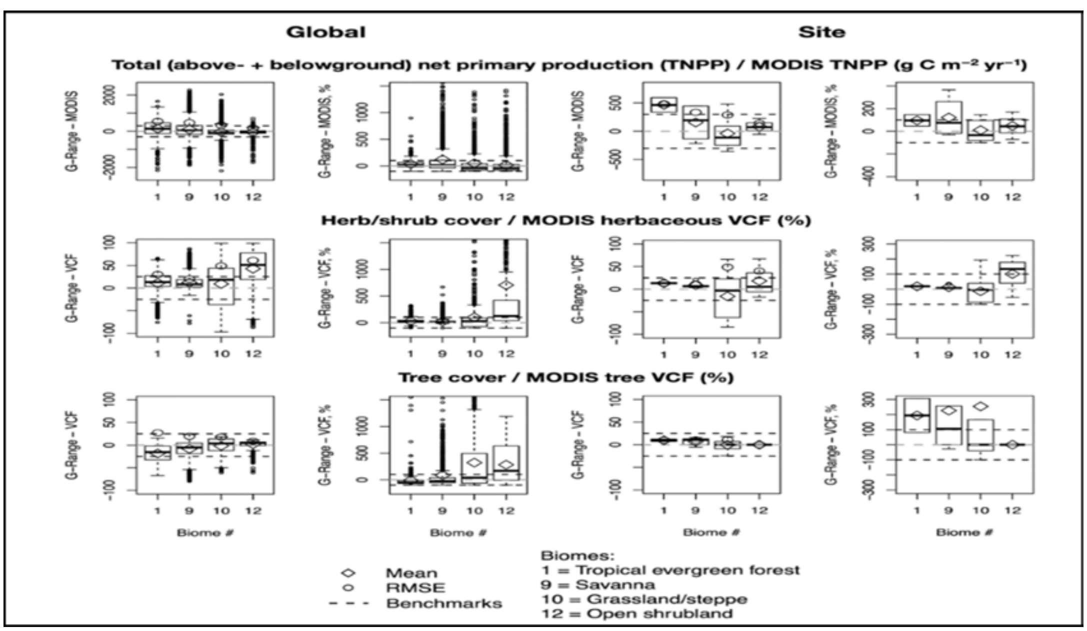

Figure 5.2. Evaluation of G-Range model, on global and site scales, against global MODIS layers for annual total net primary production and fractional vegetation cover. Boxplots show the median

and second and third quartiles, overlain with means, root mean squared error, and evaluation benchmarks (Source: Sircely et al., 2019).

In this study, we build on previous evaluation of the G-Range model to examine its ability to simulate spatial variation of rangeland across Africa. We used the MOD44B version 6.1 Vegetation Continuous Fields (VCF) yearly product, which provides global fractional vegetation cover from 2000 to the present (DiMiceli et al., 2021). The MOD44B layers include tree cover, non-tree cover, and bare ground. We compared these layers with the G-Range vegetation facet cover layers (herbaceous, shrub, and tree) and the bare ground output (Fig. 5.3). To represent the non-tree component, we combined the herbaceous and shrub layers. We then calculated the bias to assess the over- or underestimation of vegetation cover (Fig. 5.3).

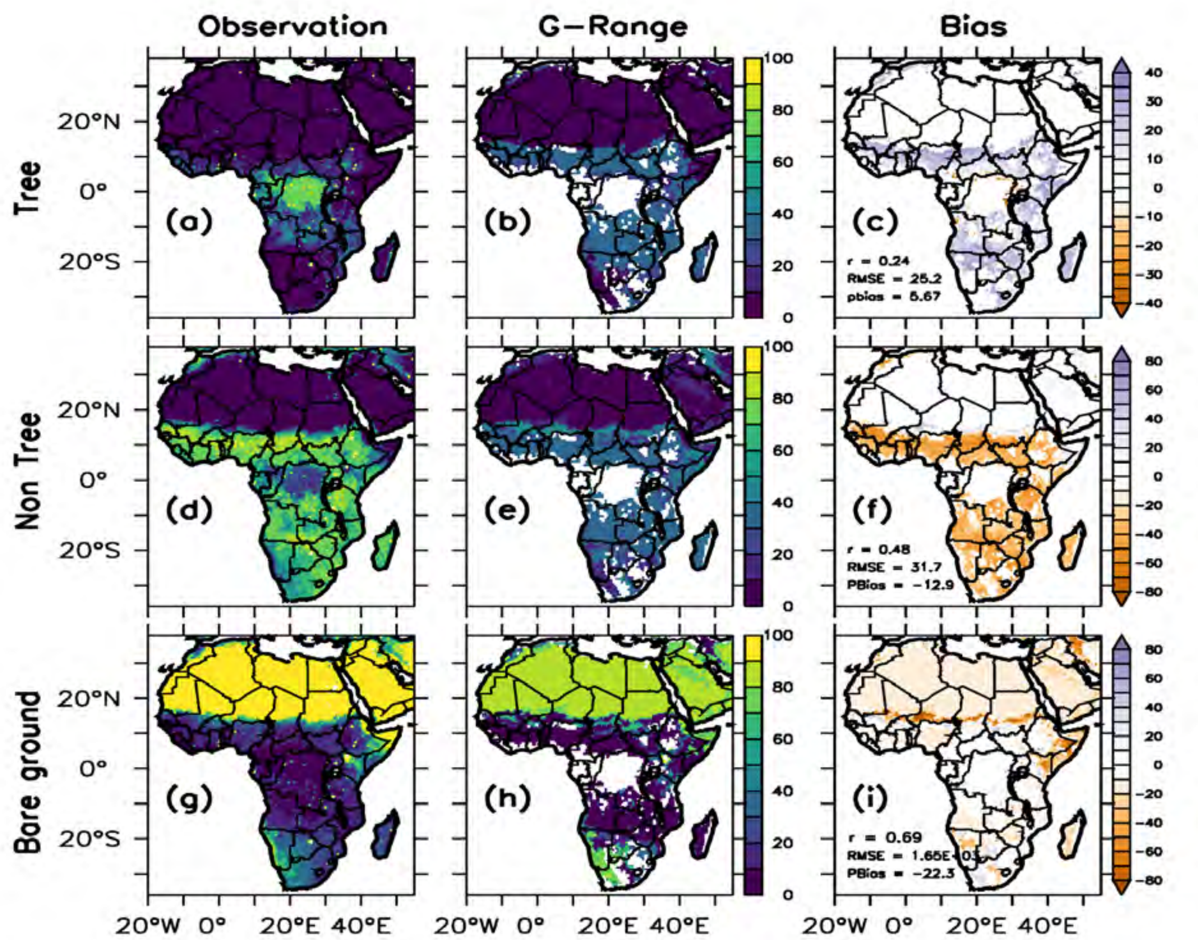

Figure 5.3. The spatial distribution of tree, non-tree and bare ground as observed by MODIS and simulated by G-Range (1982-2006). The simulation is shown in the third column; the correlation between the observation and simulation (simulation minus observation). the observation (MODIS) bare ground and fractional vegetation cover and G-Range outputs.

The general pattern of tree cover is consistent between the observational data and the G-Range spatial configuration (Fig. 5.3). However, large areas with missing data are observed in the G-

Range tree cover output, which occurs because G-Range simulates only areas classified as rangeland, leaving regions such as the tropical rainforest in Central Africa, which is characterized by high tree cover, unrepresented. Despite this, both the observations and the G-Range model exhibit a gradual increase in tree cover percentage moving northward.

However, G-Range shows a bias in the actual values of tree cover. It overestimates tree cover across most of Africa, with the exception of Central Africa, where it underestimates tree cover. The model appears to have a woody cover bias. Despite the similar distribution patterns of tree cover, the correlation in tree cover percentages between corresponding locations is quite weak (r = 0.24). This indicates a weak relationship between the observational data and G-Range values, particularly in Southern Africa.

The agreement between simulated and observed non-tree cover is less pronounced than for tree cover. However, certain features are evident in both datasets (Fig. 5.3). For instance, the low non-tree cover values along the Namibian coast extend into South Africa. Another notable feature is the hotspot of non-tree cover along the Sahel region. In contrast, G-Range shows a decrease in non-tree vegetation along the border of Namibia, Zimbabwe, Zambia, and Angola, whereas the observation data identifies this area as a hotspot for non-tree vegetation. This discrepancy in spatial patterns is clearly reflected in the bias between the model and observations. In most of Southern Africa, G-Range underestimates herbaceous and shrub cover, except in the Sahel region, where it overestimates. Despite the differences in overall spatial patterns and the bias in non-tree vegetation, the relationship between the observation and G-Range outputs (r = 0.48) is stronger than that for tree cover, indicating a moderate correlation between the two datasets.

The spatial pattern of bare ground is generally consistent between the observation and G-Range simulation (Fig. 5.3). The highest percentage of bare ground is located along the Namibian coast and continues into South Africa, where the Namib and Kalahari deserts are located. The bare ground percentage decreases gradually eastward in both spatial patterns; however, this decline is more gradual and smoother in the observation. The difference in roughness has led to patchy over- and underestimation of bare ground throughout Southern Africa. In the Sahel region, which transitions into the Sahara Desert, similarities between the observation and model results are evident. However, to the south of this transition, the model shows regions with higher bare ground than observed,. overestimatingin these areas while underestimating it near the Sahara desert. Despite these differences, the model provides largely accurate bare ground in relation to observation (r=0.69), indicating a strong correlation between the datasets.

5.3 Simulating the impact of climate change and SAI on over Africa

We applied the G-Range to simulate the impact of climate change and SAI in Africa. The model was forced with climate variables (monthly maximum temperature, minimum temperature, and precipitation) from the ARISE-SAI dataset to demonstrate how these climate variables will impact vegetation in African rangelands. The mean of the ensembles was calculated, and the mean of the reference ensemble time period was subtracted to provide a net change. The differences between the future with SAI and without were then obtained. The analysis revealed the net effect of SAI on rangeland plant functional groups (herbs, shrub and tree), bare ground, and total above-ground live biomass. The climatology of the reference period was compared to the climate change and SAI intervention scenarios to assess how the phenology and seasonality of the vegetation indices, along with selected climatic drivers, had shifted earlier or later.

5.3.1 Projected changes in temperature-related climate variables

The potential impacts of SSP2-4.5 on mean temperature-related climate variables for the period 2050-2069 vary across the African continent (Fig. 5.4). While the warming increases both maximum and minimum temperatures across the continent, the greatest increase occurs along 15°N of the equator and in Southern Africa (about +1.6°C). The smallest increase is in Northern Africa and Madagascar (about +0.8°C) (Figs. 5.2 b & f). The result of the warming is consistent with previous studies (e.g. Abiodun et al., 2021) which have explored other warming scenarios, such as RCP8.5 (Abiodun et al., 2021).

In response to this warming, potential evapotranspiration (PET) increases in tandem with temperature rise. As a result, the most widespread and highest drying is observed in West Africa (approximately +92 mm/yr) and Southern Africa (approximately +88 mm/yr). This finding is consistent with previous research (Abiodun et al., 2021), which demonstrated a positive relationship between PET and temperature, where higher temperatures intensify the vapor pressure deficit.

SAI implementation effectively mitigates the impacts of SSP2-4.5 on temperature-related climate variables (Figs. 5.4 d, h, & i). For example, SAI induces approximately 1.6°C of cooling along the 15°N parallel and in Southern Africa, both for maximum and minimum temperatures, relative to SSP2-4.5. This cooling offsets the effects of climate change across most of the continent, keeping the difference in maximum and minimum temperatures within a 0.4°C range compared to the reference period. Additionally, this cooling reduces potential evapotranspiration (PET), leading to a decrease in evaporative demand (maximum -86 mm/yr) across the continent (Fig. 5.4 i) relative to SSP2-4.5. As a result, PET stays within a 44 mm/yr range compared to the reference period. The effects of SAI on maximum and minimum temperatures and PET are consistent with previous research (e.g.??), which highlights its effectiveness in counteracting the changes driven by SSP2-4.5.

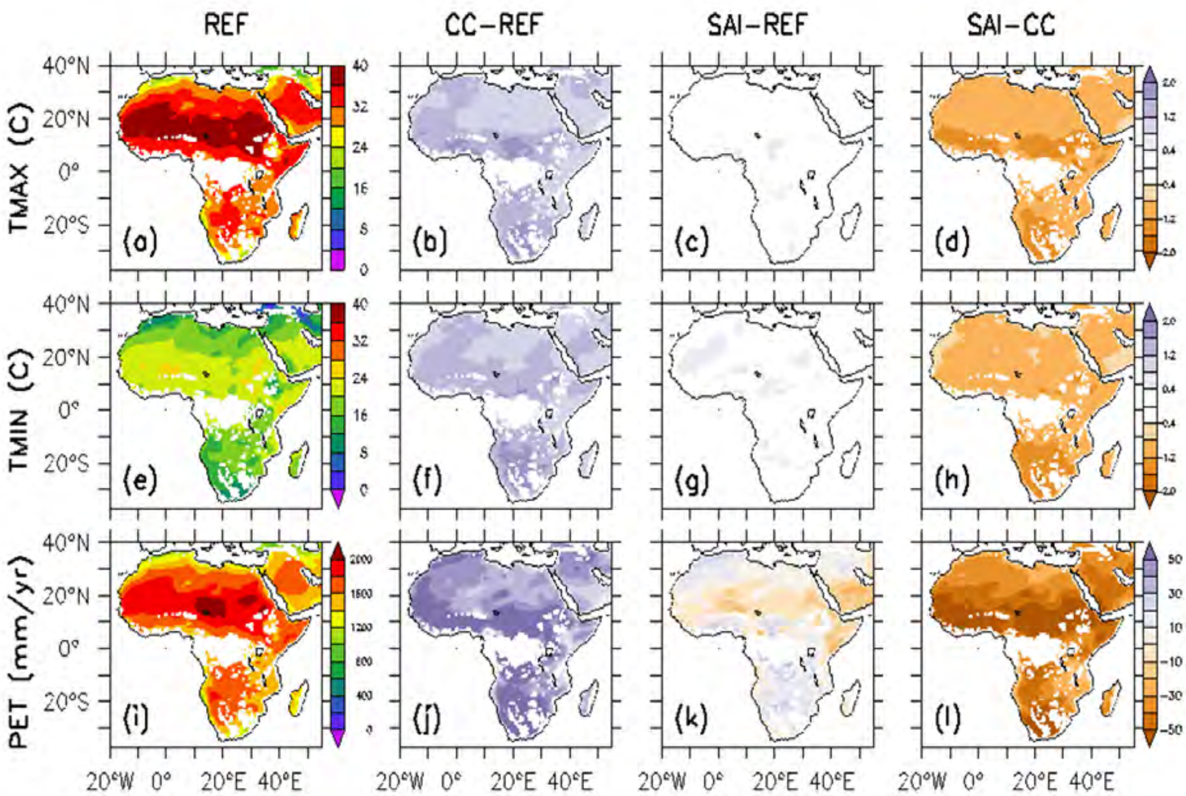

Figure 5.4. Spatial distribution of temperature-related variables during reference period (2015-2034) and the potential change due to climate change and geoengineering. These variables are maximum temperature (a), minimum temperature (e), and potential evapotranspiration (i). The change in these variables from the reference period to a future climate change (b,f,j) and SAI (c,g,k) implementation scenario. The net effect of SAI implementation (d,h,l) was calculated by subtracting climate change from the SAI scenario.

5.3.2 Projected changes in water-related climate variables

The potential impacts of SSP2-4.5 on mean water-related climate variables for the period 2050-2069 are presented in Fig. 5.5. Precipitation shows a contrasting response, with West Africa experiencing drying and East Africa getting wetter (Fig. 5.5b). The most intense drying in West Africa is around 100 mm/yr, while East Africa sees an increase of approximately 100 mm/yr.

Precipitation represents the amount of water added to the atmosphere, while actual evapotranspiration indicates how much amount of water is removed. Therefore, changes in precipitation typically influence evapotranspiration. Given the contrasting changes in precipitation – drying in West Africa and wetting in East Africa – it is expected that evapotranspiration will follow a similar spatial pattern, reflecting the availability of water. Eastern Africa shows this pattern, with evapotranspiration increasing (up to 60 mm/yr) in areas experiencing wetter conditions. In while evapotranspiration generally follows the drying pattern, there is also a decrease in atmospheric demand (around -50 mm/yr). Southern Africa also experiences a decrease in evapotranspiration (Fig. 5.5f)..

Precipitation is not the sole determinant of water availability for evapotranspiration. The intensity, magnitude, and frequency of rainfall events, as well as soil texture and ground cover, also play important roles in water infiltration and flow through the soil. These factors influence the amount of water available in the soil for plants to transpire. The water available for plant growth in the soil decreases across the entire African continent, with the maximum drying (>0.6 cm) occurring at the 15-20°N parallels and the minimum in East Africa (Fig. 5.5n).

This result is unexpected, as there is typically a positive correlation between soil moisture and precipitation. A decrease in precipitation generally implies less water available for soil infiltration. However, increased drought and more intense precipitation events can lead to crust formation or increased runoff, both of which reduce the amount of water able to enter the soil. The simulation timestep and the model's processes do not account for crust formation or the intensity of rainfall events. Therefore, it is uncertain whether these factors contribute to the observed decrease in soil water availability.

Low water availability for plants can imply water stress, but atmospheric water demand can heighten or lessen this stress. The water stress index (Fig. 5.5) is the ratio of actual evapotranspiration to potential evapotranspiration, identifying areas where there is enough moisture to meet the maximum atmospheric demand. The African continent’s rangelands have an evaporative ratio of less than one (0.5), which implies that water is a limiting factor throughout.

Water stress in East Africa decreases, while Southern and West Africa experience increased water stress, as indicated by the decline in the water stress ratio. This trend is further supported by the water balance coefficient, which shows water scarcity in Southern Africa and increased moisture in East Africa (Fig. 5.5r). However, in West Africa, water scarcity and stress increase, but this is not reflected in the water stress index. This discrepancy likely arises from the combination of decreasing precipitation and increasing potential evapotranspiration in the region.

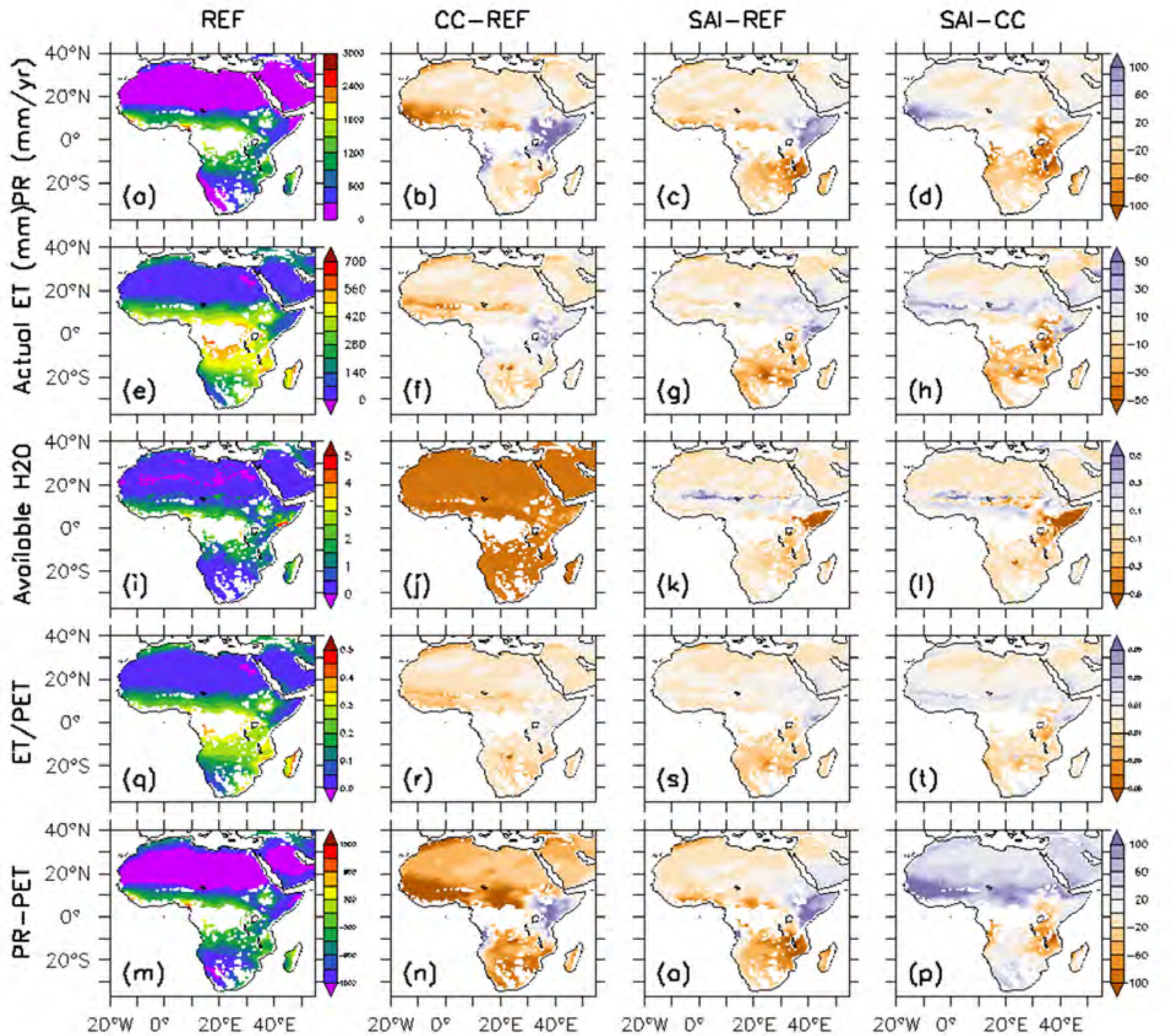

Figure 5.5. Same as Fig. 2, except for the moisture-related variables. Precipitation (a, b, c, & d), Actual evapotranspiration (i, j, k & l), Available H20 to plants for growth (m, n, o, & p), the water balance coefficient (PR-PET) (q, q, r & s), and water stress (ET/PET)(u, v, w, & x). The influence of SSP2-4.5 warming (b, j, n, r & v) and SAI implementation (c, k, o, s & w) is related to the reference period. The net effect of SAI intervention (d, l, p, t & x) on rangelands in Africa.

The SAI intervention has varying impacts on water-related variables across the African continent (Fig. 5.5). While SAI offsets the drying in West Africa, it overcompensates, leading to drying in Southern and Eastern Africa (about -100 mm/yr) (Fig. 3d). This finding is consistent with previous studies by Abiodun et al. (2021) and Cheng et al. (2019).

With SAI, the actual evapotranspiration is expected to increase in Western Africa (where SAI leads to more moisture) and decrease in Eastern and Southern Africa (where SAI leads to drier conditions). However, this is not always the case , as SAI leads to a decrease in evapotranspiration in East Africa despite the region becoming wetter, while Southern Africa's evapotranspiration remains unresponsive to the drying (Fig. 5.5c & k).The SAI intervention offsets the changes in atmospheric demand associated with SSP2-4.5 warming. The effect of precipitation and evapotranspiration on soil water availability is clear, as East Africa becomes wetter, it experiences lower atmospheric demand, and thus sees an increase in soil water (Fig. 5.5o)

Interestingly, SAI intervention has a variable response for soil moisture and tends to overcompensate between the 10-20°N parallels and in East Africa, leading to irregular patterns of wetting and drying of the soil compared to SSP2-4.5 (Fig. 5.5p). The water balance coefficient indicates that while SAI implementation offsets the water shortages caused by SSP2-4.5 warming, it also overcompensates, drying areas that would not have dried under normal climate change conditions (Fig. 5.5t). Looking at the water stress index, SAI effectively counters the increase in water stress in Southern Africa and returns East Africa to its reference water stress level..

5.3.3 Projected changes in vegetation characteristics over Africa

The impact of SSP2-4.5 on vegetation in Africa depends on the vegetation metrics used for the projection (Fig. 5.6). Under SSP2-4.5, the response of vegetation type, bare ground, and total above-ground live biomass varies with changing climate variables. Herb cover decreases significantly across large parts of the continent, with the largest declines (>2.5%) occurring along the 5°N parallel and in Southern Africa. However, there are locations, mainly in East Africa, where herb cover increases by up to about 2.5% (Fig. 5.6b).

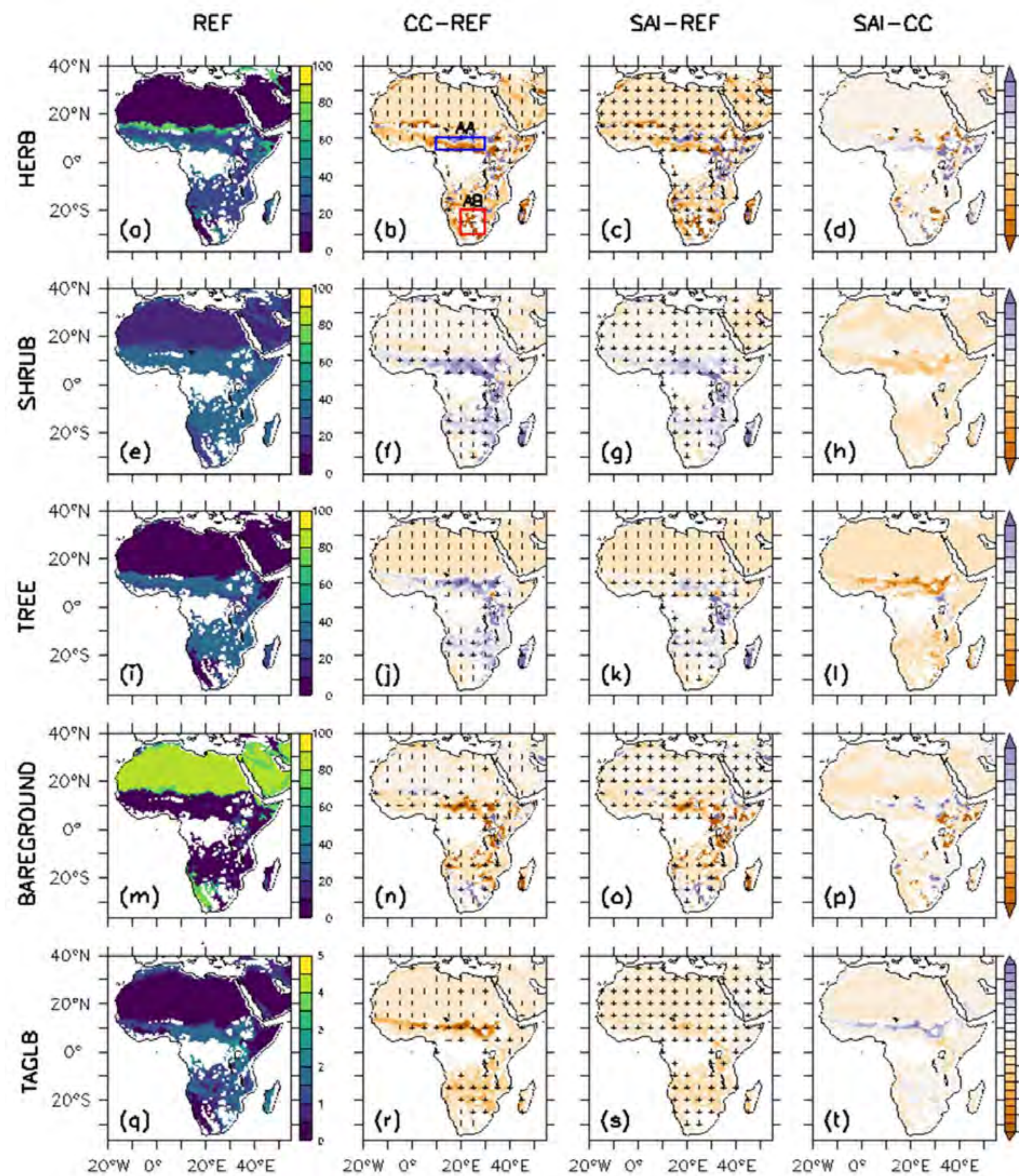

Figure 5.6. Same for Fig (2), except for grassland related variables: herb (a, b, c & d), shrub (e, f, g, & h), tree (i, j, k & l), bare ground (m, n, o, & p) percentage cover as well as total aboveground live biomass (q, r, s, & t). The influence of ssp2-4.5 (2050-2069) (b, f, j, n, & r) and SAI implementation (2050-2069) (c, g, k, o, & s) in respect to the reference period (2015-2034) (q, e, i, m & q). The net effect of SAI intervention with respect to ssp2-4.5 for the vegetation metrics (d, h, l, p & t). The vertical lines indicate that 60% of the ensembles result in a change that exceeds

natural variability. The horizontal lines indicate that 70% of the ensembles agree with the sign of the change.

Herbs are more sensitive to temperature and have an optimal growth range between 17-23°C (Lomax et al., 2024). In contrast to herb cover, shrub cover increases significantly (>2.5%) along the 5-10°N parallel, as well as in the interior of East Africa and Eastern Southern Africa (Fig. 5.6f). This increase in woody vegetation aligns with previous studies (Lomax et al., 2024).

Additionally, tree cover increases along the 10°N parallel, coinciding with the same areas where shrubs have increased (Fig. 5.6j), with a maximum increase of about 1.5%. Based on ecological competition theory, different plant types compete for the same limited resources, and it appears that herbs are outcompeted by shrubs and trees. Shrubs and trees have an evolutionary advantage over herbs due to their more complex root systems, which allow them to extract water from deeper soil levels (Lomax et al., 2024). This may be particularly important as soil moisture decreases across Africa under the SSP2-4.5 scenario (Fig. 5.6n).

Furthermore, areas that not conducive for the growth of vegetation become colonized by shrubs and trees, as indicated by a decrease of about 5% in bare ground in the same regions (Fig. 5.6n). In Southern Africa and other specific locations around the continent, there are increases in bare ground (about 5%) where herb cover declines, which aligns with the literature. This is likely due to increased water stress and the water balance coefficient linked to a strong increase in PET (Figs. 5.4 & 5.5). Despite the increase in shrub and tree cover replacing herbaceous cover in many areas, there is a decline in total above-ground live biomass. This finding contrasts with previous studies, which typically shows that trees and larger plants contribute more to above-ground live biomass than herbaceous plants.

SAI implementation on vegetation in Africa is similar in pattern to SSP2-4.5 but with a smaller magnitude. For herb cover, there was a decline; however, the large swath along the 5°N parallel is weakened (Fig. 5.6c). In East Africa, the discrete areas with an increase in herbs have grown in the area. Thus, SAI intervention may offset the decline or growth of herbs in some places compared to SSP2-4.5, while in East Africa, it intensifies the change (Fig. 5.6d).

For shrub and tree cover, SAI leads to less growth than SSP2-4.5, especially between 5-10°N. This implies that if SAI is implemented, it will result in reduced shrub (1-2%) and tree (0.6%) levels in this region compared to an SSP2-4.5 future (Fig. 5.6h & i). Along the equator, herbs, shrub, and tree cover increase, resulting in a decrease in bare ground cover (5%); however, unexpectedly, total above-ground live biomass does not increase (Fig. 5.6o & s). Bare ground responds variably to SAI in East Africa, where it enhances the increase or decrease. Meanwhile, SAI increases total above-ground live biomass (about 0.8) compared to SSP2-4.5.

5.3.4 Projected changes in area cover by vegetation types

Different regions of Africa respond with varying sensitivity, direction, and magnitude to the effect of climate change and SAI (Fig 5.7). Although the magnitude appears small (>1.5%), this can still be significant at local scales. Under the current climate in West Africa (WA), the ground composition is dominated by bare ground, then shrub, herb, and tree. Climate change leads to an increase in bare ground (+0.01%), shrubs (+0.31%), and trees (+0.13%) as herb declines (-0.44%). SAI is able to lessen the decrease in herb decline (+0.12%) and the growth of shrubs (-0.1%) and trees (-0.11%) but enhances the desertification (+0.09%).

Through the influence of geoengineering, the total above-ground live biomass remains closer to the reference than climate change which leads to a decrease in biomass. Presently in East Africa (EA), the region has high shrub coverage, then herb, trees, and bare ground. Climate change causes herb (-0.35%) and bare ground (-1.7%) cover to decrease while woody vegetation (+1.3% & +0.74% for shrub and trees, respectively) grows. SAI overcompensates for herbs (+1.44%) resulting in greater abundance than climate change and the reference. SAI restored shrub (-0.13%) closer to the reference but exacerbated the decrease in bare ground (-1.33%) and the increase in trees (+0.02%). The net effect of the changes of SAI lead to a smaller decrease in total above-ground live biomass than climate change. Central Africa's ground cover from highest percentage is shrubs, herbs, trees, and bare ground. Climate change leads to a decline in herbs (-0.08%) and bare ground (-1.36%) and the growth of woody vegetation (+1.01% & +0.42% for shrubs and trees). SAI mitigates the change for shrub (-0.21%), tree (-0.14%), and bare ground (-0.06%), however, geoengineering overcompensates for herb cover (+0.29%). The interaction between the different ground covers leads to a decrease in total above-ground live biomass for climate change. However,, SAI mitigates this decrease. Southern Africa is characterised by dominant shrubs, similar levels of tree and herb, and bare ground. Climate change leads to a decrease in herbs (-1.08%) and bare ground (-0.46%) while it increases woody vegetation (+0.97% shrubs & +0.58% trees). SAI alleviates the impacts of climate change for shrubs (-0.19%), trees (-0.22%), and bare ground (+0.43%) but elevated the decline of herbs (-0.02%). Despite the increase in woody vegetation and the decrease in bare ground, total above-ground live biomass decreases for climate change, but SAI restored it closer to reference. Northern Africa consists of mainly bare ground with some shrubs, herbs, and trees. Climate change leads to a decline of herbs (-0.148%) and bare ground (-0.27%) while shrub (0.25%) and tree (0.169%) cover increase. SAI is capable of restoring all of the ground covers closer to the reference including total above ground live biomass.

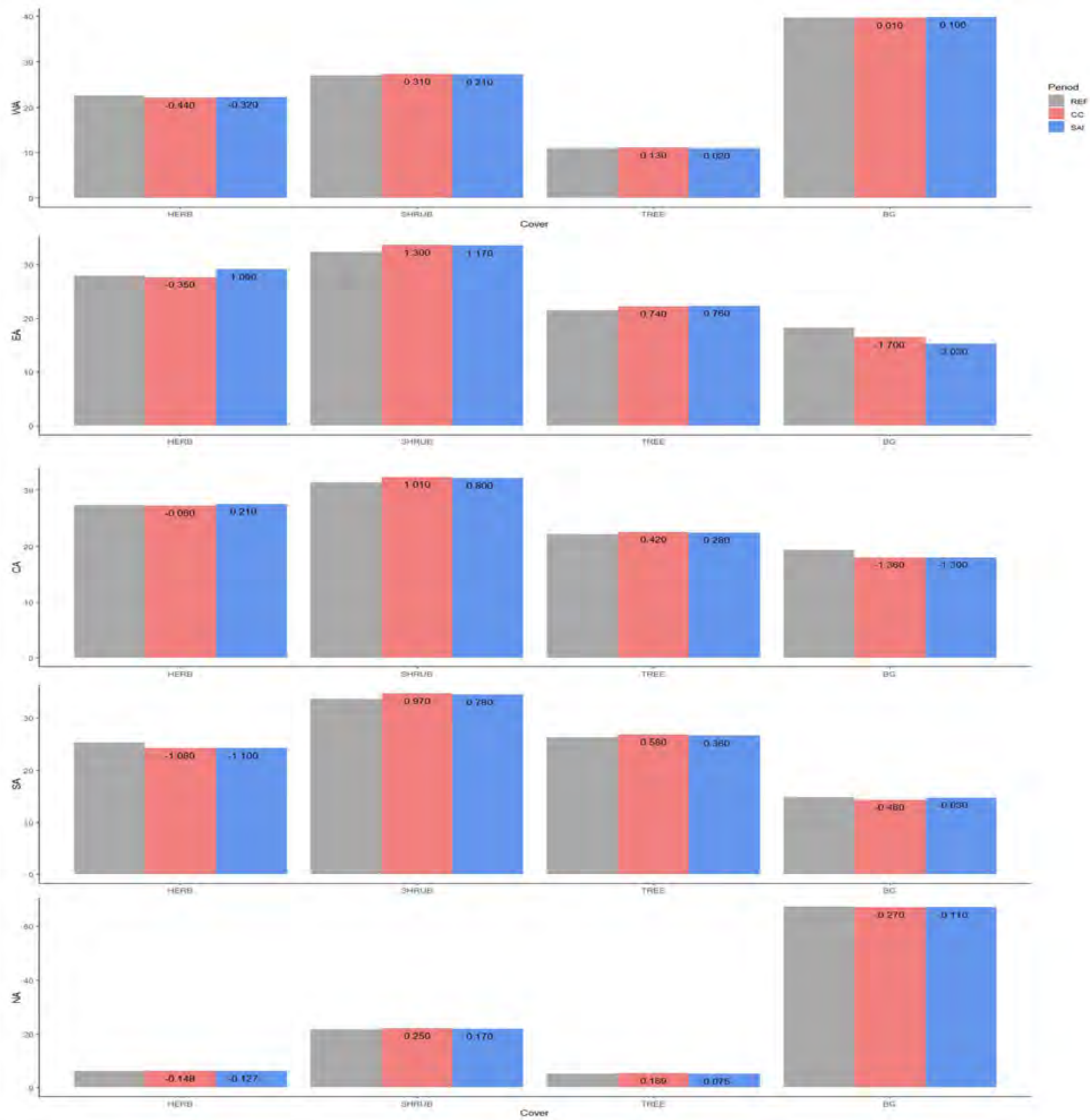

Figure 5.7: The change in ground cover (%) and total aboveground live biomass (g/m^2) in regions of Africa. West Africa (WA), East Africa (EA), Central Africa (CA), Southern Africa (SA), and North Africa (NA).

Chapter 6: Summary and Conclusions

The project examined the impacts of climate change and stratospheric aerosol geoengineering (SAG) on water yield, crop production, and grassland productivity in Africa. As part of the study, we analysed climate, hydrological, crop, and grassland simulation datasets for both past and future climate scenarios, with and without the application of SAI. The climate datasets were bias-corrected and subsequently used to drive the crop and grassland simulations.

Chapter 2 demonstrated the reliability of our bias corrections methods in improving the quality of the datasets. Reliable climate models are foundational to the study of climatic phenomena, yet biases inherent in such models often compromise their reliability. Through the application of the bias correction methodology, we were able to enhance the spatial representation of critical climate variables, including temperature and precipitation, over Africa. This bias correction of the simulations not only reduces uncertainties in datasets but also improves capability of the datasets to reproduce characteristics of African climate. Such improved datasets establish a solid framework for formulation of evidence-based policies.

Chapter 3 addressed the critical issue of water resource management by examining the impacts of climate change and SAG on major river basins across Africa. The findings indicate that climate change is likely to exacerbate freshwater scarcity in many regions, with notable exceptions in East and Central Africa, where freshwater availability may increase. The implementation of SAG introduces additional complexity to water yield patterns, underscoring the necessity for integrated and proactive planning. Hence, effective transboundary water management strategies, including the establishment of cooperative agreements, may be essential to prevent conflicts over shared water resources and to promote equitable and sustainable utilization.

Chapter 4 analysed the impacts of climate change and SAG on crop yields in Africa, highlighting regional and crop-specific variations. Soybeans, a C3 crop, benefit from elevated CO2 levels, showing increased yields across most of Africa. Conversely, C4 crops like maize and sorghum experience significant yield declines due to global warming, underscoring their vulnerability and the food security challenges this creates in the regions. SAG serves as a mitigating tool for climate change induced yield deficits, but its effectiveness varies. In Southern Africa, SAG offsets maize yield declines but worsens sorghum reductions and decreases soybean yields. In West Africa, SAG declines maize yield while lowering sorghum and soybean yields. Central Africa experiences improved maize and sorghum yields, though soybean yields drop. In Eastern Africa, SAG increases maize and soybean yields but reduces sorghum yields significantly. The findings underscore the need for tailored strategies to address regional and crop-specific challenges, ensuring sustainable agriculture and food security across Africa.

Chapter 4 extended the impacts of climate change and SAG to grassland ecosystems, which are shown to be particularly susceptible to changes induced by climate change and SAG. Alterations in vegetation composition, characterized by reductions in herbaceous species and increases in woody vegetation, have significant consequences for rangeland productivity. Such changes threaten the availability of forage resources, with potential adverse effects on the livelihoods of pastoral communities. The findings highlight the necessity of adaptive land management practices to mitigate these impacts, maintain ecosystem functionality, and support the sustainability of both biodiversity and human-dependent systems.

The project also offers valuable policy recommendations to address the multifaceted challenges posed by climate change and SAG. Key strategies include the promotion of crop diversification, the adoption of climate-resilient agricultural techniques, and the development of sustainable water management frameworks. Policymakers are urged to adopt a long-term perspective that recognizes the interconnectedness of climate, agricultural, and hydrological systems. Collaborative efforts and adaptive management approaches will be essential to ensure the resilience of communities and ecosystems in the face of ongoing environmental changes.

A particularly salient outcome of this research is the emphasis on the importance of region-specific strategies to compact impacts of climate change and SAG. Africa's heterogeneous climatic and ecological landscapes necessitate tailored approaches to address the unique challenges faced by different regions. A holistic understanding of the interdependencies between climate systems, socio-economic structures, and ecological processes is critical for devising effective solutions. By integrating scientific innovation and cross-sector collaboration, these strategies can enhance both the mitigation of and adaptation to climate impacts.

The broader implications of this work underscore the transformative potential of science in addressing global challenges. By revealing the complex interactions between climate change, SAG, and Africa's environmental systems, this research contributes to a growing body of knowledge that supports sustainable development and resilience. It also serves as a call to action, urging the translation of scientific findings into practical policies and interventions. The integration of research outcomes into actionable strategies, including the development of technologies and practices that enhance adaptability to the impacts of climate change or proposed SAG, will be instrumental in safeguarding the well-being of African communities and ecosystems.

In conclusion, the insights gained from this study provide a comprehensive understanding of the intricate dynamics linking climate change, SAG, and Africa's diverse environmental systems. These findings underscore the necessity of interdisciplinary research, cross-sectoral cooperation, and innovative policymaking to address the challenges of climate change effectively. By leveraging these insights, Africa can advance towards a future characterized by resilience, sustainability, and equitable development.

References

Abate, T., Fisher, M., Abdoulaye, T., Kassie, G. T., Lunduka, R., Marenya, P., & Asnake, W. (2017). Characteristics of maize cultivars in Africa: How modern are they and how many do smallholder farmers grow? *Agriculture & Food Security*, *6*, 30. https://doi.org/10.1186/s40066-017-0108-6

Abiodun, B. J., Odoulami, R. C., Sawadogo, W., Oloniyo, O. A., Abatan, A. A., New, M., Lennard, C., Izidine, P., Egbebiyi, T. S., & MacMartin, D. G. (2021). Potential impacts of stratospheric aerosol injection on drought risk managements over major river basins in Africa. *Climatic Change*, *169*(3-4), 31. https://doi.org/10.1007/s10584-021-03268-w

Armstrong R., Brodzik MJ, Knowles K., Sovoie M. (2009). *Global, monthly satellite-derived snow water equivalent (SWE) climatologies from November 1978 through June 2003* [Dataset]. https://doi.org/10.18739/A2GT5FG67

Bai, G. (frank), Barker, B., Scoby, D., Irmak, S., Luck, J. D., Neale, C. M. U., Schnable, J. C., Awada, T., Kustas, W. P., & Ge, Y. (2024). High-throughput physiological phenotyping of crop evapotranspiration at the plot scale. *Field Crops Research*, *316*(109507), 109507. https://doi.org/10.1016/j.fcr.2024.109507

Batjes, N. H. (2002). Revised soil parameter estimates for the soil types of the world. *Soil Use and Management*, *18*(3), 232–235. https://doi.org/10.1111/j.1475-2743.2002.tb00244.x

Bell, C., Barnes, E. A., Hurrell, J. W., Diffenbaugh, N., & Keys, P. W. (2022, September 27). Solar geoengineering might work, but local temperatures could keep rising for years. *The Conversation*. https://theconversation.com/solar-geoengineering-might-work-but-local-temperatures-could-keep-rising-for-years-190638?form=MG0AV3

Berkowitz, R. (2021). Mobile phone signals hold real-time rainfall information. *Physics*, *14*. https://doi.org/10.1103/physics.14.161

Boone, R. B., Conant, R. T., Sircely, J., Thornton, P. K., & Herrero, M. (2018). Climate change impacts on selected global rangeland ecosystem services. *Global Change Biology*, *24*(3), 1382–1393. https://doi.org/10.1111/gcb.13995

Boone R., Conant R., Hilinski T. (2011). *GRange_FINAL_Report_2011.pdf*.

Boote, E. P. K., Kim, S. H., Hsiao, J., Kinmonth-Schultz, H., Evers, J. B., Marcelis, P. L. F. M., Singh, U., Porter, C., Stöckle, P. C. O., & Meza, F. (2019). *Advances in crop modelling for a sustainable agriculture* (E. K. Boote (ed.)). Burleigh Dodds Science Publishing. https://books.google.com/books?hl=en&lr=&id=RiMzEQAAQBAJ&oi=fnd&pg=PP11&dq=Boote,+K.,+2019.+Advances+in+crop+modelling+for+sustainable+agriculture.+Burleigh+Dodds+Science+Publishing.&ots=GG_EvF46-4&sig=xI8I_UzevDhn7QVXszYMctOMRVU

Bürger, G., Murdock, T., Werner, A., & Sobie, S. (2010). *Downscaling extremes with EDS, TreeGen, and BCSD*. *2010*. https://pacificclimate.org/sites/default/files/publications/agu.pdf

Burroughs, C. H., Montes, C. M., Moller, C. A., Mitchell, N. G., Michael, A. M., Peng, B., Kimm, H., Pederson, T. L., Lipka, A. E., Bernacchi, C. J., Guan, K., & Ainsworth, E. A. (2023). Reductions in leaf area index, pod production, seed size, and harvest index drive yield loss to high temperatures in soybean. *Journal of Experimental Botany*, *74*(5), 1629–1641. https://doi.org/10.1093/jxb/erac503

Cannon, A. J. (2016). Multivariate bias correction of climate model output: Matching marginal distributions and intervariable dependence structure. *Journal of Climate*, *29*(19), 7045–7064. https://doi.org/10.1175/jcli-d-15-0679.1

Cheng, W., MacMartin, D. G., Dagon, K., Kravitz, B., Tilmes, S., Richter, J. H., Mills, M. J., & Simpson, I. R. (2019). Soil moisture and other hydrological changes in a stratospheric aerosol Geoengineering Large Ensemble. *Journal of Geophysical Research Atmospheres*, *124*(23), 12773–12793. https://doi.org/10.1029/2018jd030237

DiMiceli, C., Townshend, J., Carroll, M., & Sohlberg, R. (2021). Evolution of the representation of global vegetation by vegetation continuous fields. *Remote Sensing of Environment*, *254*, 112271. https://doi.org/10.1016/j.rse.2020.112271

Djaman, K., Irmak, S., Rathje, W. R., Martin, D. L., & Eisenhauer, D. E. (2013). Maize evapotranspiration, yield production functions, biomass, grain yield, harvest index, and yield response factors under full and limited irrigation. *Transactions of the ASABE*, *56*(2), 373–393. https://elibrary.asabe.org/abstract.asp?aid=42676

Durodola, O. S., & Mourad, K. A. (2020). Modelling the impacts of climate change on soybeans water use and yields in Ogun-Ona River Basin, Nigeria. *Agriculture*, *10*(12), 593. https://doi.org/10.3390/agriculture10120593

Ehret, U., Zehe, E., Wulfmeyer, V., Warrach-Sagi, K., & Liebert J H E S. (2012). HESS Opinions“ Should we apply bias correction to global and regional climate model data?” *Hydrology and Earth System Sciences*, *16*(9), 3391–3404. https://hess.copernicus.org/articles/16/3391/2012/

Elliott, J., Müller, C., Deryng, D., Chryssanthacopoulos, J., Boote, K. J., Büchner, M., & Sheffield. (2015). The global gridded crop model intercomparison: data and modeling protocols for phase 1 (v1. 0). *Geoscientific Model Development*, *8*(2), 261–277. https://gmd.copernicus.org/articles/8/261/2015/

Estes, A. B., Kuemmerle, T., Kushnir, H., Radeloff, V. C., & Shugart, H. H. (2012). Land-cover change and human population trends in the greater Serengeti ecosystem from 1984–2003. *Biological Conservation*, *147*(1), 255–263. https://doi.org/10.1016/j.biocon.2012.01.010

Fotso-Nguemo, T. C., Chouto, S., Nghonda, J. P., Diedhiou, A., Kravitz, B., Yepdo, Z. D., Djuidje, F. K., & Abiodun, B. J. (2024). Projected impact of solar radiation modification geoengineering on water deficit risk over major Central African river basins. *Environmental Research Letters*, *19*(9), 094046. https://doi.org/10.1088/1748-9326/ad657d

Gleeson, T., Cuthbert, M., Ferguson, G., & Perrone, D. (2020). Global groundwater sustainability, resources, and systems in the Anthropocene. *Annual Review of Earth and Planetary Sciences*, *48*(1), 431–463. https://doi.org/10.1146/annurev-earth-071719-055251

Henderson, B. B., Gerber, P. J., Hilinski, T. E., Falcucci, A., Ojima, D. S., Salvatore, M., & Conant, R. T. (2015). Greenhouse gas mitigation potential of the world's grazing lands: Modeling soil carbon and nitrogen fluxes of mitigation practices. *Agriculture, Ecosystems & Environment*, *207*, 91–100. https://doi.org/10.1016/j.agee.2015.03.029

Hoffman, M. T. (2018). Land use, land cover and vegetation change in southern Africa. In *Southern African Landscapes and Environmental Change* (pp. 91–111). Routledge. https://doi.org/10.4324/9781315537979-6

Iglesias, A., Avis, K., Benzie, M., Fisher, P., Harley, M., Hodgson, N., & Webb. (2007). *Adaptation to climate change in the agricultural sector. AEA Energy & Environment*.

Jones, J. W., Tsuji, G. Y., Hoogenboom, G., Hunt, L. A., Thornton, P. K., Wilkens, P. W., ... & Singh, U. (1998). Decision support system for agrotechnology transfer: DSSAT v3. *Understanding options for agricultural production*, 157-177.

Kirschbaum, M. U. F. (2004). Direct and indirect climate change effects on photosynthesis and transpiration. *Plant Biology (Stuttgart, Germany)*, *6*(3), 242–253. https://doi.org/10.1055/s-2004-820883

Kobayashi, K., & Salam, M. U. (2000). Comparing simulated and measured values using mean squared deviation and its components. *Agronomy Journal*, *92*(2), 345–352. https://doi.org/10.2134/agronj2000.922345x

Koo, J., & Dimes, J. (2013). *HC27 generic soil profile database*. https://cgspace.cgiar.org/items/82595601-8cdb-4109-8e59-cc145bfd3cf9

Legates, D. R., & McCabe, G. J., Jr. (1999). Evaluating the use of "goodness-of-fit" Measures in hydrologic and hydroclimatic model validation. *Water Resources Research*, *35*(1), 233–241. https://doi.org/10.1029/1998wr900018

Li, X., Zhang, K., & Li, X. (2023). The minimum temperature outweighed the maximum temperature in determining plant growth over the Tibetan Plateau from 1982 to 2017. *Remote Sensing*, *15*(16), 4032. https://doi.org/10.3390/rs15164032

Lomax, G. A., Powell, T. W. R., Lenton, T. M., Economou, T., & Cunliffe, A. M. (2024). Untangling the environmental drivers of gross primary productivity in African rangelands. *Communications Earth & Environment*, *5*(1), 1–13. https://doi.org/10.1038/s43247-024-01664-5

MacCarthy, D. S., Traore, P. S., Freduah, B. S., Adiku, S. G. K., Dodor, D. E., & Kumahor, S. K. (2022). Productivity of soybean under projected climate change in a semi-arid region of West Africa: Sensitivity of current production system. *Agronomy (Basel, Switzerland)*, *12*(11), 2614. https://doi.org/10.3390/agronomy12112614

Maraun, D. (2016). Bias correcting climate change simulations - a critical review. *Current Climate Change Reports*, *2*(4), 211–220. https://doi.org/10.1007/s40641-016-0050-x

Mengistu, M. G., Steyn, J. M., Kunz, R. P., Doidge, I., Hlophe, H. B., Everson, C. S., Jewitt, G. P. W., & Clulow, A. D. (2016). A preliminary investigation of the water use efficiency of sweet sorghum for biofuel in South Africa. *Water S. A.*, *42*(1), 152. https://doi.org/10.4314/wsa.v42i1.15

Munnoli, S., Shivashankar, K., & Golshetti, A. (2023). Influences of changes in rainfall and solar radiation on performance of kharif sorghum. *International Journal of Environment and Climate Change*, *13*(6), 186–193. https://doi.org/10.9734/ijecc/2023/v13i61814

O'Neill, B. C., Tebaldi, C., Van Vuuren, D. P., Eyring, V., Friedlingstein, P., Hurtt, G., ... & Sanderson, B. M. (2016). The scenario model intercomparison project (ScenarioMIP) for CMIP6. *Geoscientific Model Development*, *9*(9), 3461-3482.

Prasad, P. V. V., Djanaguiraman, M., Stewart, Z. P., & Ciampitti, I. A. (2018). Agroclimatology of maize, sorghum, and pearl millet. In *Agronomy Monographs* (pp. 201–241). American Society of Agronomy, Crop Science Society of America, and Soil Science Society of America, Inc. https://doi.org/10.2134/agronmonogr60.2016.0005

Ramirez-Villegas, J., & Thornton, P. K. (2015). *Climate change impacts on African crop production*. *119*, 1–25.

Randall, D., & Fichefet, T. (2007). *Climate models and their evaluation*. 589–662. https://philpapers.org/rec/BONCMA-2

Rosenzweig, C., & Tubiello, F. N. (1996). Effects of changes in minimum and maximum temperature on wheat yields in the central US A simulation study. *Agricultural and Forest Meteorology*, *80*(2-4), 215–230. https://doi.org/10.1016/0168-1923(95)02299-6

Ruesch A., G. H. K. (2008). *New IPCC tier-1 global biomass carbon map for the year 2000* [Dataset]. http://cdiac.ornl.gov

Schlenker, W., & Lobell, D. B. (2010). Robust negative impacts of climate change on African agriculture. *Environmental Research Letters*, *5*(1), 014010. https://doi.org/10.1088/1748-9326/5/1/014010

Sheffield, J., Goteti, G., & Wood, E. F. (2006). Development of a 50-year high-resolution global dataset of meteorological forcings for land surface modeling. *Journal of climate*, *19*(13), 3088-3111.

Shukla, P. R., Skea, J., Calvo Buendia, E., Masson-Delmotte, V., Pörtner, H. O., Roberts, D. C., Zhai, P., Slade, R., Connors, S., Van Diemen, R., & Others. (2019). An IPCC special report on climate change, desertification, land degradation, sustainable land management, food security, and greenhouse gas fluxes in terrestrial ecosystems. *Climate Change and Land*. https://policycommons.net/artifacts/9774155/climate-change-and-land/10669611/

Sietse, O. L. (2010). *ISLSCP II FASIR-adjusted NDVI Biophysical Parameter Fields* [Dataset]. http://daac.ornl.gov/

Sircely, J., Conant, R. T., & Boone, R. B. (2019). Simulating Rangeland Ecosystems with G-Range: Model Description and Evaluation at Global and Site Scales. *Rangeland Ecology & Management*, *72*(5), 846–857. https://doi.org/10.1016/j.rama.2019.03.002

Srivastava, A. K., Rahimi, J., Alsafadi, K., Vianna, M., Enders, A., Zheng, W., Demircan, A., Dieng, M. D. B., Salack, S., Faye, B., Singh, M., Halder, K., Ewert, F., & Gaiser, T. (2025). Modelling mixed crop-livestock systems and climate impact assessment in sub-Saharan

Africa. *Scientific Reports*, *15*(1), 1399. https://doi.org/10.1038/s41598-024-81986-8

Sultan, B., Ahmed, A. I., Faye, B., & Tramblay, Y. (2023). Less negative impacts of climate change on crop yields in West Africa in the new CMIP6 climate simulations ensemble. *PLOS Climate*, *2*(12), e0000263. https://doi.org/10.1371/journal.pclm.0000263

Thrasher, B., Wang, W., Michaelis, A., Melton, F., Lee, T., & Nemani, R. (2022). NASA global daily downscaled projections, CMIP6. *Scientific Data*, *9*(1), 262. https://doi.org/10.1038/s41597-022-01393-4

Tilmes, S., Richter, J. H., Kravitz, B., MacMartin, D. G., Mills, M. J., Simpson, I. R., ... & Ghosh, S. (2018). CESM1 (WACCM) stratospheric aerosol geoengineering large ensemble project. *Bulletin of the American Meteorological Society*, *99*(11), 2361-2371.

USGS. (2008). *Global land cover characterization, version 2* [Dataset]. http://edc2.usgs.gov/glcc/glcc.php

Werner, A., & Cannon, A. J. (2016). Hydrologic extremes – an intercomparison of multiple gridded statistical downscaling methods. *Hydrology and Earth System Sciences*, *20*, 1483–1508. https://doi.org/10.5194/HESS-20-1483-2016

Wilcke, R. A. I., Mendlik, T., & Gobiet, A. (2013). Multi-variable error correction of regional climate models. *Climatic Change*, *120*(4), 871–887. https://doi.org/10.1007/s10584-013-0845-x

Wootten, A. M., Dixon, K. W., Adams-Smith, D. J., & McPherson, R. A. (2021). Statistically downscaled precipitation sensitivity to gridded observation data and downscaling technique. *International Journal of Climatology: A Journal of the Royal Meteorological Society*, *41*(2), 980–1001. https://doi.org/10.1002/joc.6716

Xiong, W., Holman, I., Conway, D., Lin, E., & Li, Y. (2008). A crop model cross calibration for use in regional climate impacts studies. *Ecological Modelling*, *213*(3-4), 365–380. https://doi.org/10.1016/j.ecolmodel.2008.01.005

Xiong, W., Skalský, R., Porter, C. H., Balkovič, J., Jones, J. W., & Yang, D. (2016). Calibration-induced uncertainty of the EPIC model to estimate climate change impact on global maize yield. *Journal of Advances in Modeling Earth Systems*, *8*(3), 1358–1375. https://doi.org/10.1002/2016ms000625

Yang, Y., Xu, W., Hou, P., Liu, G.-Z., Liu, W., Wang, Y., Zhao, R., Ming, B., Xie, R., Wang, K., & Li, S. (2019). Improving maize grain yield by matching maize growth and solar radiation. *Scientific Reports*, *9*. https://doi.org/10.1038/s41598-019-40081-z

Zhang, K., Kimball, J. S., Nemani, R. R., & Running, S. W. (2010). A continuous satellite-derived global record of land surface evapotranspiration from 1983 to 2006. *Water Resources Research*, *46*(9). https://doi.org/10.1029/2009wr008800

Zinyengere, N., Crespo, O., Hachigonta, S., & Tadross, M. (2014). Local impacts of climate change and agronomic practices on dry land crops in Southern Africa. *Agriculture, Ecosystems & Environment*, *197*, 1–10. https://doi.org/10.1016/j.agee.2014.07.002

Zinyengere, N., Crespo, O., Hachigonta, S., & Tadross, M. (2015). Crop model usefulness in drylands of southern Africa: an application of DSSAT. *Suid-Afrikaanse Tydskrif Vir Plant En Grond [South African Journal of Plant and Soil]*, *32*(2), 95–104. https://doi.org/10.1080/02571862.2015.1006271